Studies on the Preparation and Characterization of Novel Water-Soluble Catalysts

Barbara B. Bunn

Dissertation Submitted to the Faculty of the
Virginia Polytechnic Institute and State University
in partial fulfillment of the requirements for the degree of

DOCTOR OF PHILOSOPHY
in
CHEMISTRY

APPROVED:

Brian E. Hanson, Ph.D., Chairman

Joseph S. Merola, Ph.D.

Larry T. Taylor, Ph.D.

Raymond E. Dessy, Ph.D.

G. Alan Schick, Ph.D.

November 12, 1993

Blacksburg, Virginia

STUDIES ON THE PREPARATION AND CHARACTERIZATION OF NOVEL WATER-SOLUBLE CATALYSTS

Barbara B. Bunn

Brian E. Hanson, Ph.D., Chairman

ABSTRACT

Spin-lattice (T_1) relaxation studies using solid-state and solution-state ^{31}P nuclear magnetic resonance spectroscopy have proven to be a reliable procedure for determining the onset of a "liquid-like" character of the supported phase in a supported aqueous phase catalyst. It has also been shown that the appearance of the liquid-like character, which can be determined by the length of T_1, occurs at the onset of maximum catalytic activity in a supported aqueous phase catalyst.

Direct sulfonation of 1,2-bis(diphenylphosphino)ethane (DPPE) has yielded 1,2-(bis[di-*m*-sodiumsulfonato]phenylphosphino)ethane (DPPETS), a new water soluble ligand that has been characterized and used in the synthesis of several new complexes with palladium, rhodium, platinum and nickel centers. T_1 relaxation times and the magnitude of the chemical shift anisotropy of several of the complexes have been determined with solid- and solution-state ^{31}P NMR and several complexes have been evaluated for their potential in biphasic hydrogenation and hydroformylation catalysis.

DEDICATION

This manuscript is dedicated to my husband, George S. Bunn, III, with love and gratitude for his patience, support and encouragement. He insisted that I make this effort even though it meant great sacrifice on his part. I want to thank my children, David, Jonathan and Gabrielle for their many expressions of confidence and the innumerable times they "pitched in" and helped me through the hard times. My family has made it possible for me to fulfill this dream.

I also wish to thank my mother, Eleanor K. Batt, and my friends Audrey Zaidi and Joyce Hoerner for listening to me ad infinitum.

ACKNOWLEDGEMENTS

I wish to thank my research director, Dr. Brian E. Hanson for his help, guidance, unfailing patience and never-ending good humor during my tenure at Virginia Tech. His willingness to let me go to the end of the line and then reel me back in made all this work very rewarding. I also want to thank the members of my committee, Dr. Joseph S. Merola, Dr. Larry T. Taylor, Dr. Raymond E. Dessy and Dr. G. Alan Schick for agreeing to serve on my committee and help me. I appreciate very much their confidence in me.

To the Drs. Tamas and Berit Bartik go thanks and gratitude for their willingness to share their knowledge. Their help was invaluable, and their friendship is a treasure.

Special thanks go to Bill Bebout and Tom Glass of Analytical Services for their help with the solid-state NMR.

I wish also to express my appreciation to the secretaries, Wanda, Angie, Linda, Melba, Vickie, and other staff members, particularly the glass shop, the electronics shop (Dave) and the physics machine shop; Jeannine Eddelton for her help with general chemistry, and faculty members who have been such good friends to me. The young people in our group have been a joy. Virginia Tech is fortunate to have this chemistry department. Each individual in this department has touched and enriched my life in some way.

Finally, I want to thank Dr. Thomas T.-S. Huang, chairman of the Department of Chemistry of East Tennessee State University, Johnson City, Tennessee for starting me on this course of education and for being such a good friend.

TABLE OF CONTENTS

LIST OF TABLES

LIST OF ILLUSTRATIONS

LIST OF ACRONYMS

This list of acronyms is given in order to insure brevity in this document.

TPPTS	tris(m-sodium sulfonatophenyl)phosphine
TPP	triphenylphosphine
DPPE	1,2-bis(diphenylphosphino)ethane
DPPETS	1,2-bis[di(m-sodiumsulfonatophenyl)phosphino]ethane
DPPETS-H	Acid form of DPPETS
TPPTS=O	TPPTS-oxide
TPP=O	TPP-oxide
BISBI	2,2'-bis(diphenylphosphinomethyl)-1,1'-biphenyl
DIOP	2,3-O-isopropylidene-2,3-dihydroxy-1,4-bis(diphenylphosphino)ethane
CyclobutaneDIOP	1,2-bis{(diphenylphosphino)methyl}cyclobutane
BDPP	2,4-bis(diphenylphosphino)pentane
Chiraphos	2,3-bis(diphenylphosphino)butane
Prophos	1,2-bis(diphnylphosphino)propane
Skewphos	BDPP
DPM	sodium diphenylphosphinobenzene-*m*-sulfonate
TPPMS	$PPh_2(m\text{-}C_6H_4SO_3Na)$ (Same as DPM)
SAPC	Supported Aqueous Phase Catalysis (Catalyst)
COD	1,5-cyclooctadiene
CP	Cross-Polarization
MAS	Magic-Angle Spinning

Chapter 1

Background and Objectives

1.1 Introduction to Catalysis

The feedstocks for many common compounds derived from petroleum products are oxygenated hydrocarbons such as aldehydes, ketones, alcohols and carboxylic acids. These in turn may be obtained by cracking petroleum which yields ethylene and other alkenes or from synthesis-gas-derived methanol. The conversion of alkenes to oxygenated compounds utilizes transition metals as catalysts. Hydroformylation (the Oxo process) has become the major industrial process by which alcohols and aldehydes are produced from olefins, carbon monoxide and hydrogen.[1] Hydrogenation is used extensively in the pharmaceutical industry.

Catalysts can be in either a homogeneous or heterogeneous environment. The catalyst can be in a homogeneous organic solution or on some type of support (usually polymeric) in the organic solution. The catalyst may also be in an aqueous phase with the reactants and products in an organic phase. In this case the reaction will take place at the interphase, or alternatively a phase transfer agent can be used. Finally, the catalyst may be supported in the aqueous phase with reactants and products in the organic phase. There are advantages to each system; for example, it has been shown that better selectivity and milder operating conditions are found in a homogeneous system, but a heterogeneous system allows better separation and recovery of the catalyst. The thrust of heterogeneous

systems, whether aqueous or organic, has been to recover the catalyst with minimal loss and deactivation. A catalog of some common biphasic catalytic reactions includes those shown in Figure 1.

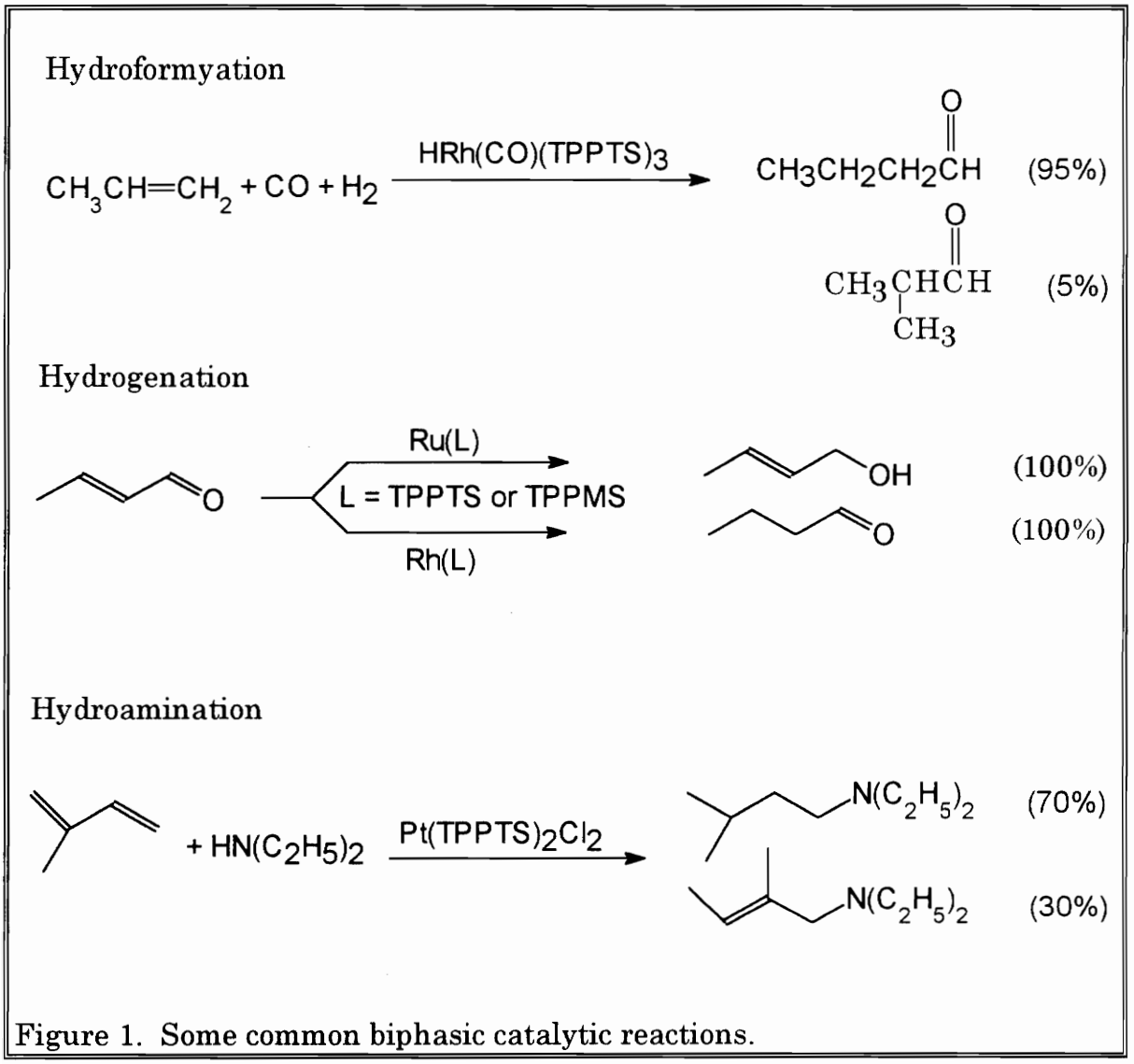

Figure 1. Some common biphasic catalytic reactions.

1.2. NMR Studies of Supported Aqueous Phase Catalysts

Supported aqueous phase catalysts (SAPC's) are water-soluble organometallic complexes supported in a thin film of water residing on a high-surface-area hydrophilic solid.[2] A schematic of an SAPC is depicted in Figure 2. The catalytic reaction is thought to take place at the organic-aqueous interphase, with the catalyst immobilized in the aqueous phase and the reactants and products in the organic (liquid) phase. A typical support is CPG-240, a controlled pore glass with a narrow pore volume distribution. The organometallic complex is made water-soluble by the addition of polar substituents on one of the ligands. For example, $HRh(CO)(TPP)_3$, a typical hydroformylation catalyst, is made water-soluble by the substitution of trisulfonated triphenylphosphine (TPPTS) for triphenylphosphine.

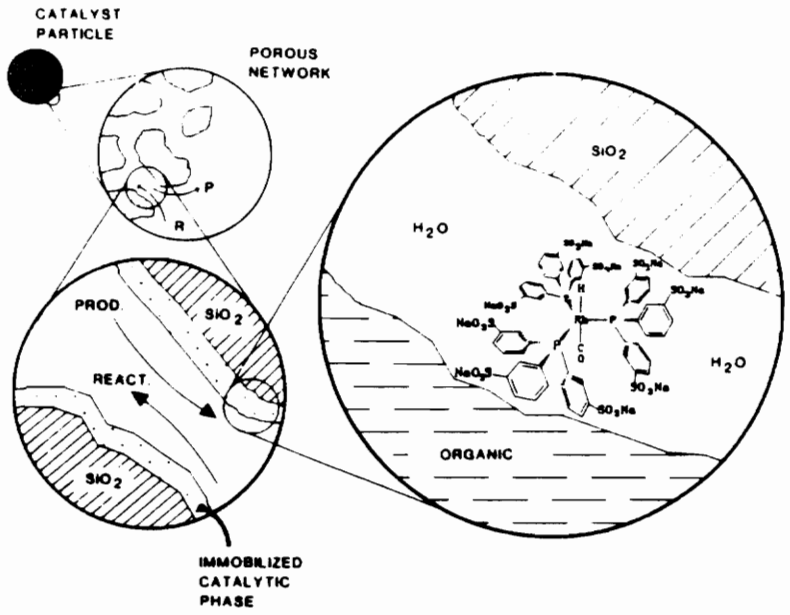

Figure 2. Schematic of a Supported Aqueous Phase Catalyst.[2]

The glass is impregnated with the water-soluble rhodium catalyst and excess TPPTS. When used for the hydroformylation of oleyl alcohol at 100°C, 5.1 MPa H_2/CO with 0.002 g Rh/g OLOH, conversions of about 97% were achieved in 5.5 hours with no significant leaching of the catalyst.[3,4]

The heterogenization of catalytic reactions by the use of two phases is still in its infancy, with the first water-soluble sulfonated phosphine (TPPMS) developed in 1958 by Chatt.[5] Kuntz[1], Dror and Manassen[6], and Wilkinson[7] were pioneers in the area of biphasic catalysis, with the initial studies reported in the mid 1970's.

With the development of magic angle spinning (MAS) and cross-polarization (CP) techniques, solid-state NMR has become a valuable source for information on local site symmetry in crystalline materials, and a bridge between solution-state NMR and x-ray crystallography.[8] NMR has in itself become one of the most powerful tools in chemistry for the elucidation of structures with the advent of Fourier transform methods, high-field super-conducting magnets and new pulse techniques.

Phosphorus-31 is an excellent nucleus for study by NMR methods because it has 100% abundance, a spin of 1/2 and a reasonably large magnetogyric ratio ($\gamma = 10.841 \times 10^{-7}$rad Tesla^{-1}). The relative receptivity of ^{31}P to the proton is 0.0665. When compared with the relative receptivity of ^{13}C, (0.0159) which also has a smaller magnetogyric ratio (6.7283×10^{-7}rad Tesla^{-1}), phosphorus is much easier to observe by NMR.[9] Another advantage of phosphorus (and all the other heavy nuclei) is the wider range of the chemical shift, from 200 to 500 ppm and higher. A large range means that signals will be spread out and inequivalent nuclei will be more easily

distinguished from one another, even when in a similar environment. Coupling constants also tend to be larger. Finally, there are usually fewer different environments for a phosphorus atom in transition metal complexes which also tends to simplify the spectrum.[10]

1.3 Sulfonation of Ligands

Several chelating water-soluble phosphines have been synthesized, including sulfonated BISBI[11], tetrasulfonated prophos[12], tetrasulfonated chiraphos[12], tetrasulfonated cyclobutanediop[12], tetrasulfonated BDPP[12], (2-sulfonatophenyl)bis-(diphenylphosphinoethyl)amide[13], and the maleic acid diphosphine[14] (Figure 3).

Many other phosphines have been rendered water-soluble through sulfonation or the addition of other functionalities. However, DPPE has not been successfully sulfonated and purified. It would be an advantage in both catalytic and coordination chemistry to have a simple water-soluble chelating phosphine that is easy to prepare and purify and is relatively inexpensive.

All the phosphines in Figure 3 are used as ligands in catalytic hydrogenation reactions except BISBI, which is used in hydroformylation reactions. While other functionalities are shown, sulfonation remains the functionalization of choice because it yields the phosphine which is soluble at most pH values. Another advantage is the fact that the sulfonated analog retains similar steric and electronic parameters relative to the parent phosphine.

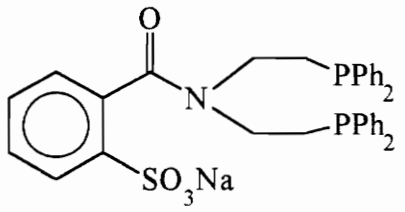

(2-Sulfonatophenyl)bis-(diphenylphosphino)amide

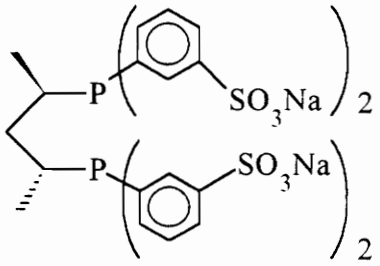

Tetrasulfonated BDPP

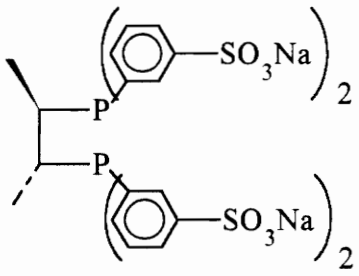

Tetrasulfonated Chiraphos

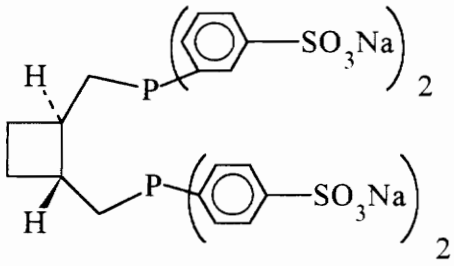

Tetrasulfonated CyclobutaneDIOP

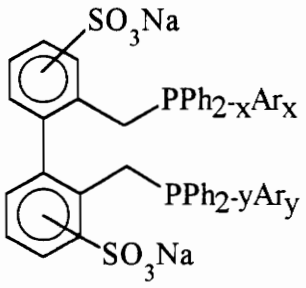

Sulfonated BISBI

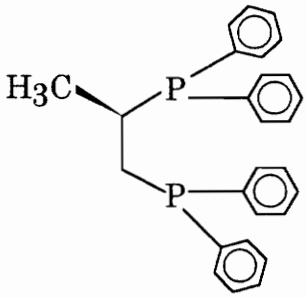

Prophos

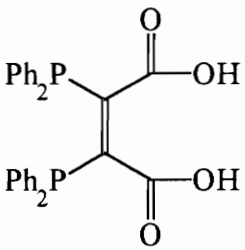

2,3-bis(diphenylphosphino)Maleic Acid

Figure 3. Some Water-Soluble Chelating Phosphines.

Sulfonated phosphines are usually prepared by direct sulfonation[1], which in all cases leads to some oxidized product; in the case of diphosphines, a mixture of mono-, di-, tri-, and tetra- sulfonated products are found along with the corresponding mixture of sulfonated oxides. Chromatographic methods have been the only reliable means of purification,[15,16] but many times the chelating ligands have been used as mixtures of sulfonated products. Interestingly, the sulfonated 1,4-diphosphine is the easiest to prepare, followed by the sulfonated 1,3- and 1,2-diphosphines. Sulfonated prophos (Figure 3) could only be prepared as the dioxide, and until this work
a 1,2-diphosphine that is unsubstituted, unoxidized and purely tetra-sulfonated has not been prepared.

There are many applications in coordination and catalytic chemistry for which it would be helpful to have a simple chelating water-soluble phosphine that is well-characterized. 1,2-bis(diphenylphosphino)ethane (DPPE) is the logical choice, because it is a prototypical chelating 1,2-diphosphine and the unsulfonated analog as starting material is relatively inexpensive compared to the others shown in Figure 3.

1.4. Statement of Objectives of Research

The objective of the solid-state NMR studies was to determine if there is a correlation between molecular motion and catalytic activity in the supported aqueous phase catalyst $HRh(CO)(TPPTS)_3$ and TPPTS on CPG-240 controlled pore glass. It has previously been shown by Arhancet[17] that there is a correlation between water-content and catalytic activity. This

study has shown that there is a relationship between the T_1 (spin-lattice) relaxation times and water content. Since T_1 is a function of molecular mobility, it may be concluded that there is a relationship between water content and molecular mobility. This study also qualitatively established that there is a point at which the supported phase takes on a "liquid-like" character, which can be determined by the magnitude of the spin-lattice relaxation time of the phosphorus atom in the ligand, and further, that it is at the onset of the liquid-like character of the supported phase that coincides with the point at which the maximum catalytic activity occurs.

The objective of the DPPETS synthesis was to attempt to find a reasonably facile synthesis and workup for a chelating diphosphine that would give it water-solubility so it can be used as a chelating ligand in biphasic and supported aqueous phase catalysis. 1,2-bis(diphenylphosphino)ethane was chosen for sulfonation because it is one of the simplest unsubstituted chelating phosphines and is relatively inexpensive. Water-soluble derivatives of platinum such as the complex $Pt(DPPETS)Cl_2$ may exhibit anti-tumor properties.

The objective of the catalytic work was to ascertain the ability of DPPETS to enhance or retard the catalytic ability of several transition metals. To date, there has been no easily accessible chelating water-soluble phosphine with which to study biphasic catalytic reactions.

Additional characterization of DPPETS and some derived complexes was also undertaken using sold-state ^{31}P NMR techniques.

Chapter 2
Literature Survey

2.1. Sulfonated Phosphines as Ligands in Organo-transition Metal Catalytic Systems

2.1.A Introduction

Historically water has been excluded from reactions involving organometallic reagents. Water destroys the Grignard reagent, and the Ziegler-Natta polymerization is also ruined by moisture. However, transition metal catalysis is an integral part of the chemical industry, providing many of the precursors for pharmaceuticals[18] which in turn are synthesized using transition metal catalysts. Oxygenated feedstocks such as aldehydes, alcohols, ketones and carboxylic acids utilized for the production of many common organic materials are produced using organo-transition metal catalysts.[19] Many biological processes also depend upon organometallic compounds.[19]

One of the major problems associated with transition metal catalysis is the recovery and recycling of the catalyst, often the most expensive and environmentally toxic component of the system. A number of methods have been developed to address the problem of leaching, and the immobilization of the catalyst in another phase such as water has recently received a lot of attention. With the catalyst in an aqueous phase it is easily and in principle completely recoverable from the reaction medium.

Among the methods that allow the catalyst to reside in another phase while remaining available to act as a catalyst is phase-transfer catalyis, in which the catalyst is allowed to move into and then out of the organic medium by a reagent that facilitates the transfer.[20]

The actual functionalization of the metal complex in order to keep it in the aqueous phase is most often accomplished by modification of the substituents on phosphine ligands. This discussion is limited to those catalysts containing phosphine ligands. There are several functionalities that can be used.

2.1.B. Non-Sulfonated Water-Soluble Phosphines and Complexes

Ellis *et al* .[21] reacted the phosphonium salt $[P(CH_2OH)_4]Cl$ with an amine base to produce tris(hydroxymethyl)phosphine, which is a crystalline solid at room temperature and is moderately air-stable. Platinum(II) and palladium(II) complexes of the type $MX_2\{P(CH_2OH)_3\}_2$ have been prepared which are soluble in water, although the pH of the aqueous solutions of the dichloro complexes are in the range of 3 - 4, indicating that coordination of the phosphine has increased the acidity of the hydroxyl protons, since the pH of typical aqueous solutions of the free phosphine is about 6.5. The hydroxyl groups are extensively involved in hydrogen bonding (Figure 4). No catalytic chemistry has been reported with these compounds, but they appear very stable at low oxidation states and high coordination numbers.

Other phosphine ligands containing hydroxy groups such as $HOCH_2CH_2PR_2$ and $Ph_2CH_2CH(OH)CH_2PPh_2$ have been reported.[22]

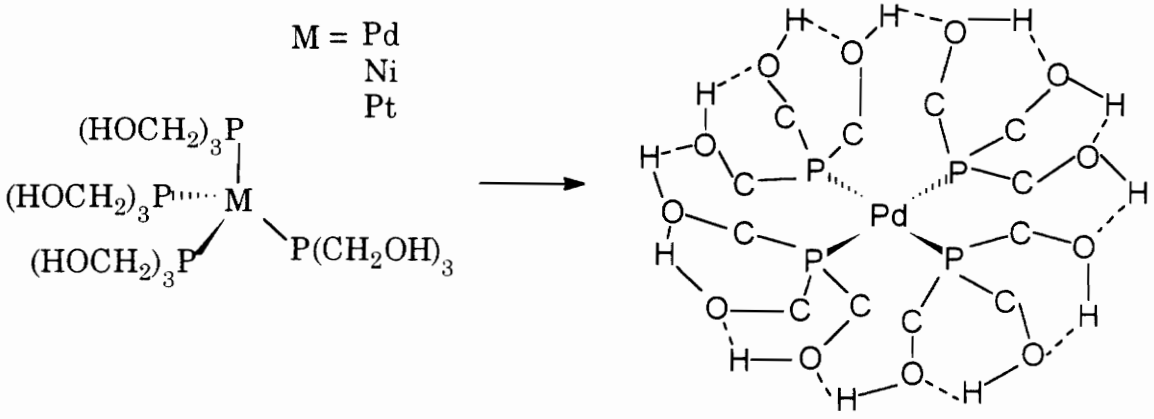

Figure 4. Tris(hydroxymethyl)phosphine complexes with Ni, Pd and Pt centers.[21]

Amrani and Sinou[23,24] used long chain ethers on the phosphine ligand to render the metal complex water-soluble. Catalytic hydrogenation with these complexes was affected by the ether chain length in one case, where rates and selectivity were both lower. One of the functionalized phosphines is the asymmetric diphosphine shown in Figure 5.

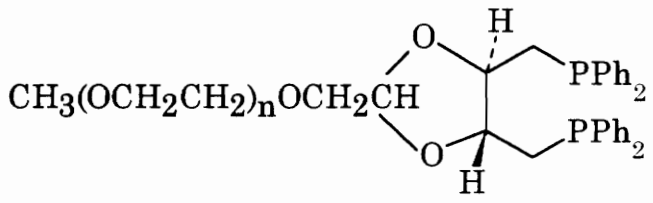

Figure 5. Ether functionalized diphosphine[23,24]

Amination has been used extensively, but requires an acidic medium unless it is in the quaternized form, and carboxylic acid functionality requires basic conditions for solubility.

A number of papers have reported the amination of phosphine ligands. Smith and Baird[25] discussed the preparation and some properties of the (2-diphenylphosphinoethyl)-methylammonium cation, $[Ph_2PCH_2CH_2NMe_3]^+$ iodide salt (AMPHOS), with carbonyl complexes of molybdenum, iron and tungsten. These complexes are reasonably soluble in 1:1 aqueous methanol or 3:1 aqueous acetonitrile.

Tyler[14] and co-workers reported the products of the reaction with water and oxygen of 2,3-bis(diphenylphosphino)maleic anhydride, which is readily soluble in aqueous solutions. The acidic ligand is soluble in solutions of pH 5 or greater. It behaves analogously to the DPPE ligand in non-aqueous solvents. Also reported are crystallographic and infrared data.

Baird, *et al.*[26] prepared and studied the catalysts derived from rhodium complexes of (2-diphenylphosphinoethyl)trimethylammonium nitrate. Also investigated[27] were rhodium complexes using this ligand in conjunction with hydride, olefin and carbon monoxide ligands. Both hydroformylation and hydrogenation were studied, and virtually complete recovery of the catalyst was possible for biphasic systems. Immobilization of a complex onto the sodium form of a strong acid, ion-exchange resin allowed hydroformylation and hydrogenation of water-immiscible olefins in an acetone solution with facile recovery of the catalyst by treatment of the resin with acid. The effects of catalyst site accessibility were also studied when these complexes were tethered to an ion-exchange resin.[28]

Acylation of bis[2-(diphenylphosphino)ethyl]amine gives a means to obtain diphosphine complexes of transition metals with a wide range of structures and solubilities. Whitesides *et al.*[29] outlined preparation and properties of various complexes.

Benhamza, Amrani and Sinou were successful in catalytic hydrogenation in water using rhodium complexes of an asymmetric water soluble diphosphine derived from 2-[(diphenylphosphino)methyl]-4-(diphenylphosphino)pyrrolidine.[30]

Nagel and Kinzel obtained 90% enantiomeric excess with hydrogenation of an aqueous solution of α-(acetylamino)cinnamic acid using [(3R,4R)-3,4-bis(diphenylphosphino)1,1-dimethylpyrrolidinium-P,P']($1,5$-cyclooctadiene)rhodium bis(tetrafluoroborate), shown in Figure 6.[31]

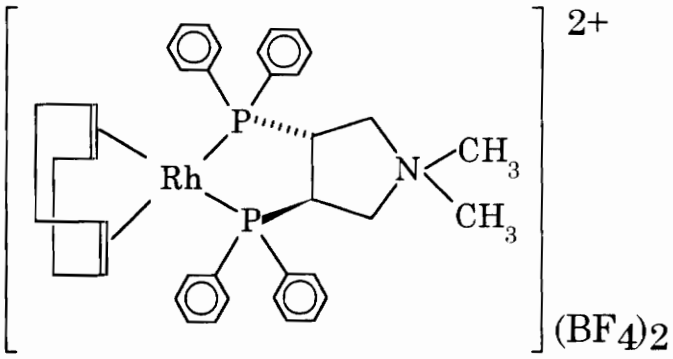

Figure 6. [(3R,4R)-3,4-bis(diphenylphosphino)1,1-dimethylpyrrolidinium-P,P'](1,5- cyclooctadiene)rhodium bis(tetrafluoroborate) [31]

Tóth and Hanson gave details on the tetra-amine functionalized derivatives of various diphosphines such as BDPP, Chiraphos and DIOP.[32] In a followup article,[33] the behavior of these ligands with rhodium-diene

catalysts under asymmetric hydrogenation conditions is discussed. The catalysts were easily recovered due to their extreme water-solubility, and the enantioselectivity was not affected by the amine groups.

Tóth, Hanson and Davis[34] also found that by immobilizing the rhodium complex $\{[CH_3CHP(p\text{-}C_6H_4NMe_2H)_2CH_2CHP(p\text{-}C_6H_4NMe_2H)_2CH_3]\text{-}RhNBD\}^{5+}$ in aqueous HBF_4 the activity for the catalytic hydrogenation of prochiral cinnamic acid derivatives is excellent at moderately high pressure and strongly acidic conditions.

Nuzzo, Feitler and Whitesides[13] developed coupling reactions which allowed the conversion of (bis(2-diphenylphosphinoethyl)amine to a number of water-soluble diphosphines. The catalytic activity of the rhodium complexes of some of these diphosphines for hydrogenation and other less well-known reactions is discussed.

Darensbourg and co-workers[35] used water-soluble 1,3,5-triaza-7-phosphaadamantane complexes of rhodium and ruthenium (Figure 7) for catalytic hydrogenation of aldehydes and olefins. The ruthenium complex is active for the conversion of α,β-unsaturated aldehydes to unsaturated alcohols, while the rhodium complex is very active for olefin hydrogenation. This ligand (PTA) is small, air-stable, non-ionic and water-soluble.

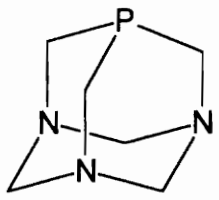

Figure 7. 1,3,5-triaza-7-phosphaadamantane.[35]

2.1.C Sulfonated Phosphines, Derived Catalysts and Catalytic Studies

The first sulfonated phosphine was prepared by Ahrland, Chatt, Davies and Williams[36] in 1958. By adding oleum (H_2SO_4/SO_3) to triphenylphosphine (TPP), the monosulfonated species $Ph_2P(m\text{-}C_6H_4SO_3Na)$, (TPPMS) was obtained upon neutralization. Kuntz[37] modified the reaction conditions to obtain the trisulfonated form, tris(m-sodium sulfonatophenyl)-phosphine, (TPPTS). Since that time, sulfonation has become the major procedure for functionalization of aryl phosphine ligand in order to give transition metal complexes water-solubility. Sulfonated phosphines are soluble at virtually any pH, and sulfonation has relatively little steric effects on the behavior of the phosphine compared to the unsulfonated analog. Small changes in electronic effects such as infrared stretching frequencies are attributed to the electron-withdrawing sulfonato group.

Kalck and Monteil[22] have written a comprehensive review on the use of water-soluble ligands in homogeneous catalysis. While other water-solubilizing functionalities are mentioned, the bulk of the discussion concerns sulfonation. Preparation of the ligands and the complexes is reviewed, along with their use as hydroformylation, hydrogenation and other catalytic reactions. The review is well-organized and complete.

Barton and Atwood[38] have also reviewed water-soluble organometallic complexes. Hydroformylation, hydrogenation and water-gas shift reactions are discussed, including photo-induced reactions.

The synthesis and purification of TPPTS has occupied a great deal of the literature on sulfonated phosphines. Gel-permeation chromatography[39]

has been reliably used to purify aqueous solutions of TPPTS. Herrmann and co-workers [40,41] also used the gel permeation method to purify complexes of Mn, Fe, Ru, Co, Rh, Ir, Ni, Pd, Ag, and Au. It is also claimed that these complexes are the first examples of homoleptic TPPTS metal complexes. That is, $M(TPPTS)_3$, with each containing one water molecule per sodium ion. It is also noted that the Au and Ag complexes are of the type $Au(TPPTS)_2(TPPTS^*)$ [TPPTS* = $P(C_6H_4\text{-}m\text{-}SO_3^-Na^+)_2P(C_6H_4\text{-}m\text{-}SO_3^-)$]. These TPPTS complexes have lower coordination numbers (TPPTS/metal ratios) than those of the unsulfonated analog TPP.

Aquino and Macartney[42] studied the kinetics of ligand substitution reactions of dirhodium(II) tetraacetate with water-soluble charged phosphines of the type PR_3^{n+}, where n+ can be a varied charge such as found in $Ph_2P(m\text{-}PhSO_3)^-$ and $Ph_2PCH_2CH_2NH(CH_3)_2^+$. The mechanism is discussed as well as the dissociation constants of the protonated phosphine ligands. Darensbourg[43] investigated the kinetics of dissociative phosphine substitution processes with water soluble group 6 metal carbonyl derivatives containing TPPTS in water and water/THF mixtures. It was found for analogous processes that TPPTS-containing complexes behaved similarly to TPP-containing complexes.

A trisubstiuted red-violet cluster of the form $Ru_3(CO)_9[P(C_6H_4\text{-}m\text{-}SO_3^-Na^+(H_2O))_3]_3$ was obtained by Fontal, *et al.*[44] by three different routes. The yellow disubstituted osmium derivative $Os_3(CO)_{10}$ $[P(C_6H_4\text{-}m\text{-}SO_3^-Na^+(H_2O))_3]_2$, and the trisubstituted yellow $Ir_4(CO)_9[P(C_6H_4\text{-}m\text{-}SO_3^-Na^+(H_2O))_3]_3$ were also obtained and characterized. These complexes have potential as catalysts and the ruthenium cluster has been shown to be an

intermediate for the preparation of tetrameric water-soluble ruthenium hydrides as $H_4Ru_4CO_4$.

Chain length is a factor in the catalytic activity of phosphine complexes [NBDRhCl(n-phosphos)]X, where NBD = norbornadiene, and phosphos = $[Ph_2P(CH_2)_nPMe_3]X$ (n = 2,3,6,10; X = NO_3^-, Cl^-, PF_6^-). It was found [45] that while all the catalysts were active, the longest chain length gave the greatest activity. for hydrogenation of olefins in a biphasic system.

Roundhill and co-workers[46] synthesized and characterized tertiary water soluble phosphines having terminally substituted alkylene sulfonate or alkylene phosphonate chains. Sodium 2-(diphenylphosphino)-ethanesulfonate, $Ph_2PCH_2CH_2SO_3Na$, and disodium 2-(diphenylphosphino)-ethanephosphonate, $Ph_2PCH_2CH_2P(O)(ONa)_2$ are described.

Hanson and co-workers[47] described a new and more efficient process for the synthesis and purification of TPPTS. Monitoring the reaction by ^1H NMR spectroscopy to determine the extent of sulfonation and concurrent oxidation gives greater control over products. A facile method of purification is outlined, and data are reported for ^1H, ^{13}C and ^{31}P NMR parameters.

Hanson *et al.*[48] synthesized a series of water soluble tris(ω-phenylalkyl) phosphines of the type $P[(CH_2)_x(C_6H_5)_3$, x = 1,2,3 and 6. The para- and ortho- positions are sulfonated, and the para isomer is easily isolated. Interestingly, for x = 2, 3 and 6, the corresponding oxide is not formed during reaction. For phosphines with $x \geq 2$, stable phosphonium salts are formed, which could account for the lack of oxide formation. Derived steric and electronic parameters for the phosphines were determined from the palladium and nickel complexes, respectively.

The diphosphine 2,2'-bis(diphenylphosphinomethyl)-1,1'-biphenyl (BISBI) was sulfonated using 60% oleum and recovered as a mixture of sulfonated products[11]. In the biphasic hydroformylation of propene, BISBI yields quite high n/iso ratios (ca. 95% normal) with rhodium catalysis. Dependence upon concentration, temperature and pressure were studied.

Darensbourg, Bischoff and Reibenspeis[49] reported the synthesis, characterization and x-ray structure of [Na-kryptofix-221]$_3$[W(CO)$_5$P{C$_6$H$_4$-*m*-SO$_3$}$_3$].

Dror and Manassen[6] used the method of biphasic catalysis in 1977 with rhodium-TPPMS complexes to hydrogenate cyclohexene. This was one of the first reports on biphasic catalysis.

Wilkinson, *et al.*[7] provided an early example of biphasic hydrogenation and hydroformylation catalysis with ruthenium, rhodium, palladium and platinum complexes with TPPMS as the water-soluble phosphine.

Joó, Tóth and Beck[50] were also among the early investigators of biphasic catalysis. They explored the hydrogenation of carbonyl and olefin functionalities with ruthenium complexes made water-soluble with TPPMS at various pH values.

Tóth and Joó[51] discussed the role of pH in terms of selectivity, and speculated upon future work in the area of biphasic catalysis. Studies on the reaction mechanism of hydrogenation were begun for reactions catalyzed by ruthenium-sulfonated triphenylphosphine complexes.

Sinou *et al.*[52] sulfonated a series of chiral ligands for use in asymmetric hydrogenation. They found that while 1,4-diphosphines are relatively easy to sulfonate, 1,3-diphosphines are harder, and were

unsuccessful at sulfonating 1,2-unsubstituted diphosphines. It was found that rhodium(I) catalysts formed with sulfonated diphosphines are efficient catalysts for asymmetric hydrogenation.

Quinn and Taylor[53] were able to selectively hydrogenate and hydroformlyate 9-decene-1-ol and 10-undecen-1-ol using water-soluble $HRh(CO)(TPPMS)_3$ in phospholipid bilayers. The substrate is packed into the phospholipid bilayer in a close-packed hexagonal fashion to give a structure characteristic of a gel. The reaction presumably takes place on the surface of the bilayer. It is postulated that the bilayer orients the substrate and the catalyst anchors to the surface through the sulfonate groups. Both catalyst and substrate partition from water and associate with the bilayer at rates considerably faster than in simple homogeneous catalysis.

Isoprenylation of β-dicarbonyl compounds was reported by Mignani, *et al.*[54] Rhodium/TPPTS selectively catalyzed the condensation of isoprene with active methylene compounds (Figure 8).

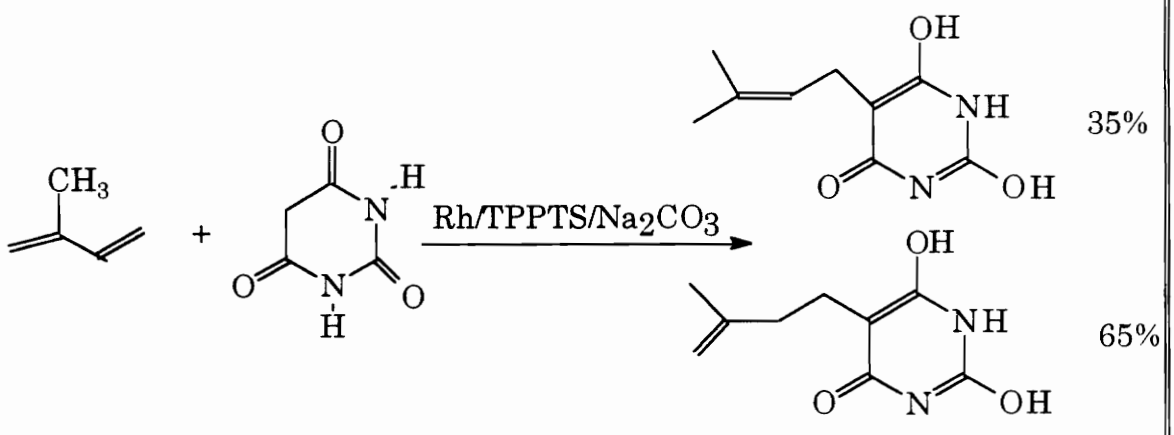

Figure 8. Isoprenylation of barbituric acid. [54]

Jensen and Trogler [55] reported the catalytic hydrogenation of terminal alkenes to primary alcohols using *trans*-$PtHCl(PMe_3)$ with a phase transfer catalyst in base under mild conditions. However, Marsella *et al*[56] were unable to repeat the experiment.

Casalnuovo and Calabrese[57] efficiently alkylated and cross-coupled biomolecules and organic substrates to yield compounds such as 5-propargyltrifluoroacetamido)-2'-deoxyuridine using the water-soluble palladium(0) complex $Pd(TPPMS)_3$ as catalyst. Crystallographic data for the complex is reported. Syntheses of the complex and all the substrates are reported. Reactions were either in a single basic aqueous phase or basic aqueous-organic medium, and were complete within several hours under mild conditions.

Benzyl chloride was carbonylated by the water-soluble complex $PdCl_2(TPPMS)_2$ in an aqueous NaOH/organic system, where the organic medium was n-heptane, benzene or anisole.[58] Yields of 89% - 93% of phenylacetic acid were obtained.

Bahrmann, and Bach[59] reviewed the use of water-soluble phosphines as ligands for hydroformylation catalysts. Advantages to the biphasic method were discussed.

Escaffre, Thorez and Kalck[60] examined hydroformylation of alkenes using water as both solvent and hydrogen source. Low temperatures and pressures gave high rates and complete selectivity with ratios of 18:1 and 23:1 n/b for 1-hexene using $Rh_2(\mu\text{-}SBu^t)_2(TPPTS)_2$ and 1:1 $CO:H_2$.

Water-soluble ruthenium-phosphine complexes have been found to be selective to the aldehyde functionality in α,β-unsaturated aldehydes under

hydrogenation conditions. On the other hand , rhodium appears to be completely selective to the double bond in the same species.[61,62]

Sinou *et al.*[63] reduced the double bond in α,β-unsaturated carboxylic acids in water or a two-phase system using formate as the hydrogen donor with rhodium complexes prepared *in situ* from $[Rh(COD)Cl]_2$. They found enantioselectivities up to 43 % using tetrasulfonated cyclobutanediop as ligand. (Figure 9).

Asymmetric hydrogenation of enamides in a biphasic system using rhodium complexes and chiral sulfonated diphosphines yielded enantiomeric excesses up to 88%.[64]

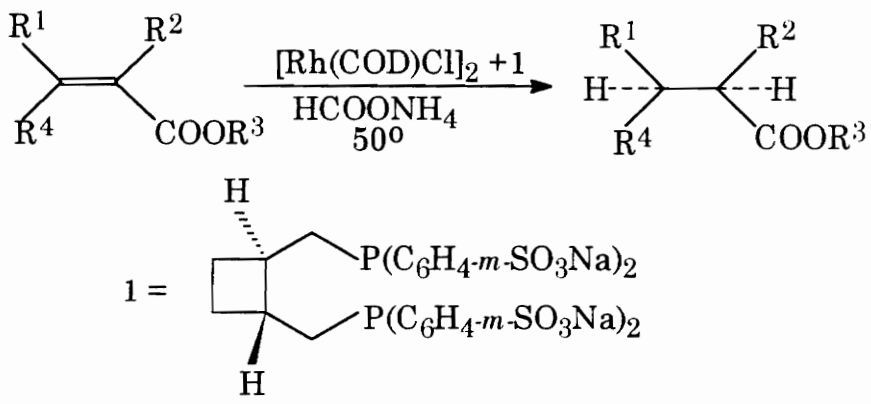

Figure 9. Hydrogenation of α,β-unsaturated carboxylic acids.[63,64]

Joó and Beck[65] found that unsaturated aldehydes can be reduced to unsaturated alcohols under mild conditions using ruthenium(II) species and formate as the hydrogen donor. Selectivity was between 78% and 98%.

The kinetics of the hydrogenation of unsaturated compounds with rhodium and ruthenium were studied by Joó and Beck.[66,67] A highly polar solvent such as water complicates the pathway because of its ability to act as a proton acceptor. It is also believed that catalytically inactive substrate-complex species can form.

The presence of alkaline, alkaline earth and ammonium salts such as NaI, etc., increases the activity of water-soluble ruthenium(II) complexes such as $RuH(TPPTS)_3$ without any loss of selectivity for the hydrogenation of aldehydes such as propionaldehyde. It is postulated that there are two different mechanisms for hydrogenation with and without salt. Fache, *et al.*[68,69] have investigated this phenomenon with a number of ruthenium complexes.

Bartik, Bartik and Hanson[70] investigated the hydroformylation of 1-octene with Rh complexes associated with trisulfonated tris(ω-phenyl)-alkylphosphines and compared with TPPTS as ligand under similar conditions. The phosphines, of the general type $P[(CH_2)_xC_6H_4\text{-}p\text{-}SO_3Na]_3$, where x = 1, 2, 3, or 6, are electron donating. It was found that when low L/Rh ratios are used for conversion, donating phosphines are more active,while at high L/Rh ratios, catalytic activity declines.

The catalytic hydrogenation of the double bonds of the fatty acid core of membrane lipids can be used as a probe for studying the role in membrane-bound physiological processes.[71] Water-soluble $RuCl_2(TPPMS)_2$ is a highly active catalyst for short-chain fatty acids, and can also be used for hydrogenation of the unsaturated fatty acid component of liposomes and biomembranes. The catalyst appears to be an effective tool for changing the

fatty acid content, hence the microviscosity of lipids, in particular for plant cell membranes.

Larpent, Dabard and Patin[72] found that a redox reaction between water and a highly active rhodium(III) species takes place when rhodium trichloride is dissolved in water, and is responsible for the oxidation of the water-soluble phosphine being used. (Figure 10). Preliminary studies with $RuCl_3$ indicate the same process occurring under similar conditions.

In a follow-up paper, Patin *et al.*[73] outlined a sequence of reactions for this process.

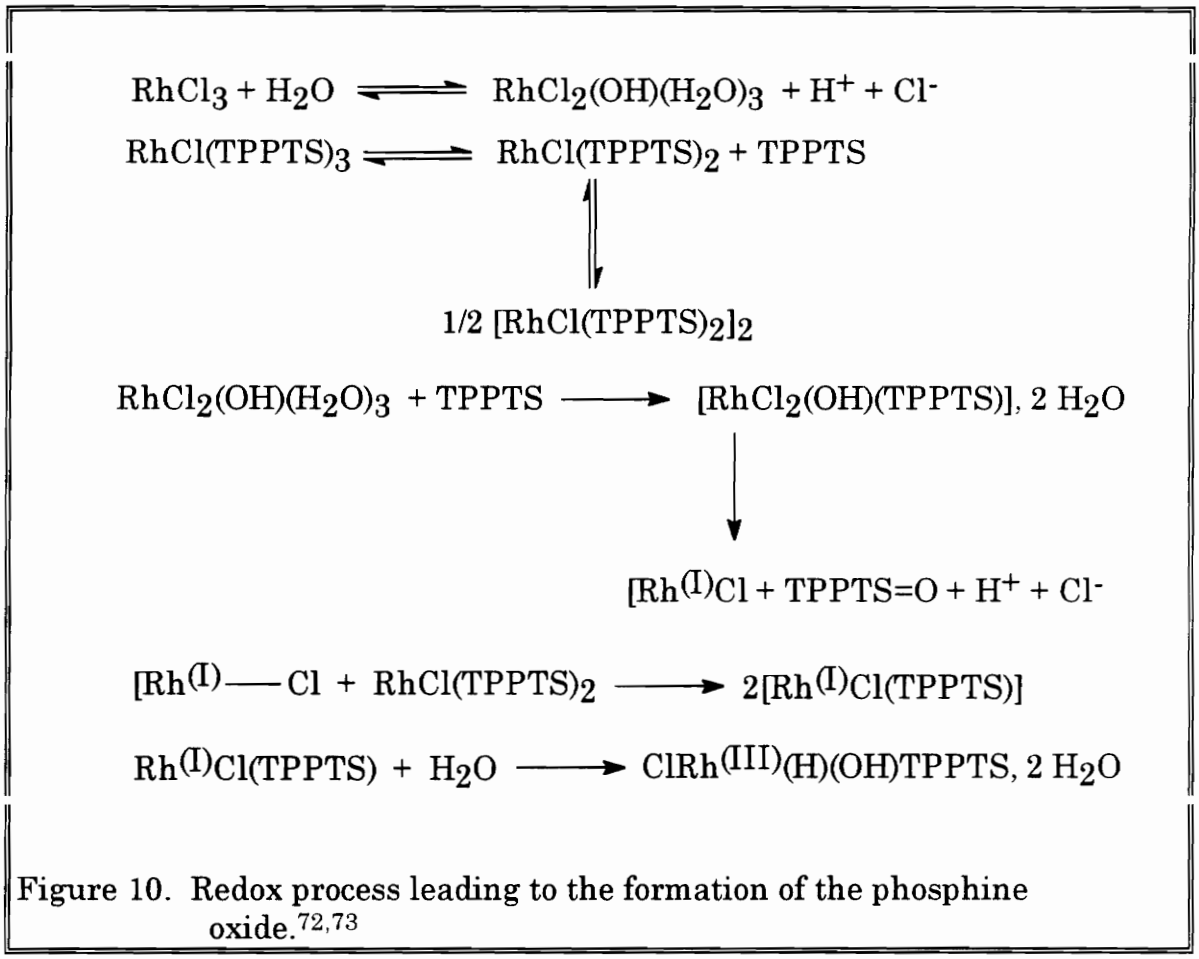

Figure 10. Redox process leading to the formation of the phosphine oxide.[72,73]

Willner and Maidan[74] reported that with the use of water-soluble rhodium TPPMS complexes visible light photo-induced hydrogenation of ethylene and acetylene takes place, and hydroformylation of ethylene occurs. They theorize a possible route that utilizes the photo-generated hydridorhodium species in the evolution of H_2, as well as hydrogenation and hydroformylation processes.

High pressure NMR studies of the water-soluble rhodium hydroformylation sytem were accomplished by Horváth, *et al.*[75] It was found that when $HRh(CO)(PPh_3)_3$ is under 30 atm of CO/H_2 (1/1) the organic-soluble $HRh(CO)(PPh_3)_2$ is the only species detectable, yet under 200 atm the water-soluble complex $HRh(CO)(TPPTS)_3$ does not show the formation of a new species. Detailed mechanistic studies show that for the $HRh(CO)(PR_3)_3/PR_3$ hydroformylation system that there are two key catalytic species, both coordinatively unsaturated, $HRh(CO)(PR_3)_2$ and $HRh(CO)(PR_3)$ (Figure 11). It is also believed that the n/b ratio of aldehyde production is controlled by competitive reactions of the olefins with these species resulting in high or low n/b ratios, respectively. Since a similar species to the monophosphine intermediate in the water-soluble analogue could not be detected even at extremely high pressures, this provides an explanation for the observed high n/b ratios for aldehydes even at low P/Rh ratios (Figure 11).

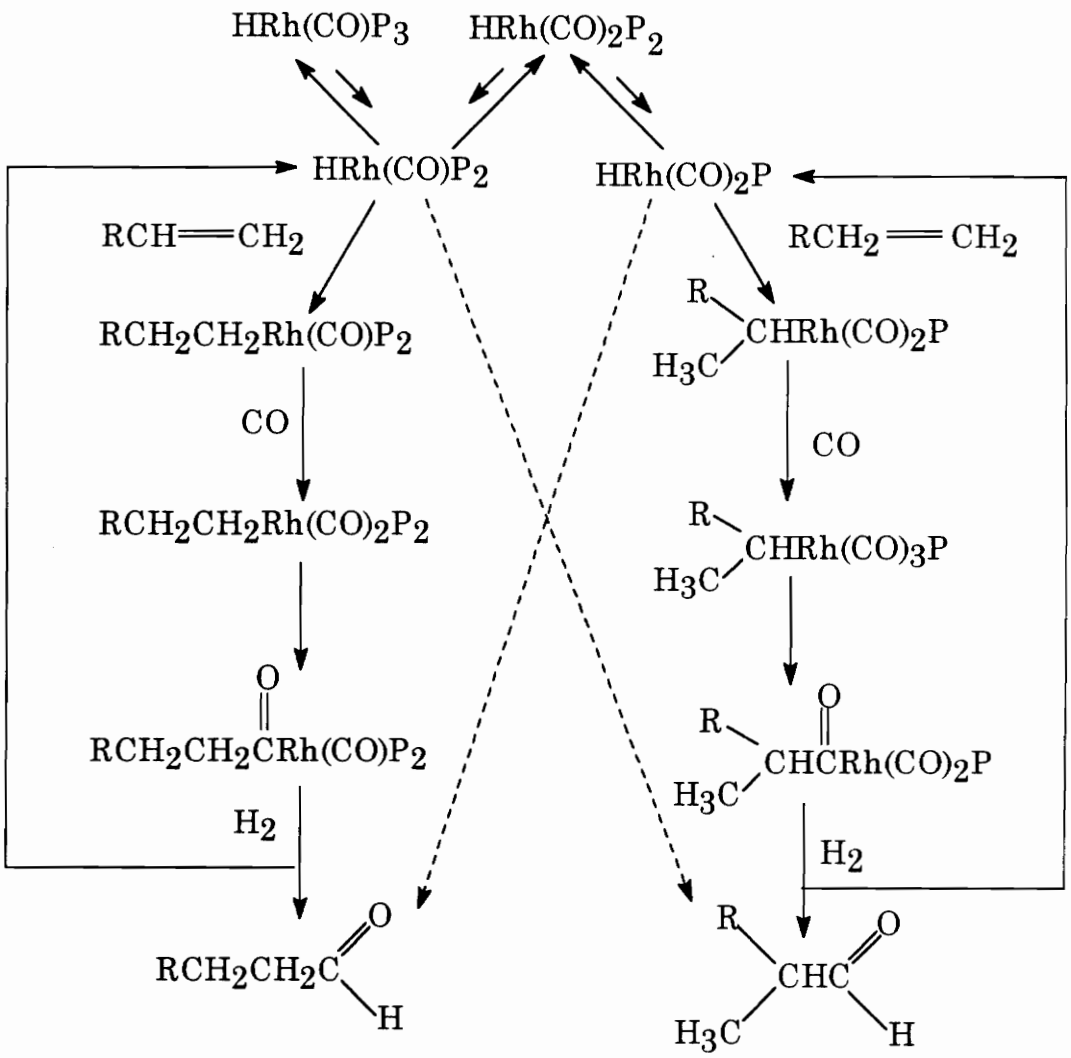

Figure 11. Scheme depicting the formation of normal and branched aldehydes and the role of the coordinatively unsaturated catalytic intermediates.[75]

2.2 Supported Aqueous Phase Catalysis

The driving force behind biphasic catalysis is the ability to recover and recycle the catalyst. By immobilizing the catalyst, the ability to recover it is greatly enhanced, but there are problems associated with this technique. In solution an equilibrium can occur between the supported metal complex and the complex in solution, with resultant leaching of the catalyst into solution. An additional problem arises because the nature of the supported complex and the environment in which it resides is neither completely understood nor completely controllable.[76]

There are a number of methods for the immobilization of a complex onto a support.[77] For example, Joò and Beck[78] immobilized water-soluble complexes of triphenylphosphine with rhodium(I) and ruthenium(II) on strongly basic anionic exchangers. The hydrogenation of various olefins in the gas phase at moderate conditions was accomplished. It was postulated that the same molecular pathway existed whether the catalyzing complex was supported or not.

Arhancet, Davis, Merola and Hanson developed a new class of heterogeneous catalysts called Supported Aqueous Phase Catalysts (SAPC), which have the ability to enhance the interaction of the catalytic species with the substrate at the interface of the aqueous-organic phases.[17,79]
A schematic of the supported aqueous phase catalyst is shown in Figure 2, page 3. The support is CPG-240, a controlled pore glass with a pore volume of 0.95 mL/g, a mean pore diameter of 237Å with a pore volume deviation of ± 4.3% from the mean, and a surface area of 77.5 m^2/g. This is considered a very homogeneous support.

A distinct advantage is the ability to use reactants in the liquid phase, whereas supported liquid phase catalysis, in which the complex is immobilized on a polymeric support and all species are soluble in the organic phase, requires that the reactant and products be in the gas phase.[80]

Arhancet, *et al.*[2] described the system and gave results of the hydroformylation of oleyl alcohol. Methods of preparation for impregnation of the complex onto the CPG-240 support are outlined, initial activity and stability studies are discussed.[3]

Horváth[81] questioned whether SAPC is really aqueous, or merely a precipitated complex phase that organic reagents can flow past, since the solubility of the olefin in the aqueous phase is no longer a limiting factor. However, it has been shown definitively that the rate of conversion of substrate to product is dependent upon the total weight percent water of the system.[82] Horváth postulated that the mode of immobilization is by hydrogen bonding of the sodium sulfonate groups to the surface of the glass.

Hydroformylation of linear, terminal and internal olefins by SAPC is presented.[4] Due to the availabilty of isomers, heptenes were selected; 1-tetradecene, 1-heptadecene and *t*-7-tetradecene were also hydroformylated. The results as to n/b ratios, % conversion (total and total aldehydes) and the influence of pressure, temperature and P/Rh ratio are discussed. It was found that the activity of SAP catalysts is approximately the same for internal olefins as it is for terminal olefins, but isomerization of the internal olefins is much greater than for terminal olefins, with the *cis* isomers more prone to isomerization than the *trans* species. For the higher alkenes, it was found that the n/b ratio does not show significant change with chain length.

The increase of pressure increases the rate of reaction, particularly between 100 and 300 psig. Catalytic activity is strongly dependent upon total water content. At low pressures and high temperatures, n/b ratios are increased as is isomerization activity. It was also found that SAP catalysts do not respond in the same fashion as homogeneous catalysts do with an increase in P/Rh ratio.

Renaud and Baird[82] used ^{31}P spin-lattice relaxation times to assess the relative molecular mobilities for amphiphilic tertiary phosphines of the type $[Ph_2P(CH_2)_nPMe_3]^+$ (n = 2, 3, 6 and 10), with the phosphines in D_2O and tethered to cation exchange resin. It was found that immersion of the resin-sorbed ligands in D_2O shortened the correlation time for the molecules which allowed well-resolved $^{31}P\{^1H\}$ NMR spectra of the solid materials.

2.3 Solid-State ^{31}P Nuclear Magnetic Resonance Spectroscopy

A great deal of literature has been published on solution state ^{31}P NMR spectroscopy, and as more sensitive and powerful instruments are developed, solid-state ^{31}P NMR spectroscopy is becoming an important chemical tool for structure analysis; it also provides a link between solution state NMR and X-ray diffraction. Here follows a survey of some methods and results obtained.

Recently several review articles on the status of solid-state NMR spectroscopy applied specifically to inorganic chemistry have been published.[83,84,85] The application of high resolution solid-state NMR (SS NMR) spectroscopy to the study of the coordination chemistry of tertiary phosphines with transition metals is discussed by Davies and Dutremez[85] with emphasis on metals in groups 8-11. In his study Yamasaki[84] includes many spin 1/2 nuclei, covers briefly the analysis of paramagnetic solids, quadrupolar nuclei and touches on variable temperature measurements. An exhaustive review by Davies and Dutremez[83] covers SS NMR spectroscopy of the d-block and p-block metal nuclei.

An early (1980) article by Suwelack, Rothwell and Waugh[86] described an approach for detecting and analyzing slow molecular motions in solids which is closely related to the study of rates of site exchange in liquids. Site exchange in solids is more complicated due to the anisotropy factor, but the changes in line shape associated with the spin jump gives an accompanying frequency jump and this distorts the powder pattern. Rothwell and Waugh also studied the spin-spin relaxation of dipolar coupled spin systems to detect motions in solids.[87] Neither of these methods was specific to phosphorus, but

could be adapted. Duncan[88] compiled an extensive list of ^{13}C shielding anisotropies organized by carbon functionality, another project that could be accomplished for phosphorus.

Tolman[89] has discussed steric and electronic parameters of phosphorus ligands with mention of chemical shifts in the solution state, and Bartik and Himmler[90] looked specifically at ^{31}P NMR spectra of palladium complexes to determine a correlation between chemical shift in solution and steric parameters. In another article, Bartik, *et al.*[91] determined deviations from the additivity rule of Tolman which were related to the donor/acceptor character of the atoms in the α position relative to phosphorus. They found a correlation between solution-state ^{31}P NMR chemical shifts in terms of steric parameters.

Herzfeld and Berger[92] developed a procedure for using spinning sideband intensities to extract the principal values of the chemical shift tensors. Interestingly, if the chemical shift tensor principal values are known, the intensities of the spinning sidebands can be calculated. The method also allows the contributions of various functional groups to the spectrum to be determined. This method is especially useful for systems that have so many signals the isotropic chemical shifts are difficult to distinguish.

Solid-state ^{31}P NMR spectroscopy has also shown its usefulness in biochemistry for the determination of variations in backbone configurations of DNA with respect to the phosphodiester moiety.[93]

Soderquist *et al.*[94] measured the principal values of the chemical shift tensors for several aromatic compounds using ^{13}C SS NMR spectroscopy. The orientation of the chemical shift tensor on the molecule can be related to

theoretical electron distributions using standard quantum mechanical methods. Again, ^{31}P SS NMR spectroscopy could be used for this purpose.

The first literature for solid-state studies of phosphines appeared in 1980.[95] It was confirmed that Wilkinson's catalysts, $RhCl(PPh_3)_3$ has a square planar configuration that is slightly distorted toward tetrahedral geometry. However, another study found the determination of ^{31}P chemical shielding tensors in single crystals of the same complex, chlorotris(triphenylphosphine)rhodium(I) which showed a large chemical shift anisotropy and an approximately square planar geometry.[96]

Much information about molecular motion in polycrystalline solids is contained in Spin-Lattice relaxation times (T_1). Torchia and Szabo[97] devised a method for eliciting this information by developing equations for the frequency of a spectral line as a function of the angles that describe the orientation of a the external magnetic field and the orientation of the coupling tensor principal axis in a crystal-fixed system for both static and spinning samples. The correlation functions contained in the expressions for T_1 can be evaluated by assuming axially symmetric coupling for an N-site jump model. A related article describes in detail the study of molecular motion of ethylene adsorbed on a silver surface;[98] this method would lend itself very nicely to a ^{31}P NMR spectral study.

The magnitude of coupling constants between ^{31}P nuclei and metal centers such as ^{195}Pt have proven to be a convienient parameter for determining the geometry of the complexes. For example, in square planar platinum(II) bis(phosphine) complexes, cis geometry gave $^1J_{iso}$ (^{31}P, ^{195}Pt) values around 3500 Hz, whereas the trans geometry yielded values on the

order of 2500 Hz.[99] This relationship has been known for a number of years through solution state NMR[100] and is based upon the amount of electron density contained on the phosphorus atoms. The argument states that the *cis* compound has higher electron density in a square planar complex such as platinum(II), a result of increased π bonding by the use of the platinum d_{xz} and d_{yz} orbitals in addition to the in-plane bonding by the d_{xy} orbitals. The *trans* complex has only the d_{xz} orbital available in addition to in-plane d_{xy}. (The x-axis is defined as the P-Pt-P axis.) The *cis* arrangement allows for increased back donation from the platinum orbitals.

Rahn, Baltusis and Nelson[101] used CP-MAS ^{13}C, ^{31}P NMR and solution state NMR spectroscopy for a number of $(R_3P)_2PtX_2$ complexes to compare structures in the solid state with those in solution. They found that most of the complexes studied have regular square planar structures in solution, but are distorted towards a tetrahedral arrangement in the solid state as a result of steric bulk. Interestingly, the $^{31}P\{^1H\}$ spectra in solution and solid state for *cis*-$(Me_3P)_2PtCl_2$ are very similar, but the ^{13}C NMR spectra are very different for solution and solid states. The crystal structure shows that there are four molecules in the unit cell, and no methyl group is symmetry equivalent to another. The solid state NMR spectrum shows agreement with the crystal structure.

Other metal complexes have been studied by ^{31}P solid state NMR spectroscopy. Lindner, *et al.*[102] studied cyclic and acyclic phosphine-metal complexes using as metal centers ^{55}Mn, $^{95/97}Mo$, and ^{183}W. The chemical shift tensors were extracted and correlated to structural features of the compounds. The ring effect is discussed; in five-membered metallacycles the

phosphorus signal is shifted 20-50 ppm to lower field, while in six-membered rings the signal is found 2-17 ppm at higher fields.

Cu-P quadrupole effects were studied with ^{31}P solid state NMR spectroscopy [103] using two-coordinate (tris[2,4,6-trimethoxyphenyl]-phosphine)copper(I) chloride and bromide compounds. The highly basic, very bulky ligand was chosen to form metal complexes with low coordination numbers. The quadrupole coupling constants were estimated from the NMR data. The fluoro compound was also characterized in the same manner.[104] Tertiary phosphine complexes of gold(I) halides, which have anti-arthritic properties and are also used as anti-tumor drugs have been studied extensively by solution and solid state NMR spectroscopy. Attar *et al* [105] reported on phosphole complexes of gold(I) halides and compare solution and solid state spectra as well as crystal structures.

Solvation effects on tertiary phosphine derivatives and metal complexes were studied using ^{31}P solid state NMR spectroscopy. The chelating diphosphine oxide bis(diphenylphosphino)methane dioxide, and several platinum complexes showed that CP-MAS NMR spectra are sensitive to solvation effects in crystalline compounds.[106]

Rhodium complexes of the type $(R_3P)_2Rh(CO)Cl$ are used as catalysts in hydroformylation of alkenes, and it has been shown that the nature of the phosphine heavily influences the normal to branched ratio of aldehyde products.[107] They are also good catalysts for C-H bond activation under photolytic conditions.[108] Solution and solid state NMR characterization of *trans* rhodium complexes with PR_3 as a phosphole such as 1-phenyl-3,4-dimethylphosphole as well as triphenylphosphine were also characterized at

the same time by Wu and Wasylishen.[109] It was found that these complexes show hindered rotation about the Rh-P bond in solution with increasing steric bulk, and in the solid state crystallize with considerable tetrahedral distortion.

Phosphorus sulfides have several interesting uses, as constituents of non-oxide chalcogenide glasses which have infrared transmitting properties, and in low-equivalent weight batteries as solid electrolytes. Correlations between solid state NMR spectral characteristics and x-ray crystal structures were possible for these stoichiometric compounds; it was shown that NMR spectroscopy can yield valuable information on local phosphorus environments. Chemical shift tensors contain anisotropic chemical shift information which is lost in solution or liquid state. Distortions from axial symmetry are revealed by spinning side band patterns.[110]

In the areas of immobilized homogeneous catalysis, chromatography and surface chemistry, phosphine-modified polysiloxane frameworks have been developed. Both ^{31}P and ^{29}Si solid-state CP-MAS NMR spectroscopy have proven to be valuable probes of these systems due to the insolubility of the frameworks.[111]

Solid state ^{31}P NMR spectroscopy of phosphines has been used to determine the number of crystallographically nonequivalent molecules in the unit cell. Penner and Wasylishen[112] studied the variation of the chemical shift tensor components with molecular structure for thirteen different phosphines and found that the number of crystallographically nonequivalent phosphorus atoms in a solid phosphine is reflected by the number of resonances perceived in the ^{31}P CP-MAS spectrum. The data proved

consistent with the x-ray structures. Davies, Dutremez and Pinkerton[113] used the same method and reached the same conclusions about other phosphines and phosphine derivatives.

Spin-lattice relaxation (T_1) measurements yield accurate information about the mobility of a nucleus. There are a number of methods for measuring T_1 values, the most common of which is the inversion-recovery method. Several modifications of this method were reviewed by Frye,[114] and he concluded that the most accurate method is the Freeman-Hill modification which is especially helpful for systems which obey complicated relaxation rate laws.

^{31}P spin-lattice relaxation measurements were used by Baird *et al.*[82] to appraise the relative molecular mobilities for amphiphilic tertiary phosphines both in solution and tethered to a cationic exchange resin through the tetra-alkylphosphonium groups. The conventional inversion-recovery method was used in both solution and CP-MAS measurements. The rhodium(I) complexes containing the phosphines of the type $[Ph_2P(CH_2)_nPMe_3]^+$ where n = 2,3,6 or 10, were found to become more solution-like with longer phosphine chain length. It was found that the longer the chain length the greater the catalytic activity, which was attributable to the solution-like character of the supported complex. It was postulated that there was less steric hindrance from the support and so increased motion was possible. Differences in catalyst site mobilities could be measured by ^{31}P relaxation times.

Wu and Wasylishen[115] have used two-dimensional CP-MAS NMR techniques in a homonuclear J-resolved experiment to study metal

phosphine complexes. They were able to obtain homonuclear J connectivity information when the J splittings are unresolved in conventional spectra, particularly for couplings such as $^2J(P,P)_{cis}$ in square planar and octahedral complexes. Also discussed are other 2-D experiments.

Dutasta, Robert and Weisenfeld[116] were among the original discoverers of the valuable information contained in the chemical shift tensor components. They investigated a number of phosphine oxides, selenides and sulfides. The ^{31}P chemical shift tensor principal components of a number of phosphine oxides, selenides and sulfides were obtained using a proton enhanced nuclear induction technique.[117] It was found that the chemical shift anisotropy for the oxide is larger than its selenium or sulfur analogue. Robert and Weisenfeld also found that CSA was larger in the selenides and sulfides when going from alkyl to aryl substituents. The conclusion reached is that the electronic anisotropy distribution about the phosphorus atom parallels the ^{31}P CSA.

The principal components of the chemical shift tensor of four cyclic organophosphorus compounds of different size but where the phosphorus atoms are in the same chemical environment were studied by Dutasta, *et al.*[118] They determined that for a phosphorus atom in a given chemical environment, the ^{31}P chemical shift shows a large anisotropy and a linear variation when the asymmetry parameter η is plotted as a function of the intracyclic bond angle around the phosphorus atom.

Gobetto[119] reviewed the use of SS ^{31}P NMR techniques to investigate phosphorus ligands coordinated to transition metals. Included are examples which deal with crystallographic sites in organometallic solids and the

characterization of transition metal complexes on surfaces. An example is $HRu_3(CO)_7(PPh_2)_3$, in which a large difference in chemical shift anisotropy of the three diphenylphosphido ligands is associated with a difference in the M-P-M bond angle. This is shown in Figure12. For the unique PPh_2, which is bonded in the same edge as the hydrido ligand, the bond angle MPM = 73.5-74.3°, and the CSA is 192 ppm. The other two PPh_2 moieties have MPM = 77.3-80.1° , and CSA = 408 ppm.

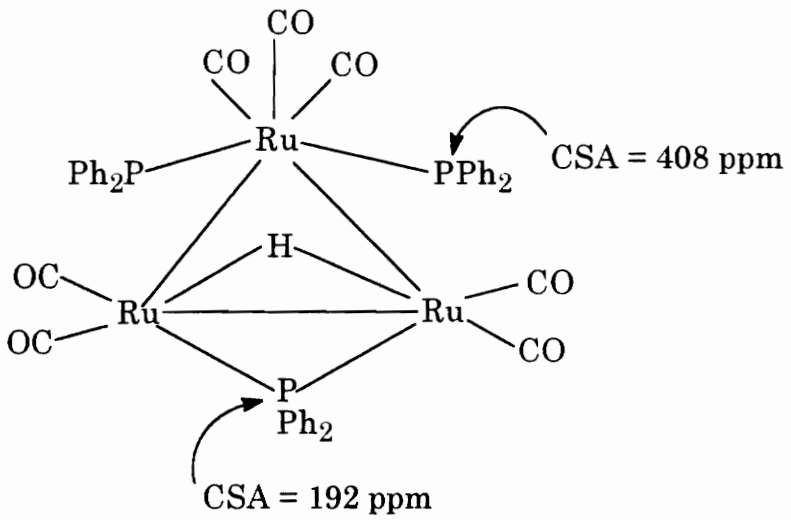

Figure 12. Varied CSA for phosphorus in $HRu_3(CO)_7(PPh_2)_3$.[119]

Using ^{13}C and ^{31}P solid state NMR Chu, *et al.*[120] determined the principal chemical shift tensors for three bis(dialkoxythiophosphoryl)-disulfides. This appears to be the first time thiophosphates with an S-S linkage have been studied by solid state NMR, yet these types of thiophosphates are commonly used in pesticides, motor oil additives, and in vulcanization processes.

Phosphorus ligands and complexes of Nickel(II), palladium(II) and platinum(II) were immobilized on an insoluble support and studied by ^{31}P MAS NMR spectroscopy. The geometry of the complexes in the solid state could be determined and surface reactions monitored. Bemi *et al.*[121] showed that the schemes representing the supposed routes of immobilization are more complicated than previously thought, demonstrating yet another use of SS NMR techniques.

Platinum complexes of the type $(R_3P)_2MX_2$ were studied by CP-MAS ^{13}C and ^{31}P NMR spectroscopy and it was found that while the complexes have square-planar geometries in the solution state, some have distorted geometry in the solid state as determined by additional resonances.[122]

^{31}P NMR spectroscopy has been recently shown to be a useful tool for determining the enantiomeric purity of chiral organophosphorus compounds. The chemical shielding tensors of both ^{13}C and ^{31}P vary as a result of different crystal symmetries. Andersen *et al.*[123] have shown that through integration or deconvolution of the MAS NMR signals one can determine enantiomeric purity because impure samples give different signals than the samples of racemic or pure samples.

To conclude this review, there are a number of short articles available to give the reader a general idea of the ability and power of solid-state NMR spectroscopy. Harris[124] , Jelinski[125], Dybowski[126], and Maciel[127] are among those who have written short informative reviews on the solid state techniques.

Chapter 3
Solid-State Nuclear Magnetic Resonance Spectroscopy

3.1 Introduction to Solid-State Nuclear Magnetic Resonance Spectroscopy

3.1.A History

Nuclear magnetic resonance spectroscopy has become one of the most powerful tools in science for the study of physical phenomena. The idea that some nuclear isotopes have the property of spin and so possess a nuclear magnetic moment was discovered by Pauli in 1926 and established in 1933 with modifications of the Stern-Gerlach experiment.[128] The 1952 Nobel Prize for Physics was awarded jointly to Bloch, Hansen and Packard of Stanford and Purcell, Torrey and Pound from Harvard for their pioneering discoveries of NMR signals with water and paraffins in the years preceding 1944. The first observation of the NMR phenomenon was rewarded by the Nobel prize in 1944 to Rabi for work done as early as 1939.

When a nucleus with the property of spin is placed in a strong homogeneous magnetic field, the magnetic moments align themselves parallel to the field, with a very slight excess aligned with the field at equilibrium. Energy in the radio frequency range will displace the macroscopic nuclear magnetization and cause it to precess about the field at a specific frequency. The precessing magnetization will induce an electrical current which is detectable. With this beginning and

tremendous strides in magnet and computer technology, NMR has become an indispensable tool for all branches of science. With solution-state NMR so widely used in all areas of chemistry, this outline will cover the basics of solid-state NMR. For enlightening discussions of the phenomenon of NMR and applications in the liquid state, any of the texts listed in the bibliography are recommended[130].

3.1.B. Interactions in NMR

There are a number of interactions involving a nucleus with a magnetic moment when placed in a magnetic field. All these interactions contribute in some manner to the NMR spectrum of a solid material, because they are all dependent upon the orientation of the molecule (hence the nucleus). The inherent anisotropy of each interaction is averaged either to zero or to a single average value in solution because of the rate of Brownian motion compared to the rate of the interaction. This results in a spectrum of high resolution in the liquid or solution state. When the conditions are carefully determined for an experiment in the solid state it is possible to generate a spectrum of quite good resolution for solids.

A Hamiltonian may be written for the interactions experienced by a nucleus in a magnetic field. Each Hamiltonian contains a tensor quantity:

$$\begin{aligned} H_{NMR} &= H_{ext} + H_{int} \\ &= (H_Z + H_{RF}) + (H_{CS} + H_{SR} + H_{DD} + H_J + H_Q + H_{NE}) \end{aligned} \quad (1)$$

H_Z = Zeeman interactions
H_{RF} = Radiofrequency
H_{CS} = Chemical shift
H_{SR} = Spin rotation
H_{DD} = Dipolar
H_J = Scalar coupling
H_Q = Quadrupole
H_{NE} = Nuclear-electron

The external factors include Zeeman interactions with the external static magnetic field B_0 and interactions with radiofrequency magnetic fields B_1, B_2, etc. These terms are essential for the NMR experiment. (Figure 13.) The other six quantities are considered internal, having to do with the make-up of the system.

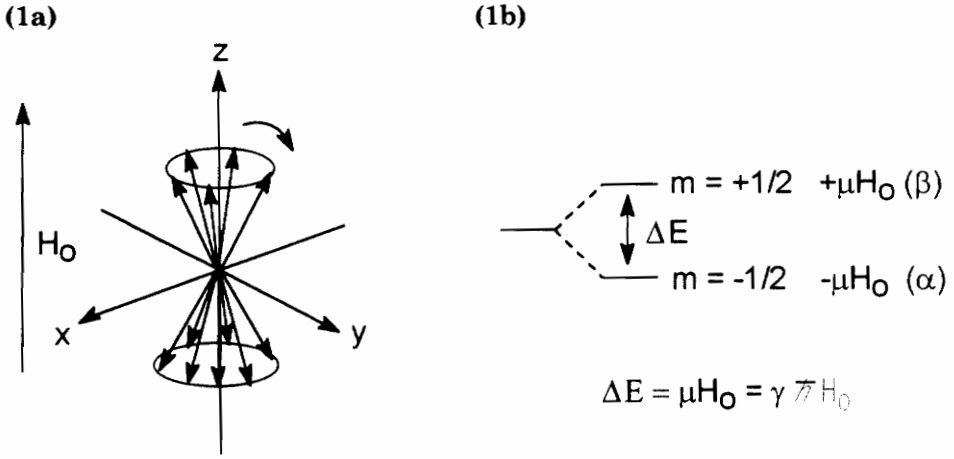

Figure 13a. Dependence of the macroscopic magnetization on a radio frequency field.
Figure 13b. Dependence of Zeeman energy levels on the magnetic field.

3.1.C. Zeeman Interactions

The basic interaction in NMR is the Zeeman interaction of the nucleus with the applied magnetic field B_0. The result is 2I + 1

quantized energy levels. Transitions between these levels produce resonance when the appropriate energy is supplied. The Zeeman levels are degenerate in the absence of B_0, but lose that degeneracy when the nucleus is placed in B_0. The difference in energy depends upon the strength of B_0 (figure 11) with greater population differences and larger signal to noise ratios at higher fields. Zeeman spin interactions are in the range of 10^6 - 10^9 Hz. At 4.7 Tesla, the Zeeman interaction occurs at 200 MHz for ^1H, 50.3 MHz for ^{13}C and 81.01 MHz for ^{31}P. Other interactions can perturb the Zeeman interactions. At 4.7 T, most of these other interactions are about 1% of the Zeeman, on the order of 50 kHz for ^{13}C.

3.1.D. Scalar Coupling

Scalar coupling consists of indirect magnetic moment spin-spin coupling by way of the electronic surroundings. This coupling arises because of the tendency of a bonding electron to correlate its spin to that of a nearby nucleus. Scalar coupling is transferred through bonds and depends upon the spin state of the adjacent nucleus. The splitting of the signal into more than one peak is the result of scalar interactions and is also called J-coupling or spin-spin coupling. The neighboring nuclei can be in one of two possible spin states, α (lower energy, aligned with B_0) or β (higher energy, aligned against B_0) (Figure 13). Therefore the nucleus being observed can couple with both these states in another nucleus with spin. This is applicable to rhodium and platinum, both of which couple with phosphorus. Scalar coupling interactions range from 0 to 10^4 Hz.

and are independent of the field. They do not average to zero in solution, and can be similar in solution- or solid-state spectra.

3.1.E Dipolar Coupling

Dipolar coupling is direct, through space coupling of the magnetic moments of nuclei. Each dipolar interaction produces a splitting which depends upon the orientation of the nucleus. If the local magnetic field is averaged over all possible orientations of the molecule, then the average local field is zero. Dipolar interactions usually are in the kHz range and produce severe line broadenings. In order to generate sharp lines, the averaging process must be fast compared with the splitting generated by the local field. The Brownian motion which takes place in solution is sufficiently fast to fulfill this condition. In solids however, motions are slow and broad lines are a problem. The dipolar interaction is dependent upon the magnitude of the magnetic moments of the nuclei (as γ) and the internuclear distance, r. I and S are nuclear spin operators for different nuclei and θ is the angle that the internuclear vector makes with the applied field (Figure 14). The Hamiltonian for dipolar interactions for an isolated heteronuclear pair is:

$$H_D^{IS} = \frac{\gamma_I \gamma_S \hbar^2}{r^3}(1 - 3\cos^2\theta\ ) I_Z \cdot S_Z \qquad (2)$$

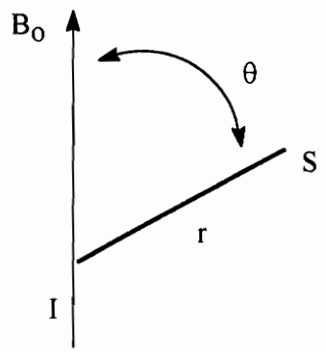

Figure 14. Dipolar interactions.

Dipolar interactions are very important in solid-state NMR. In solution, where molecules are tumbling very rapidly, all angles are sampled so the term must be integrated over a sphere. The integration yields zero for this term, so dipole interactions are not a factor in solution. In solids, magic angle spinning approximates molecular tumbling in solution. The macroscopic sample (S) is spun about an axis making an angle θ with the static field, B_0 (Figure 14). Dipolar interactions (and, as a matter of fact, chemical shift anisotropy) have an energy term in which is found the function $(1- 3\cos^2\theta)$. Spinning the sample about this angle will give a time averaged function $\langle 1- 3\cos^2\theta \rangle$. If the angle θ is set to 54° 44', the magic angle, this function averages to zero. This means that in principle when the sample is rotated faster than the dipolar interactions [and the chemical shift anisotropy (*vide infra*)] and at the magic angle, the resulting spectrum will resemble a solution state spectrum in that the dipolar couplings will disappear. However, this is normally not the case because dipolar couplings are usually far larger than can be removed by

magic angle spinning, and other methods such as high power decoupling must be applied to remove the dipolar coupling.

3.1.F Chemical Shielding

Chemical shielding arises from the interaction of the electrons about a nucleus with B_0. The applied field generates currents in the electronic charge distribution and these induced currents in turn generate additional magnetic fields at the nucleus. The consequence is that the nucleus sees not only B_0 but B_0 plus or minus some small contribution to the magnetic field called the screening or shielding constant. The fundamental NMR equation, $\omega = \gamma B_0$, which defines the resonant frequency of a nucleus, becomes:

$$\omega = \gamma(B_0 - \sigma B_0) = \gamma B_{eff} \qquad (3)$$

where B_{eff} is the actual field seen by the nucleus and σ is a shielding constant which when related to some reference becomes the chemical shift.

If every different nucleus in a sample felt exactly the same magnetic field, the NMR spectrum would be composed of many lines of identical frequency. Due to electronic shielding, each magnetically equivalent nucleus resonates with a characteristic frequency called the chemical shift. This yields a single line for each type of nucleus in solution. The resonant frequency is determined by the local magnetic fields and electric field gradients which depend upon molecular

orientation. The screening constant is a fraction and therefore a larger σ means a smaller B_{eff}. If we set up the spatial distribution of the electrons of a molecule on an axis system using polar coordinates, the chemical shift is dependent upon θ and ϕ and takes on the values σ_{xx}, σ_{yy}, and σ_{zz} when B_0 lies along the x, y and z axes respectively, and various intermediate values elsewhere. In liquids the molecule assumes all possible orientations in a very short time relative to 1/CS so the anisotropy is averaged to $\sigma = 1/3(\sigma_{xx} + \sigma_{yy} + \sigma_{zz})$. A nucleus in a powder sample has microcrystallites randomly oriented with respect to the magnetic field., and as a result feels a spread of frequencies which can range from a few kilohertz to megahertz depending upon the anisotropy of the local fields. Different orientations of the magnetic field relative to molecular coordinates will result in different resonance line positions for magnetically equivalent nuclei and a resonance pattern called a chemical shift tensor powder pattern results. The Hamiltonian for chemical shift anisotropy is:

$$H_{CSA} = \gamma_I \hbar \vec{I} \cdot \hat{\sigma} \cdot \vec{B}_o \; (\; 1 - 3\cos^2\theta \;) \qquad (4)$$

where σ is a tensor quantity representing the anisotropy. The Hamiltonian for CSA also contains the term $1 - 3\cos^2\theta$ which vanishes at the magic angle, 54.7°.

In solution, the single resonance line represents the isotropic average of the CS tensor. In solids, with restricted motion, the electronic distribution causes the chemical shift to take on directional properties.

The chemical shift tensor powder pattern describes the magnitude and direction of shielding; the shape of the powder pattern is determined by the symmetry of the molecule. The shapes of the pattern are related to the principle values of the tensor,which are obtained through diagonalization. When $\sigma_{zz} \neq \sigma_{xx} \neq \sigma_{yy}$ the pattern is asymmetric. If $\sigma_{xx} = \sigma_{yy}$ or σ_{zz} then the pattern is axially symmetric. Since the isotropic average is defined as $1/3(\sigma_{zz} + \sigma_{xx} + \sigma_{yy})$, the most intense line is not necessarily the isotropic chemical shift. When the molecular symmetry axis is perpendicular to B_o, the symbol is $\sigma_{\perp}$. When the symmetry axis is parallel, the symbol is $\sigma_{\parallel}$ (Figure 15). Figure 16 depicts types of powder patterns. Cubic symmetry (such as that possessed by adamantane) yields an isotropic chemical shift in the solid state.

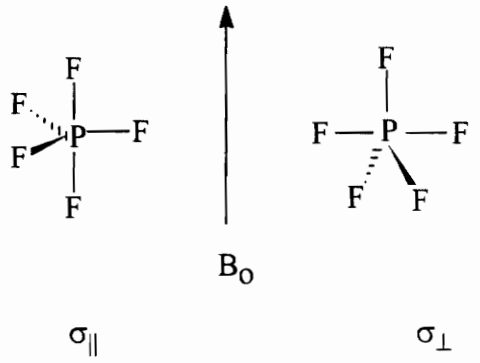

Figure 15. Orientation of symmetry axes with B_o.

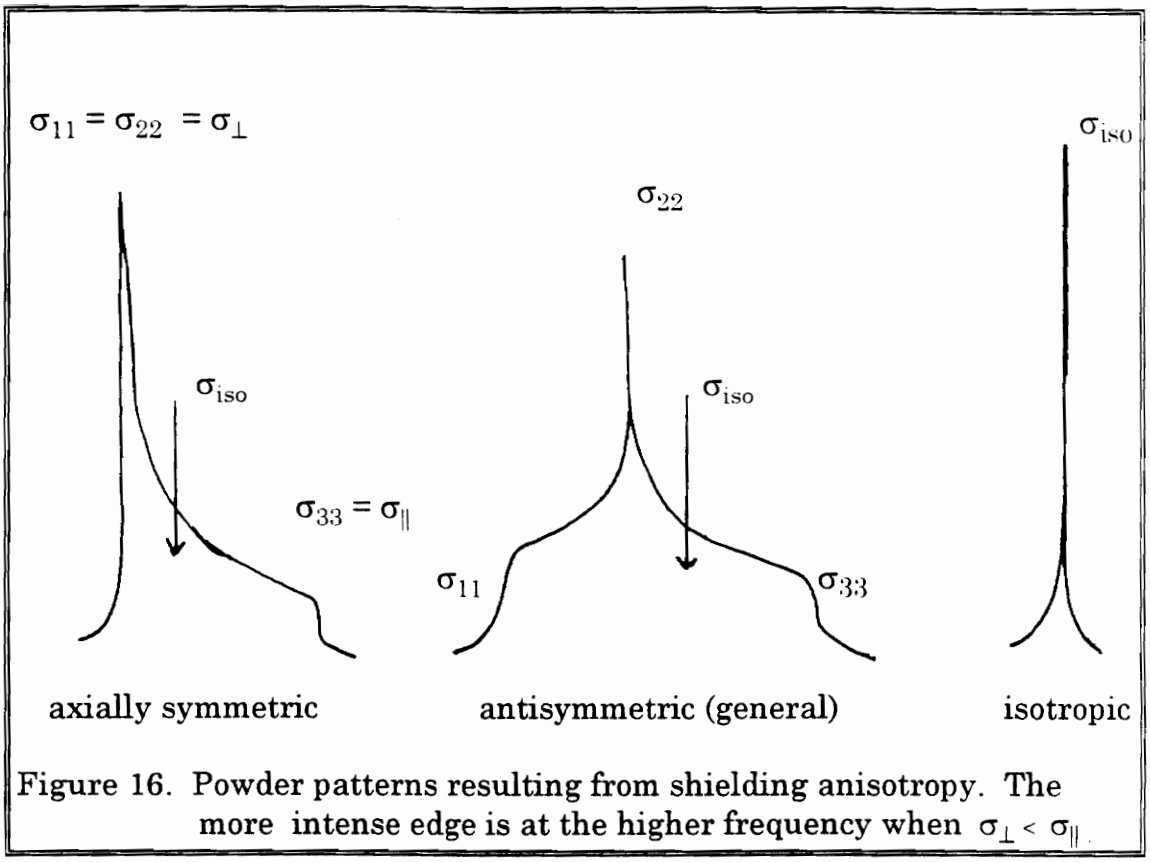

Figure 16. Powder patterns resulting from shielding anisotropy. The more intense edge is at the higher frequency when $\sigma_{\perp} < \sigma_{\parallel}$.

3.1.G. Other Interactions

Other interactions which perturb the Zeeman effect include quadrupolar effects, spin rotation and paramagnetic effects. Since these do not apply to this research, they will not be discussed here.

3.1.H. Time Considerations

Molecular motion that is faster than the line width caused by an interaction with the magnetic field will yield a sharpened spectrum (motional narrowing). The motion must be isotropic in order to reduce the interaction to its isotropic average. Since motions in solids are restricted and rates of motion are slower, this type of averaging is rare.

3.1.I. Methods for Spectral Enhancement: High Power Decoupling, Magic Angle Spinning and Cross Polarization

The two major sources of line-broadening in solid-state NMR are dipole-dipole (DD) coupling and chemical shift anisotropy (CSA). The Hamiltonian for both of these interactions contain the $1\text{-}3\cos^2\theta$ term, which goes to zero at the angle of 54.7°, the magic angle. Theoretically, these interactions should disappear if the sample is spun rapidly at the magic angle (Magic Angle Spinning, MAS). However, dipole-dipole interactions cannot usually be averaged out because the interactions are usually larger than the spin rate. Dipole-dipole coupling between abundant nuclei such as protons or fluorine can be a major problem; with phosphorus and other dilute spins the interactions are not as severe. High power decoupling solves this problem. Two radio frequencies are used; one for the nucleus to be observed and the other at the frequency of the nucleus to be decoupled (usually hydrogen or fluorine). By strongly irradiating the nucleus to be decoupled, it is effectively saturated and the nucleus of interest can be observed.

If the CSA is smaller than the spin rate, the isotropic average of the powder pattern is the only peak seen when spun at the magic angle. Many times it is not mechanically possible to spin the sample rapidly enough to average all the interactions to zero, and spinning side bands result. These spinning side bands are found at the rate of spinning about the isotropic resonance. They move according to the spinning rate of the sample, coalescing into a powder pattern when static. There is useful information contained in the sidebands. (Figure 17).

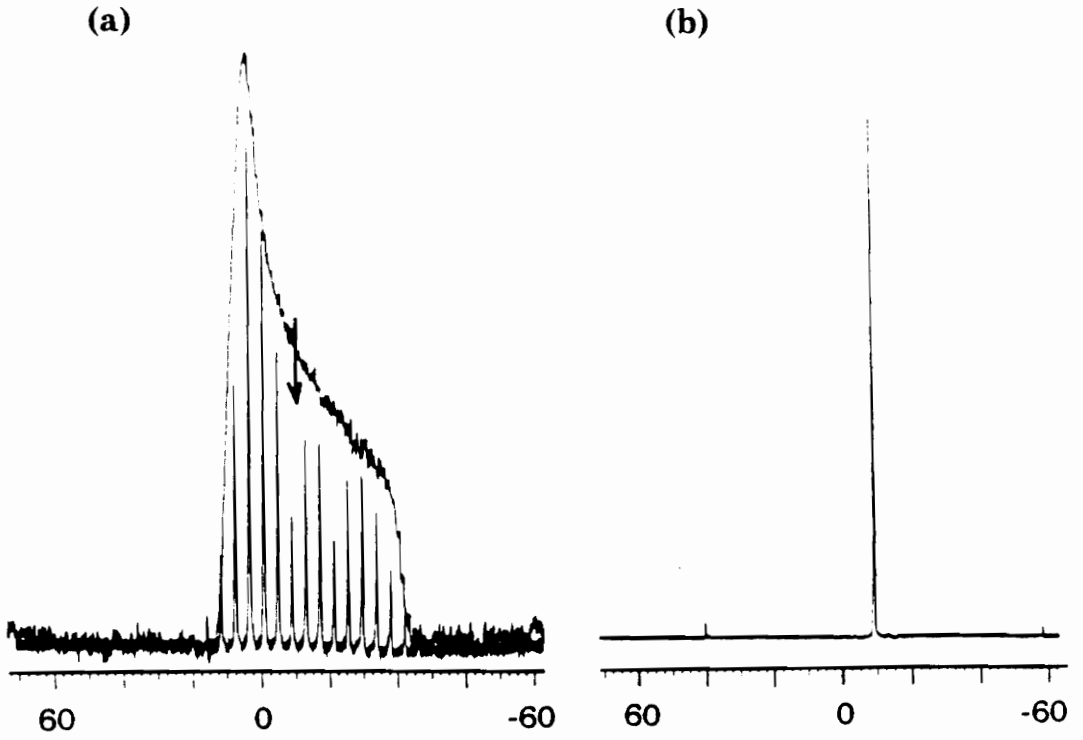

Figure 17. (a) Spinning sidebands (500 Hz) superimposed on a static powder pattern for triphenylphosphine. The isotropic shift in is indicated with an arrow. (b) Spectrum of TPP at 7000 Hz, when sidebands are virtually non-existent. The CSA for TPP at 7.1 Tesla is about 7000 Hz.

Cross-polarization is a technique that allows the magnetization of a dilute spin such as ^{13}C to be derived from an abundant spin (^{1}H). By fulfilling the Hartmann-Hahn condition:

$$\gamma_H B_{1H} = \gamma_C B_{1C} \qquad (5)$$

where $B_{1,}$ representing the two applied radiofrequency fields are adjusted so the the two spins are "locked" together. The two spins precess at the

same rate and their effective energies are equivalent, which allows transfer of magnetization from the more abundant to the dilute spin.

Cross-polarization was not used for this work because historically the inversion-recovery pulse sequence for the nucleus of interest is a more accurate method of determining spin-lattice relaxation times.

3.I.J. Signal Averaging

Signal averaging is not a technique unique to solid state NMR or indeed to NMR at all, but is essential to most NMR experiments. It is a process by which many spectra (or FID's) may be accumulated and added together, thereby enhancing the signal to noise ratio. The signal to noise ratio (S/N) is improved with the number of transients (NT) collected:

$$S/N \approx (NT)^{1/2} \tag{12}$$

Signal averaging is only possible because of advancements in magnet technology (giving precise stability of the fields and frequencies) and computer technology (allowing storage and transformation of data).

3.2. Relaxation Methods and Measurements

Relaxation in the solid state is dominated by dipole-dipole interactions, chemical shift anisotropy or a combination of both. The other mechanisms will be neglected for the purposes of this discussion.

Relaxation mechanisms give a means of obtaining information on the dynamics of a molecule through the behavior of certain nuclei.[129] In order to extract this information, the system must be perturbed from its equilibrium state, allowed to relax and regain equilibrium with its environment, called the "lattice".

The T_1 relaxation, referred to as spin-lattice relaxation, is a first-order process which allows the system to return to thermal equilibrium with its environment after perturbation. T_2 relaxation, called spin-spin relaxation, allows the return of equilibrium between the nuclear spins themselves.[130]

The macroscopic magnetization, **M**, can be considered in the laboratory frame of reference as a vector which is rotating at the Larmor frequency, $\omega_o = \gamma B_o$, about the Z axis. When viewed in the rotating frame of reference, the frame itself is rotating at this frequency which has the effect of making the vector **M** stationary on the Z' axis (Figure 18).

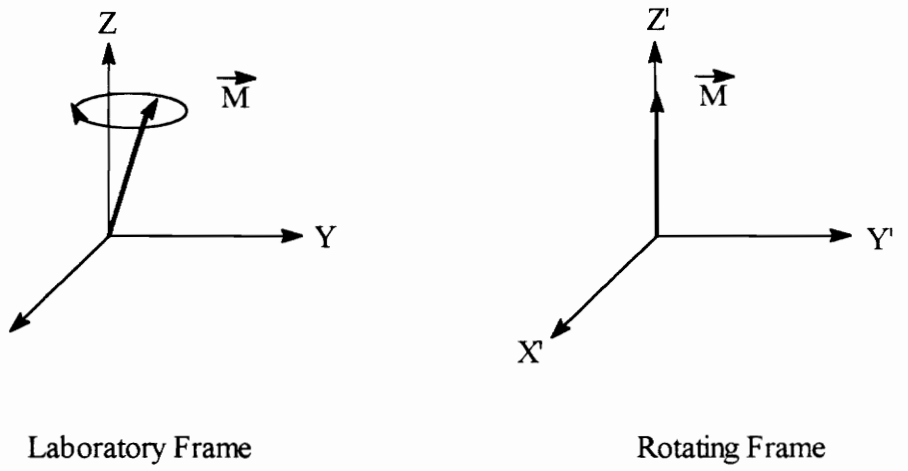

Figure 18. Moving from the laboratory to the rotating frame of reference.

If the macroscopic magnetization $\mathbf{M_o}$ is tilted from the Z' axis by an angle α it will be composed of three components, M_x, M_y and M_z. If it is then allowed to return to its equilibrium position, the component M_z will return by obeying a first order rate law with a time constant T_1 called the longitudinal or spin-lattice relaxation time:

$$dM_z/dt = (M_z - M_o)/T_1 \qquad (7)$$

M_z is related to the Zeeman energy levels, and this equation determines the populations and the transitions between the energy levels.[131]

M_x and M_y are zero at equilibrium. They relax due to exchange of energy between spins and also are first order processes:

$$dM_x/dt = -M_x/T_2 \quad \text{and} \quad dM_y/dt = -M_y/T_2 \qquad (8)$$

where T_2 is a time constant called the spin-spin or transverse relaxation time. The dephasing of the spins is a process of entropy; it changes the Larmor frequencies of the spins and yields a distribution of frequencies about the unperturbed resonance frequency. T_2 is thus responsible for the line width of the absorbance peak.[131]

The distribution of frequencies of motion in the molecular system affect the relaxation times of the spin systems; these motions have a very wide range of frequencies. The correlation time (τ_c) is the average time a molecule in a system remains in a given position; for liquids this is short indeed, on the order of 10^{-12}s for non-viscous liquids. That is, after 10^{-12}s there is a collision or some event such as rotation occurs and the molecule changes its state of motion. The frequency components for this system are from 0 to 10^{12} Hz.

Considering **M** in the rotating frame, if it is perturbed from its equilibrium Z' position, there will be components of the vector along the X', Y', and Z' axes. (Figure 19.)

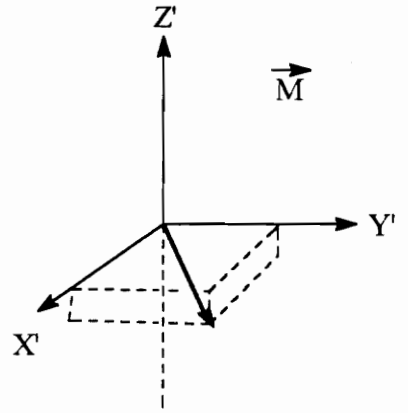

Figure 19. **M** has components along X',Y', and Z' axes when perturbed from equilibrium.

Since the nucleus is charged and is spinning, it has a magnetic moment which generates a fluctuating magnetic field, **b**, which has components b_x, b_y . and b_z. It is these fluctuating magnetic fields which allow the relaxation processes to occur.

Dipolar interactions and chemical shift anisotropy both depend upon orientation, and are therefore major contributors to relaxation in the solid state. There are general expressions for the orientation dependence of spin-lattice relaxation times in solids; these are beyond the scope of this discussion.[97,132] However, the dipolar spin-lattice relaxation time can be defined as:

$$\frac{1}{T_1} = C\left[\frac{\tau_c}{1 + \omega_o^2 \tau_c^2} + \frac{4\,\tau_c}{1 + 4\,\omega_o^2 \tau_c^2}\right] \qquad (9)$$

and the chemical shift anisotropy spin-lattice relaxation time can be defined as:

$$\frac{1}{T_1} = C\left[B_o^2\left(\sigma_{\parallel} - \sigma_{\perp}\right)^2 \frac{2\,\tau_C}{1 + \omega^2 \tau_C^2}\right] \qquad (10)$$

where τ_c = the correlation time

ω_o = the nuclear precession frequency

C = a collection of constants including the magnetic moment.

B_0 = magnetic field

It can be seen from these equations that T_1 depends upon τ_c.[129] In the solid state, the more mobile the molecule, the shorter τ_C. As τ_C increases, (as mobility decreases) the T_1 increases. It follows that most solids will have long relaxation times.

Dipolar relaxation results from the effect of the fluctuating field of one nucleus on another. Chemical shift anisotropy is a factor if the environment of the spin is not symmetrical.

T_1 in the solid state can also be affected by sample impurity and paramagnetic impurities such as oxygen as well as other factors.

3.3. Methods of Measuring T_1[129]

There are threee common methods for measuring T_1: inversion-recovery, (IR), progressive-saturation (PS) and saturation-recovery (SR). The method used for this work was inversion-recovery; a brief synopsis of the other two processes is given, followed by a more comprehensive discussion of IR.

PS uses a series of repetitive pulses separated by a fixed time delay, τ:

$$[90°\text{-acquisition-}\tau]_n \qquad (11)$$

where τ is a variable time and n = the number of transients.

Following the first three or four pulses the Z magnetization reaches a steady state and data acquisition can then follow each pulse. After several FIDs are collected and stored, τ is changed and the operation begins again. The signal intensity varies with τ as:

$$I_t = I_\infty(1 - e^{-\tau/T_1}) \qquad (12)$$

where I_∞ is the intensity at $\tau > 5\ T_1$ and I_t is the intensity at time t.

This method can be used when $T_1 >> T_2$, which is almost always the case in solid state. The problems with this method include the inability to measure very short T_1's and the fact that the 90° pulse must be accurate.

SR uses a combination of pulses to destroy all magnetization and saturate the sample:

$$[90°\text{-}\tau\text{-}90°\text{-acquisition-t}]_n \qquad (13)$$

During a time τ relaxation occurs and after the application of a 90° pulse a FID is collected and stored. The signal intensity varies as a function of time as in P-S.

3.II.C. Inversion-Recovery Method

Inversion-recovery is the method that is considered the most accurate, and is the most widely used. The pulse sequence is:

$$[180°\text{-}\tau\text{-}90°\text{-acquisition-t}]_n \qquad (14)$$

where τ = a variable delay time,
t = a relaxation delay > 5 T_1,
n = number of transients

τ is a variable delay that determines the orientation and intensity of the signal. The length of the relaxation delay between sequences must be greater than 5 T_1 to allow the system to return to thermal equilibrium. The pulse-timing diagram in Figure 20 gives the sequence of events in chronological order. The FID is collected after the 90° pulse.

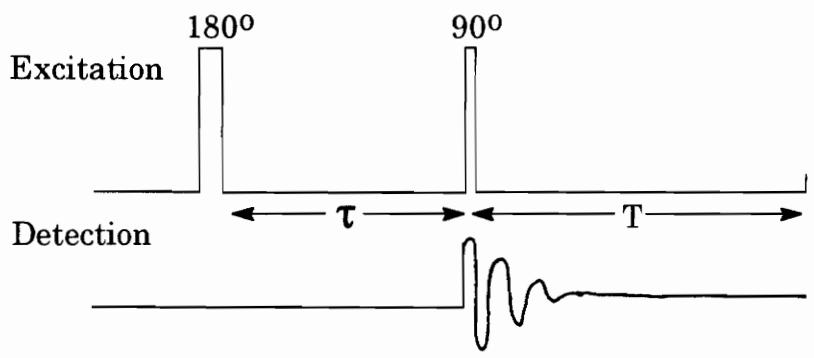

Figure 20. Pulse-timing diagram for inversion-recovery sequence.

The intensity of the signal as a function of τ is:

$$I_t = I_\infty[1-2e^{(-\tau/T_1)}] \qquad (15)$$

where I = the intensity of the signal.

One of the greatest advantages to the inversion-recovery method is that it does not require accurate setting of the 90° pulse. There are a number of variations to this experiment;[97] all the variations are optimized when at least eight intensities are collected and of these intensities at least one has the phase reversed; that is, the null has been approached from both sides. The reduction in the number of adjustable parameters and the relaxation of the requirement for collecting long τ spectra are two advantages to modified versions of the I-R method.[114]

Figure 21 shows the effect upon a sample of solid trisulfonated triphenylphosphine (TPPTS). Figure 22 depicts a plot of the results.

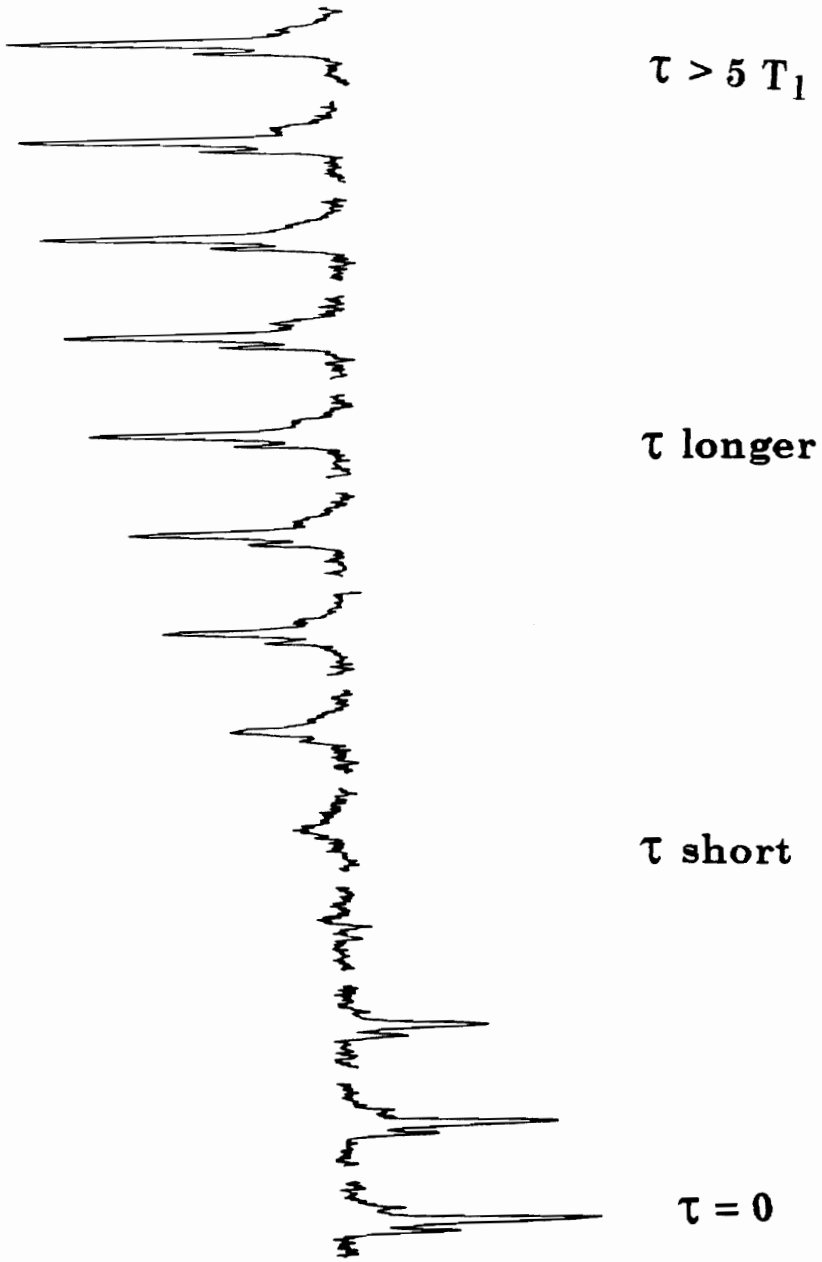

Figure 21. ^{31}P NMR spectra of TPPTS corresponding to I-R pulse sequences.

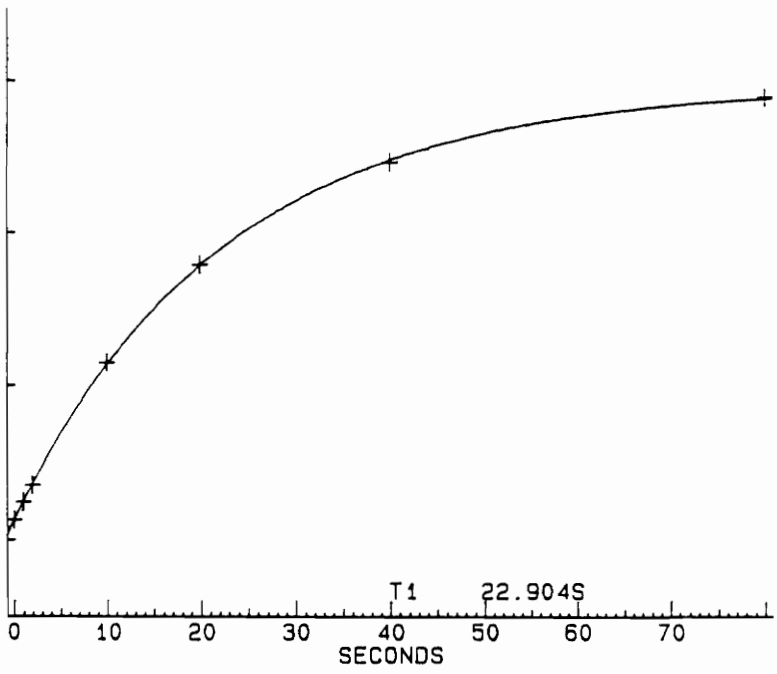

Figure 22. T_1 plot for TPPTS. The program loop = 50; T_1 = 1100 s.

Chapter 4
Experimental Procedures

4.1. Preparation of Solid-State NMR Spectrometer for Use

Solid-state NMR measurements were carried out on a Bruker MSL-300 multinuclear spectrometer with a wide bore magnet (7.05 T) at an observation frequency of 121.496 MHz for ^{31}P. Samples (approximately 200 mg) were placed in 4 mm rotors of zirconium dioxide. Magic angle spinning used spinning rates between 6000-9000 Hz. Before each experiment, the pulse angle was set at 90° using the Bruker HPDEC program on a sample of NaH_2PO_4.

Chemical shift data were referenced to 85% H_3PO_4 contained in a sealed glass vial and inserted into the probe without spinning. This procedure allowed the spectrometer reference to be set before inserting the sample. All experiments were begun under the program TPPP31 QUADCYCL especially meant for collection of ^{31}P data. The T_1 data were collected using the Bruker MMIRTONE program were manipulated using the T1 POINTS program supplied by Bruker. Variable spinning experiments were measured using the HPDEC program.

To ready the MSL 300 spectrometer for data acquisition, the 4 mm tunable multinuclear probe and stack were inserted into the magnet. The preamp and power amps were changed for the correct frequency range. The probe was tuned and matched using HPDEC and WOBL. These and other pulse programs can be found in Appendix A. The preamp was tuned with a receiver gain of 0 on H_3PO_4. The power amp was tuned using HPDEC on

H_3PO_4. The best 90° pulse width was determined by setting the power gain for the ^{31}P channel to an arbitrary setting of 10 and varying the pulse width. NaH_2PO_4 or $NaH(PO_4)_2$ was utilized to determine the pulse angle because of their relatively short spin-lattice relaxation times compared to TPPTS and TPP. Cross-polarization was not used. The receiver gain was set based upon the relative amount of phosphorus in the sample. The number of experiments to determine T_1 values was generally 8, although more or less than 8 were collected in some cases. The number of transients depended on the concentration of phosphorus in the sample. Instrument parameters are defined in Appendix A and the parameters for each experiment are also found in Appendix A.

4.2. Preparation and Impregnation of Compounds for Solid-State NMR Studies

All manipulations involving air-sensitive compounds were performed under argon by standard Schlenk techniques. Fuming sulfuric acid (18-24%), triphenylphosphine and D_2O were obtained from Aldrich and used without further purification. Methanol, ethanol, acetone (all purchased from Fisher) and water were distilled under nitrogen prior to use. D_2O was degassed by the freeze-pump-thaw method. $Rh(acac)(CO)_2$ was purchased from Strem and used as received. CO/H_2 1/1 (syn gas) was purchased from Airco and used with a deoxygenating column. Characterization by NMR to assure the purity of each sample for solid-state study was executed on a Bruker 200 MHz spectrometer at an observation frequency of 200.133 MHz for ^1H, 80.015 MHz for ^{31}P and 50.323 MHz for ^{13}C.

Thermogravimetric analyses to determine the water content of certain samples was performed by Polymer Solutions, Inc. All samples were kept under argon prior to analysis, and the TGA was performed under nitrogen.

Sulfonation of TPP and purification of the ligand TPPTS was accomplished by the procedures outlined by Kuntz[37b] and Bartik, *et al* .[47] The preparation of the complex $HRh(CO)(TPPTS)_3$ was achieved using the techniques outlined by Arhancet, *et al.*[3] and Bartik, *et al.*[134] Immobilization of the ligand and the complex on CPG-240 was described by Arhancet.[79]

Additonally, carefully measured amounts of CPG-240 (purchased from Electronucleonics, Inc., Fairfield, NJ) were carefully degassed and precisely measured solutions of the sample compound of interest were introduced slowly with stirring. The "dry" glass/sample/water was allowed to stir several days and then evacuated for at least 48 hours to remove any excess water. Hydration was attained by the use of a "hydration vessel" constructed by the glass shop, in which the sample was placed in one depression of a Schlenk-type vessel and the degassed water in another (Figure 23).

The rotor was filled as shown in Figure 24. By using the "pair of pants", a glass bowl fitted with joints to which the hydration vessel and the rotor-tube holder could be attached, the samples could be transferred under a positive inert gas pressure. The samples were transferred by forcing portions into the "squisher", a 12 gauge 12" syringe needle fitted with 14 gauge copper wire and transferred from the hydration vessel to the combination rotor/tube holder under argon.

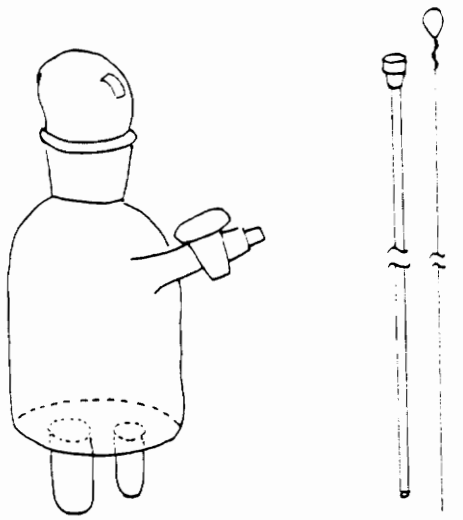

Figure 23. Hydration vessel and "squisher".

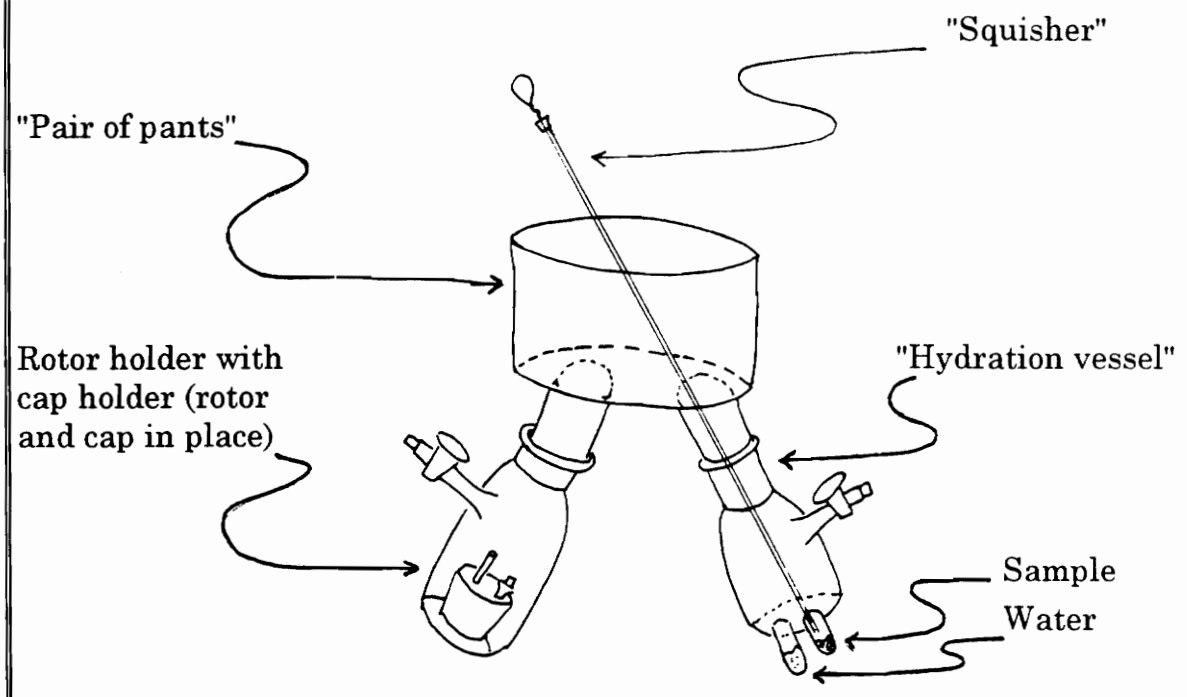

Figure 24. Method of filling the rotor for solid state NMR measurements.

4.3. Ligand and Complex Syntheses, Characterization and Catalysis

All manipulations were performed under argon or prepurified nitrogen using standard Schlenk techniques. THF and pentane were distilled from sodium benzophenone ketyl. CH_2Cl_2 was distilled under nitrogen from P_2O_5. Other reagent grade solvents, methanol, acetone, ethanol and deionized water were distilled under inert gas just prior to use. All solvents were purchased from Fisher. Argon, hydrogen and carbon monoxide were purchased from Air Products, Inc. Triphenylphosphine, 1,2-bis(diphenylphosphino)ethane (DPPE), oleum (fuming sulfuric acid; 18-24% SO_3), and D_2O were obtained from Aldrich; D_2O was degassed by the freeze-pump-thaw method; oleum was used without further purification. The water-soluble chemical shift standard 3-(trimethylsilyl)tetradeutero sodium propionate (TSP) was purchased from Wilmad Glass Co. Sodium hydroxide was purchased from Mallinckrodt AR. Hydrochloric acid (36%) was obtained from Fisher and used as supplied. $Ni(CO)_4$ was purchased from Alfa Chemicals. $(PhCN)_2PdCl_2$, $(PhCN)_2PtCl_2$, $Rh_2COD_2Cl_2$ and $Rh(acac)(CO)_2$ were obtained from Strem Chemical Co. $CO:H_2$ (1:1) was received from Airco and used with a deoxygenating column.

The series of high pressure catalytic reactions were carried out in four stainless steel reaction vessels (autoclaves) equipped with the appropriate high pressure guages purchased from Dibert Valve and Fitting. The volume of each autoclave is 30 mL. Reaction products and starting materials were determined by gas chromatography on a Varian 3300 gas chromatograph fitted with a HP-1 cross-linked methyl silicone gum phase column 25m x 0.32 mm x 0.52 μm and a temperature range of -60° to 325°C.

Helium was the carrier gas and a FID detector was employed. The temperature program for each series of experiments can be found in Appendix C with the appropriate experiment. An Omega CN 2000 temperature process controller was used for the temperature control of the silicone oil bath for the catalytic reactions. Stirring rates were kept constant at 360 rpm as determined by a Lutren photo-tachometer. Stirring was accomplished by a Corning hot plate - magnetic stirrer.

NMR measurements were performed on a Bruker WP200 spectrometer at 200.133 MHz for ^{1}H, 50.323 MHz for ^{13}C, and 81.015 MHz for ^{31}P. Solution ^{31}P T_1 studies on DPPETS and derived complexes were measured on a Varian 400 spectrometer at 162.03 MHz for ^{31}P observation. Potentiometric titrations were carried out using a Microcomputer pH Vision, Cole-Parmer Model 05669-20 and a standard Ag/AgCl electrode purchased from Fisher. Elemental analysis was performed by Galbraith Laboratories, Inc. Mass Spectra were measured by K. Harich, Biochemistry Dept., Virginia Tech.

Key to NMR data: s, singlet; d, doublet; t, triplet; q, quartet; quin, quintet; sex, sextet; m, multiplet; br, broad; asterisk, pseudo. Carbon atoms in the phosphines are numbered from the CH_2 group as (1)C and continue with the α carbon (ipso) on the phosphorus atom labeled (2)C-P through the γ (4)C with attached SO_3Na. Key to IR data: vs, very strong; s, strong; w, weak.

4.3.A Hydroformylation Reactions

To insure good reproducibility in the series of catalytic reactions, separate stock solutions of the hydroformylation catalysts were prepared and used for each reaction. The concentrations and other parameters for the reactions can be found in Appendix B. The components of the catalytic reactions were combined at room temperature in the small reactors under CO. Nonane or octane was added as an internal standard for the GC analysis. The reaction vessel was closed, pressurized with $CO:H_2$ (1:1) and placed in a silicone oil bath preheated to the reaction temperature. In all reactions the stirring rate for the silicon oil bath was kept to the same value, 360 rpm. The initial pressure of the reaction was 200 psig. After the appropriate reaction time, the reactor was removed from the oil bath, allowed to cool to room temperature, depressurized and the contents removed. The products were immediately analyzed by gas chromatography. All catalytic reactions were batch reactions.

To facilitate mixing of the aqueous and nonaqueous phases 0.5% (w/w) dodecylbenzene sulfonic acid sodium salt was added to each hydroformylation reaction mixture. In a separate series of experiments the surfactant concentration was varied from 0.5 - 10% (w/w) with no effect on product yields or selectivity.

4.3.B Hydrogenation Reactions

To insure reproducibility in the series of catalytic reactions, separate stock solutions of $Rh(DPPETS)_2^+$ and Rh(COD)(DPPETS)Cl were prepared and used for each reaction. For hydrogenation, the isolated, purified

complexes were used. The concentrations for each series of experiments can be found in Appendix B with all reaction parameters as well as GC parameters. The components of the catalytic reactions were combined at room temperature in the small reactors under nitrogen. Octane or decane was added as an internal standard for the GC analysis. The reaction vessel was closed, pressurized with H_2 (200 psig) and placed in a silicon oil bath preheated to the reaction temperature . In all reactions the stirring rate for the silicon oil bath was kept to the same value, 360 rpm, as measured with a photo-tachometer. After the appropriate reaction time, the reactor was removed from the oil bath, cooled to room temperature under water, depressurized and the contents removed. The products were immediately analyzed by gas chromatography. The GC program was altered slightly when a lower boiling solvent was used.

4.3.C Carbonylation Reactions

Carbonylation reactions were run under similar coditions to the hydrogenation reactions. Appendix B contains all pertinent parameters.

4.4 Synthesis of Compounds

4.4.A Synthesis and Characterization of 1,2-bis[di-m-sodium-sulfonatophenyl)phosphino]ethane (DPPETS)

1,2-bis[diphenylphosphino]ethane (DPPE) (10.0 g, 0.025 mol) was added slowly to 125 mL (2.83 mol) of oleum (18-24% SO_3) at 0°C with vigorous stirring. The mixture was kept at 0°C for approximately eight hours. The course of the reaction was monitored by ^{31}P NMR (Figure 23.). Aliquots were prepared by pipeting about 1 mL of the reaction mixture into a small Schlenk vessel. The mixture was chilled and neutralized slowly with 25% NaOH with strong stirring. Methanol (25 mL) was added and the mixture refluxed for ten minutes followed by hot filtration to remove the Na_2SO_4 side product; the filtrate was vacuum dried and analyzed by ^{31}P NMR. Aliquots were taken every 24 hours, and when it could be seen that the reaction had peaked and begun to decline (as determined by oxide formation), the reaction mixture was neutralized with 25% NaOH at 0°C while stirring, and the pH brought to 8-9.

The volume of the neutralized mixture was reduced to about 200 mL and 800 mL of methanol was added. After refluxing for one hour, hot filtration was carried out, and the salt washed with an additional portion of 4:1 hot methanol/water to recover any remaining phosphine. The solution of methanol/water/phosphine was distilled to dryness and methanol/water in a 10:1 ratio was added to the solid; the mixture was refluxed and cooled to allow fractional crystallization, which yielded the desired phosphine in >95%

purity. Further purification to 99-100% can be accomplished by fractional precipitation with acetone/water in a 5:1 ratio. The impurities include variously sulfonated phosphines and the corresponding oxides. The crude product contains about 50% of the tetrasulfonated product. The final product is a white crystalline solid. The yield, based on DPPE is 30-40% pure DPPETS (6 - 8 g). A flow chart for the synthesis of DPPETS and a schematic of the possible products is depicted in Figure 27.

Spectral Data:

^{1}H NMR $\delta(D_2O)$: 2.31 [t,$J_{P\text{-}H}$ = 4.8 Hz, 4H, (1)CH_2], 7.49 [d, $J_{H\text{-}H}$ = 7.8 Hz, 8H], 7.81 [t, $J_{H\text{-}H}$ = 4.2 Hz, 4H], 7.87 [s br., 4H].

^{13}C NMR δ (D_2O): 25.3 [s, (1)CH_2], 140.67 [t, $J_{C\text{-}P}$ = 5.8 Hz, (2)C-P], 137.70 [t, $J_{C\text{-}P}$ = 7.4 Hz, (3)CH], 145.64 [s, (4)C-SO_3Na], 132.15 [t*, (5)CH + (7)CH], 128.85 [s, (6)CH].

^{31}P NMR $\delta(D_2O)$: -12.45[s].

Elemental Analysis:

Calcd. for $C_{26}H_{20}Na_4O_{12}P_2S_4$ x $6H_2O$ M_r = 914.68): C, 34.14; H, 3.53.

Found: C, 34.71; H, 3.43.

Mass Spectrum:

[MH^+] at 807 by F.A.B.

4.4.B Synthesis of [Pd(DPPETS)(H)]Cl_2

$(PhCN)_2PdCl_2$ (0.08g, 0.2 mmol) dissolved in 2 mL CH_2Cl_2 was added to a solution of DPPETS(H) (acid form of DPPETS) (0.16g, 0.2 mmol) in 2 mL water at room temperature, with vigorous stirring. After one hour the water phase of the mixture was slightly yellow. The aqueous phase was separated and washed twice with 5 mL pentane to remove the residual organic solvent, and then reduced in volume under vacuum to 1 mL. Precipitation of the white product was effected by the addition of 15-20 mL ethanol. The product was filtered and dried (yield: 92% based on DPPETS; 825 mg). Recrystallization can be accomplished using ethanol/water in a 20:1 ratio.

Spectral data:

^{1}H NMR $\delta(D_2O)$: 2.86 [t, J_{P-H} = 12.4 Hz, 4H, (1)CH_2], 7.45 [q, J_{H-H} = 5.8 Hz, 4H, (7)CH], 7.68 [t, J_{H-H} = 7.7 Hz, 4H], 7.85 [t, J_{H-H} = 5.1 Hz, 4H], 7.99 [d, J_{H-H} = 8.0 Hz, 4H].

^{13}C NMR $\delta(D_2O)$: 31.15 [t*, (1) CH_2], 138.90 [s, (2)C-P], 133.99 [s br., (3)CH], 147.47 [s, (4)C-SO_3Na], 133.45 [s br., (5)CH + (7)CH], 131.67 [s, (6)CH].

^{31}P NMR $\delta(D_2O)$: 61.21 [s].

4.4.C Synthesis of $Rh(DPPETS)_2^+$

A solution of $Rh_2(COD)_2Cl_2$ (0.154g, 0.40 mmol) in 4/1 THF/water (20 mL) was added to a solution of DPPETS (0.322g, 0.40 mmol) in 4/1 THF/water (20 mL) with stirring. After one hour the volume of the solution

was reduced to 5 mL and the yellow complex precipitated with 75% ethanol. Yield: 83% based upon DPPE; 1.42 g.

Spectral Data:

^{1}H NMR $\delta(D_2O)$: 2.34 [t br., $J_{P\text{-}H}$ = 11.6 Hz, 8H, (1)CH_2], 7.51 [d*, 16H], 7.81 [d*, 16H].

^{13}C NMR $\delta(D_2O)$: 31.45 [s, (1)CH_2], 139.88 [s, (2)C-P], 131.07 [s, (3)CH], 145.85 [s, (4)C-SO_3Na], 130.72 [s, (5)CH], 132.41 [s, (6)CH], 134.12 [s, (7)CH].

^{31}P NMR $\delta(D_2O)$: 60.71 [d, $J_{Rh\text{-}P}$ = 132.7 Hz,].

Elemental Analysis:

Anal. calcd. for $C_{52}H_{40}Na_8O_{24}P_4Rh_1S_8 \times 8H_2O$ (M_r = 1860.20): P, 6.66; Rh, 5.53; C, 33.58; H, 3.03.

Found: C, 33.55; H, 3.56.

4.4.D Synthesis of [Rh(DPPETS)(COD)]Cl

A solution of DPPETS (0.17g, 0.2 mmol) in 30 mL of a 4/1 THF/water mixture was added very slowly to a yellow solution of $Rh_2COD_2Cl_2$ (0.043g, 0.11 mmol) in 75 mL of the 4/1 THF/water mixture at room temperature with vigorous stirring. The yellow solution gradually turned orange. After the additon of DPPETS was complete, the THF was removed by vacuum and the remaining water solution filtered to remove any excess rhodium dimer. The aqueous solution was reduced in volume to 5 mL and 100 mL ethanol was

added until a fine orange crystalline precipitate formed. Upon filtration the desired product was obtained (yield: 96% based on DPPETS; 1.01 g).

Spectral Data:

^{1}H NMR $\delta(D_2O)$: 2.45 (s br., 12H, 2 x (1)CH_2 + 4 x CH_2(COD)), 5.07 (s, 4H, CH(COD)), 7.72 (t, J_{H-H} = 7.6 Hz, 4H), 7.84 (t, J_{H-H} = 9.8 Hz, 4H), 8.02 (d br., J_{H-H} = 7.8 Hz, 4H), 8.23 (d br., J_{H-H} = 10.9 Hz, 4H).

^{13}C NMR $\delta(D_2O)$: 32.05 (s, (1)CH_2 + CH_2(COD)), 105.91 (s, CH(COD)), 131.27 (s, (6)CH), 133.69 (s, (3)CH + (5)CH + (7)CH), 137.66 (s, (2)C-P), 146.01 (s, (4)C-SO_3Na).

^{31}P NMR $\delta(D_2O)$: 59.24 (d, J_{RhP} = 151.7 Hz).

4.4.E Synthesis of Pt[DPPETS(H)]Cl_2

A yellow solution of $(PhCN)_2PtCl_2$ (0.17g, 0.2 mmol) dissolved in 2 mL CH_2Cl_2 was added to a solution of DPPETS(H) (acid form of DPPETS) (0.16g, 0.2 mmol) in 2 mL water at room temperature, with vigorous stirring. After one hour the reaction was complete and the two phases were separated. The aqueous layer was washed twice with 5 mL pentane to remove any residual organic material and then reduced to a volume of 1 mL. The white solid product was precipitated with 15-20 mL ethanol, filtered and dried under vacuum (yield: 92% based on DPPETS; 856 mg).

Spectral Data:

^{1}H NMR $\delta(D_2O)$: 2.62 [t, $J_{P\text{-}H}$ = 12.3 Hz, 4H, (1)CH_2], 7.38 [q*, 4H], 7.56 [t, $J_{H\text{-}H}$ = 7.8 Hz, 4H], 7.73 [s br., 4H], 7.83 [d, $J_{H\text{-}H}$ = 7.8 Hz, 4H].

^{13}C NMR $\delta(D_2O)$: 31.27 [t*, (1)CH_2], 139.14 [s, (2)C-P], 133.89 [s, (3)CH], 147.36 [s, (4)C-SO_3Na], 133.60 [s, (5)CH + (7)CH], 131.95 [s, (6)CH].

^{31}P NMR $\delta(D_2O)$: 52.97 [t, $J_{Pt\text{-}P}$ = 2310 Hz].

Elemental Analysis:

Anal. calcd. for $C_{26}H_{24}Cl_2O_{12}P_2Pt_1S_4$ (M_r = 984.64): C, 31.72; H, 2.46; Pt, 19.81. Calcd. for $C_{26}H_{24}Cl_2O_{12}P_2Pt_1S_4 \times 4H_2O$ (M_r = 1056.74): C, 31.15; H, 3.22; Pt, 19.46.

Found: C, 28.84; H, 2.69; Pt, 8.11.

4.4.F Synthesis of $Ni(CO)_2$(DPPETS)

DPPETS (0.17g, 0.2 mmol) was dissolved in 0.5 mL water and 2.2 mL of a solution (0.1 M) of $Ni(CO)_4$ in THF was added slowly to the phosphine solution at room temperature with vigorous stirring. Argon was bubbled through the mixture during the addition in order to remove the CO. The color of the reaction mixture changed to a pale yellow. After one hour, ^{31}P NMR and IR spectra indicated the presence of the desired product as well as the intermediate state, a nickel tricarbonyl dimer with a bridging DPPETS between two Ni centers. After four hours of stirring the reaction was complete and the solvent was removed under vacuum. The pale yellow crude product was dissolved in 0.5 mL water, filtered and precipitated with 10 mL

acetone. The final product, a white-yellow powder (yield: 88% based on DPPETS; 184 mg) was filtered and dried under vacuum.

Spectral Data:

^{1}H NMR $\delta(D_2O)$: 2.52, 2.61 [2 x s br., 2 x 2H, (1)CH_2], 7.61 [t, J_{H-H} = 7.8 Hz, 4H], 7.85 [t*, 8H], 8.0 9 [d*, 4H].

^{13}C NMR $\delta(D_2O)$: 27.56 [s, (1)CH_2], 139.64 [t, J_{C-P} = 15.3 Hz, (2)C-P], 137.22 [t*, (3)CH], 145.6 [d*, (4)C-SO_3Na], 132.24 [d*, (6)CH], 131.21 [t, J_{C-P} = 9.1 Hz, (7)CH], 202.28 [s, CO].

^{31}P NMR $\delta(D_2O)$: 48.47 [s].

IRν**CO**(D_2O): 1953.9(vs), 2010.1(s), cm^{-1}.

Elemental Analysis:

Anal. Calcd. for $C_{28}H_{20}Na_4O_{14}S_4P_2Ni_1$ x $4H_2O$ (M_r = 993.38): C, 33.85; H, 2.82.

Found: C, 34.21; H, 3.01.

Chapter 5
Results and Discussion

5.1 Results of Syntheses and Characterization

5.1.1 Sulfonation of DPPE to Yield DPPETS

The sulfonation of DPPE results in a mixture of *meta* sulfonated products and analogous oxides, but by rigorous attention to reaction times and Schlenk techniques the optimum yield of tetra-sulfonated unoxidized product can be obtained. The ^{31}P NMR spectra of the aliquots taken at various times during the reaction (Figure 25) indicate the best time to terminate the reaction. The shaded peak in the inset is assigned to DPPETS and typically represents about 55% of the total phosphorus by integration. The overall yield, based upon DPPE, is about 30 - 40%; the low, variable yield is attributed to oxide formation, which is changeable from experiment to experiment as well as the number of intermediate sulfonations possible (Figure 26). This in turn is attributed to the lack of control over the SO_3 content of the oleum. It is felt that most oxidation results from the reaction medium rather than improper handling. Fractional crystallization with methanol followed by selective precipitation with acetone produces DPPETS that can be considered >99% pure based upon the ^{31}P NMR spectrum of the final product. Figure 27 depicts a flow chart for the sulfonation of DPPE. DPPETS is relatively air-stable.

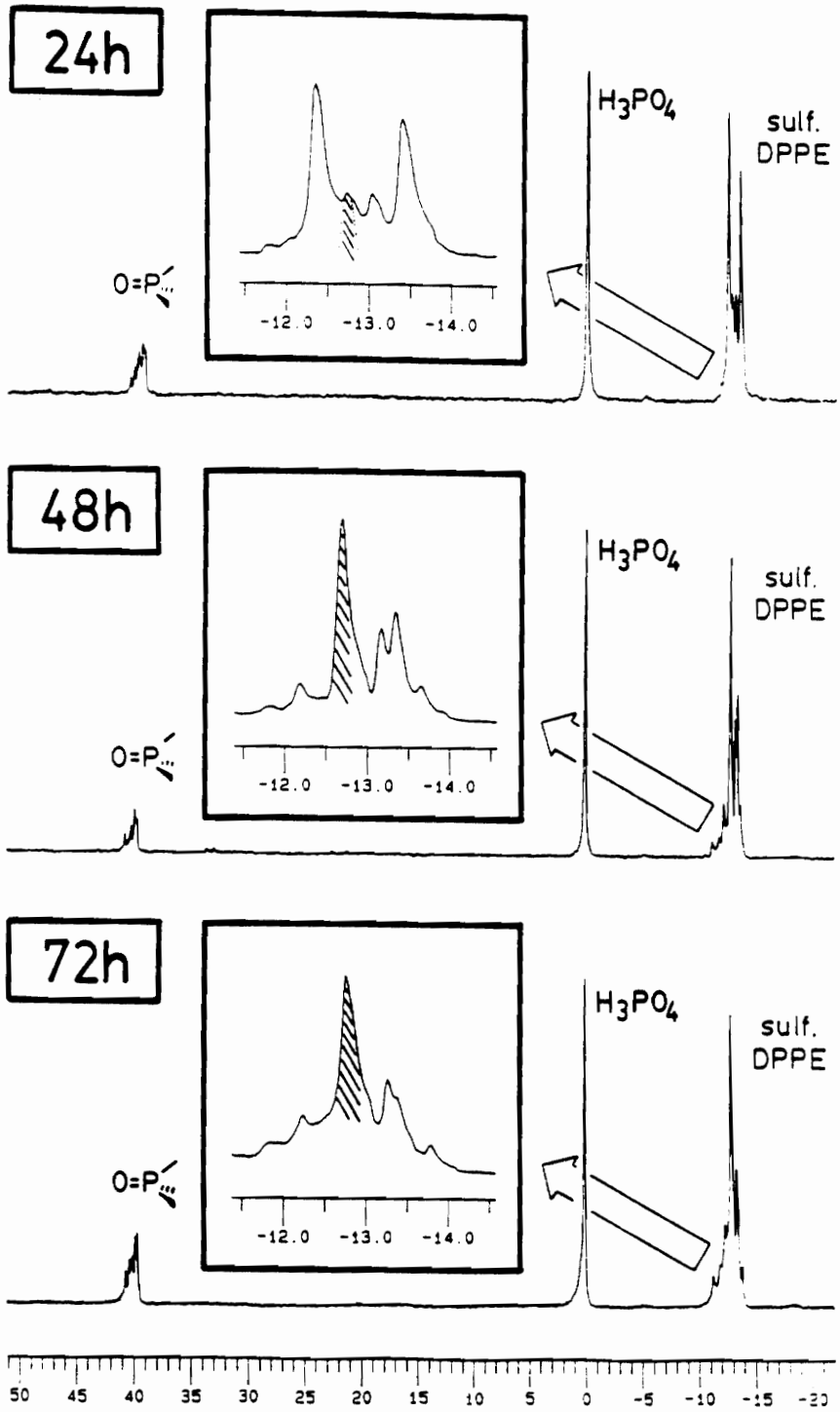

Figure 25. ^{31}P spectra of aliquots (in D_2O) taken during the course of the sulfonation reaction of DPPE.

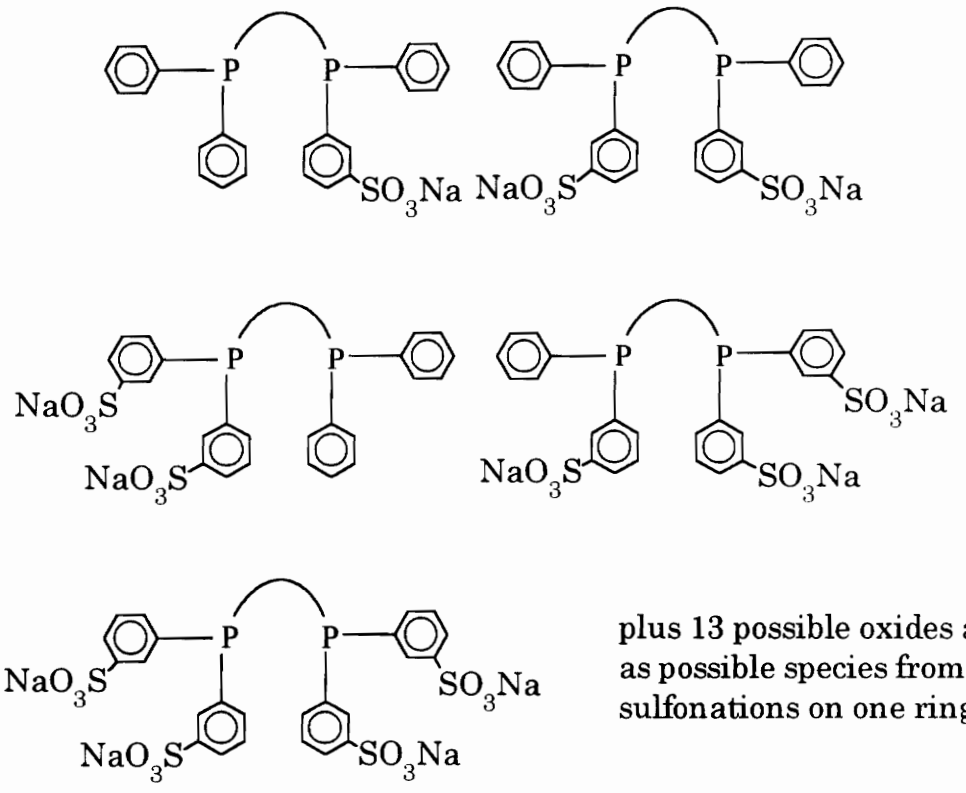

Figure 26. Possible intermediate sulfonation products.

There have been numerous attempts to separate sulfonated products by various methods.[12,16] This method is a variation of the method developed to separate TPPTS from its oxides,[47] and is simple and efficient.

Figure 28 represents the ^{31}P NMR spectrum of purified DPPETS. The quality of the signal to noise ratio indicates the presence of less than 1% impurities. ^{13}C and ^{1}H NMR spectra for DPPETS are shown in Figures 29 and 30.

In the ^{31}P NMR spectra of the aliquots, it appears that the more sulfonation on the molecule, the farther downfield the shift. It also seems

that more than tetra-sulfonation is possible, but this has not been confirmed. The resonances for the oxides appear downfield between δ = 39 - 43 ppm. No attempt has been made to separate the oxides or characterize them. The resonances in the ^{13}C spectrum were assigned on the basis of electronegativity.

The ^{1}H spectrum is interesting in that the triplet (inset, Figure 30) results from phosphorus coupling to hydrogen. The triplet arises from the fact that the hydrogen atoms see phosphorus atoms that appear to be inequivalent atoms but are in fact magnetically and chemically equivalent. A doublet of doublets is expected, but coincidentally the inner resonances lie atop each other. The pattern in the aryl region is consistent with *meta* substitution.

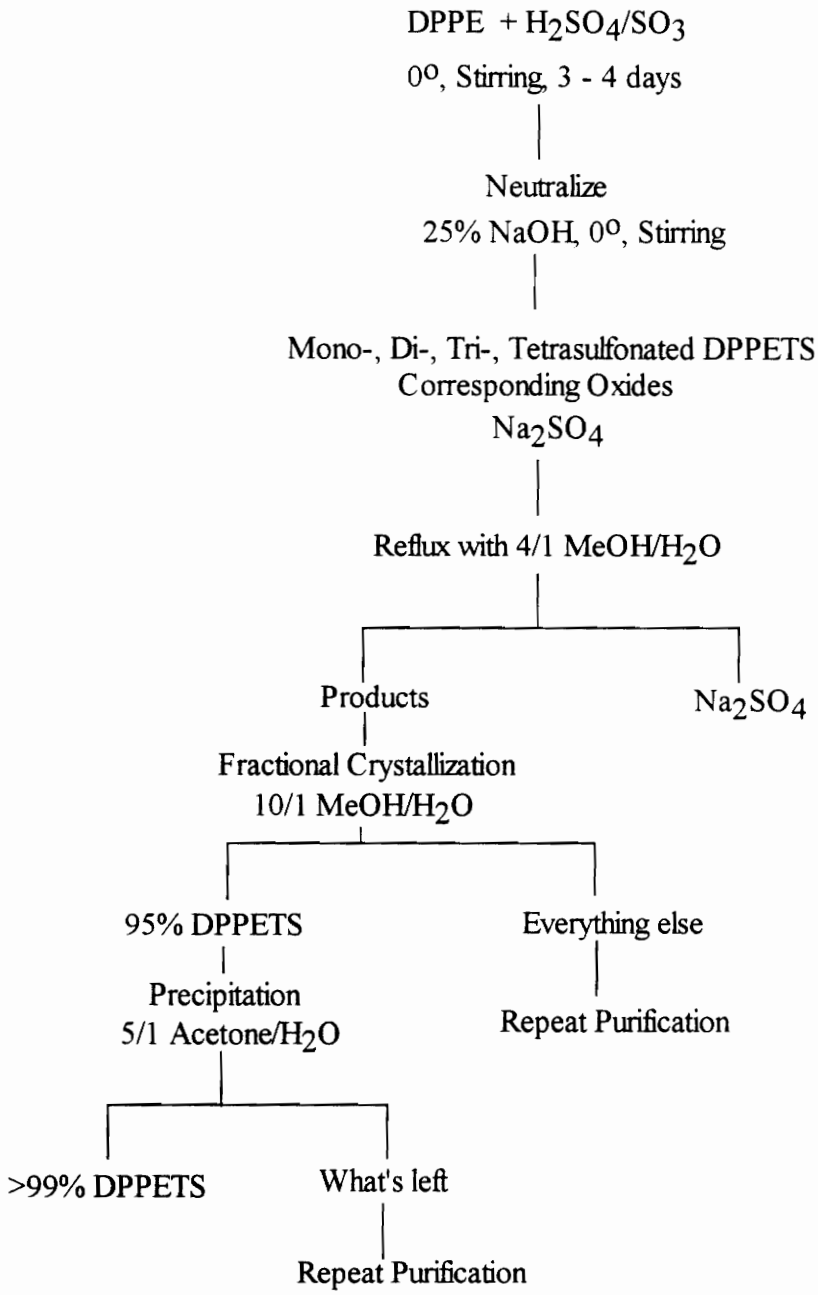

Figure 27. Flow chart for the sulfonation of DPPE to yield DPPETS.

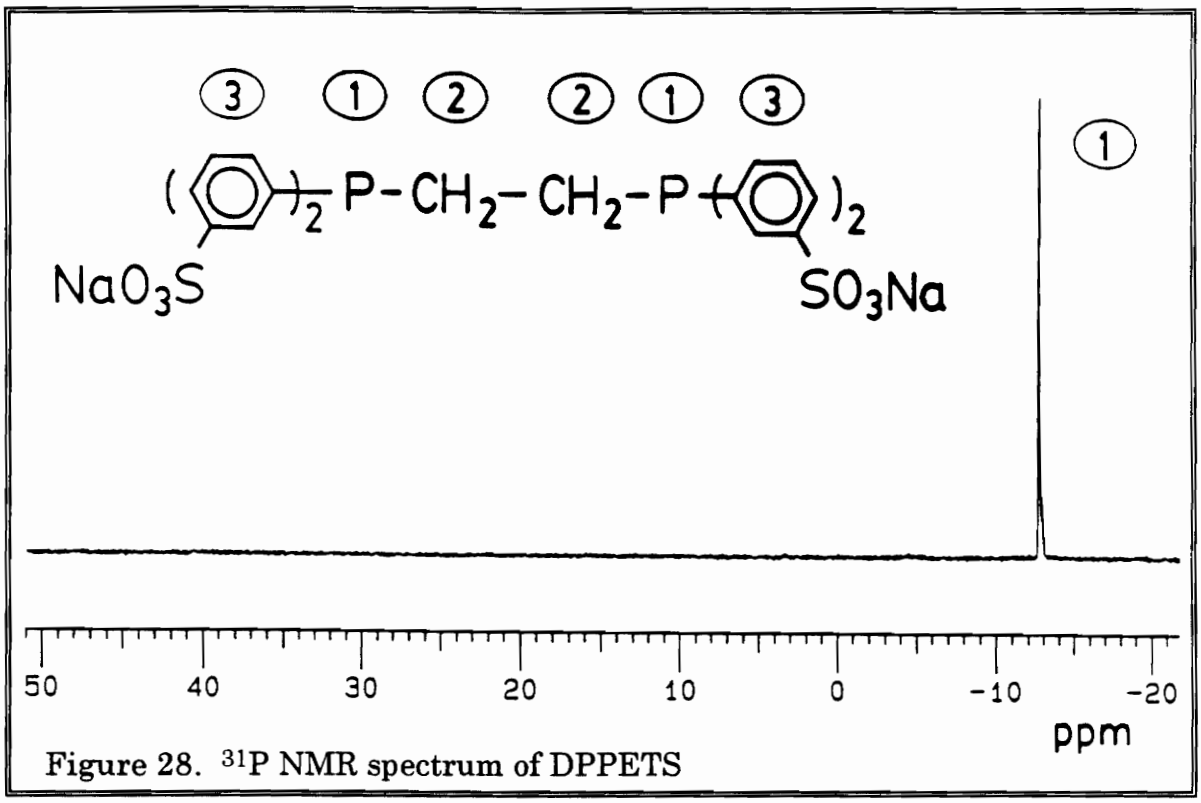

Figure 28. ^{31}P NMR spectrum of DPPETS

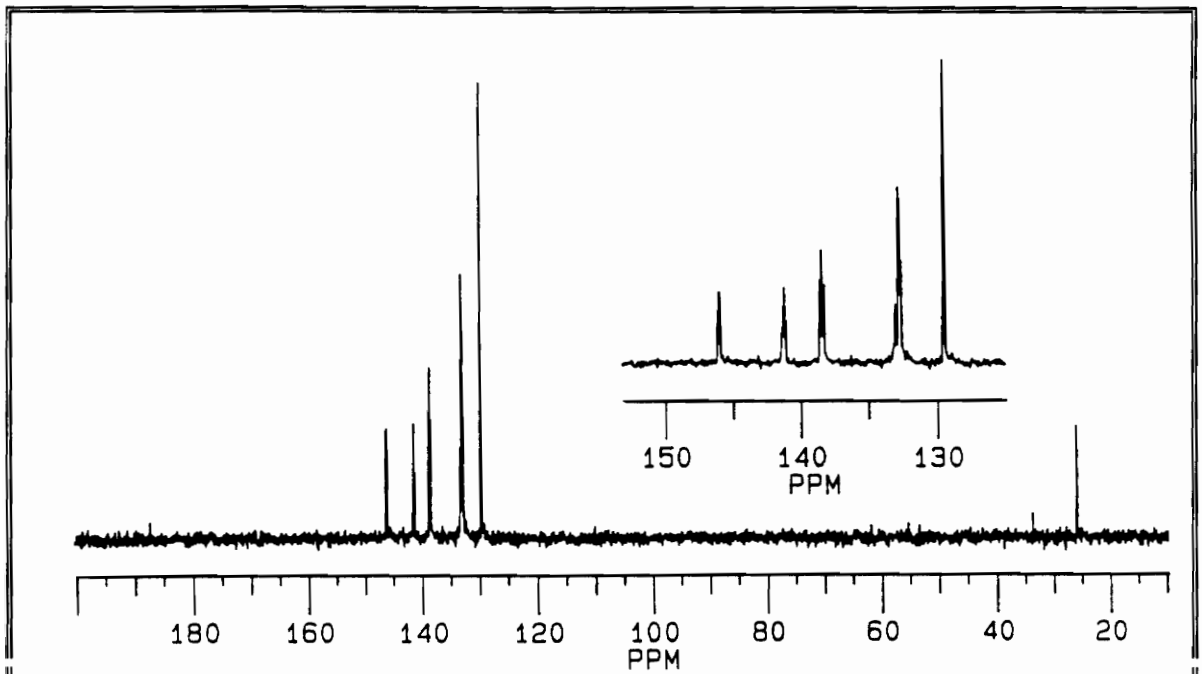

Figure 29. ^{13}C NMR spectrum of DPPETS.

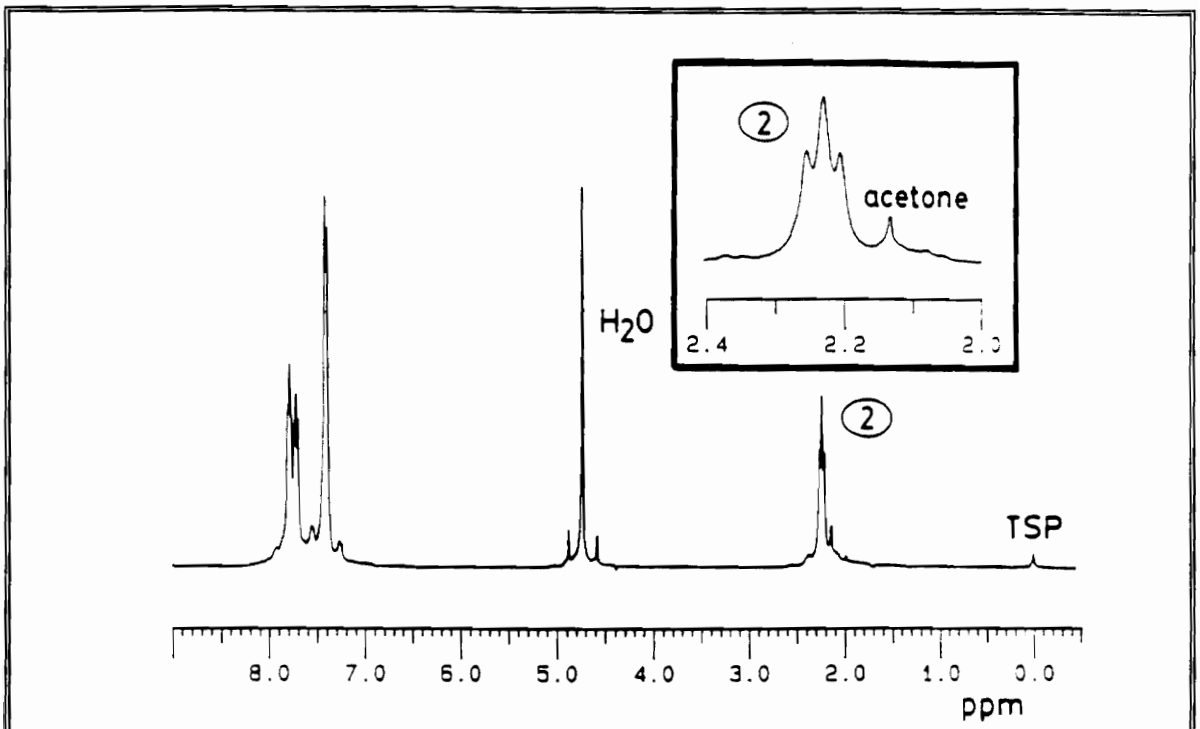

Figure 30. ^{1}H NMR spectrum of DPPETS.

Figure 31 shows the titration curve for DPPETS. Titration was accomplished by carefully acidifying a measured solution of DPPETS with HCl and titrating with aqueous NaOH. While trisulfonated tris-ω-phenylalkyl phosphines form stable phosphonium salts in water at pH between 7 - 10.5, DPPETS shows no evidence of this behavior in this pH range. There is an inflection point at pH = 6.6 which is assigned to different phenylsulfonato groups bound to the same phosphorus atom. This situation is also seen in TPPTS.[48] The equivalence point for DPPETS is found at pH = 7.8. Potentiometric data can be found in Appendix A.

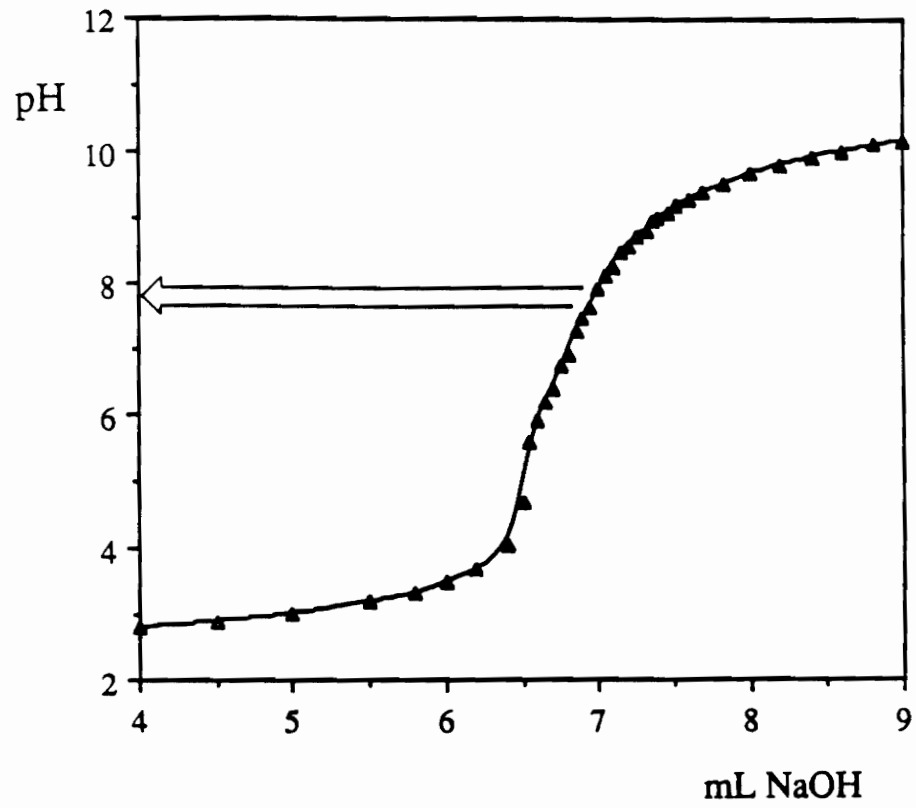

Figure 31. Potentiometric titration curve for DPPETS.

Elemental Analysis, Mass Spectrum:

The C,H elemental analysis is consistent with the hexa-hydrate. While a thermogravimetric analysis has not been performed on DPPETS, a number of TGA's were obtained for TPPTS and showed conclusively that TPPTS precipitates with varying water content. It seems reasonable to assume that DPPETS would have the same property. The fast-atom-bombardment mass spectrum gave a very poor signal to noise ratio, but a peak at 807 assigned to $[MH]^+$ was observed. Additional peaks at 785 and 763 were also observed; these can be assigned to the net loss of sodium with concomitant gain of a proton.

5.1.2 Complexes Synthesized With DPPETS as a Ligand

5.1.2.A $Ni(CO)_2$(DPPETS)

This complex was synthesized in order to determine the relative electron-donating ability of DPPETS. The infrared data[136] for the unsulfonated analog of the complex shows carbonyl stretching bands at 1998 and 1936 cm^{-1} while the sulfonated complex $Ni(CO)_2$(DPPE) shows bands at 2010 and 1954 cm^{-1}. The inductive effect of the electron withdrawing sulfonato groups reduces the donating ability of water-soluble phosphines. It has also been found that trisulfonated triphenylphosphine (TPPTS) is less electron donating than triphenylphosphine.[48]

5.1.2.B $PdCl_2$(DPPETS-H)

The palladium complex was made for use in carbonylation catalysis. There was nothing unusual about the spectral data. It is similar to its non-sulfonated analog. While it is known that chloro palladium and platinum complexes undergo hydroolysis reactions in water, $PdCl_2$(DPPETS-H) is stable at pH's ranging from 2-10.

5.1.2.C $Rh(DPPETS)_2Cl$

$Rh(DPPETS)_2Cl$ could be prepared from either $Rh(acac)(C0)_2$ or $Rh_2COD_2CL_2$. When $Rh(acac)(C0)_2$ was used, inevitably the products was the bis-DPPETS compound, whereas $Rh_2COD_2Cl_2$ would give $Rh(DPPETS)_2^+$ or Rh(COD)(DPPETS)Cl depending upon concentration. The ^{31}P NMR spectrum (Figure 32) shows a doublet at 60.7 ppm with a coupling

constant J_{Rh-P} = 132.7 Hz. This is in excellent agreement with the unsulfonated analog, $Rh(DPPE)_2Cl$, with δ = 55.2 ppm and J_{Rh-P} = 133 Hz.[133] The ^1H spectrum (figure 33) is also consistent with the compound. This compound formally contains Rh(I), which is cationic if one ignores the charges on the sulfonato groups.

All efforts to generate and detect a hydride were fruitless. If one of the sulfonato groups weakly coordinates to the rhodium, the compound could be considered zwitterionic in the sense that the counterion to the Rh(I) center is part of the same complex.

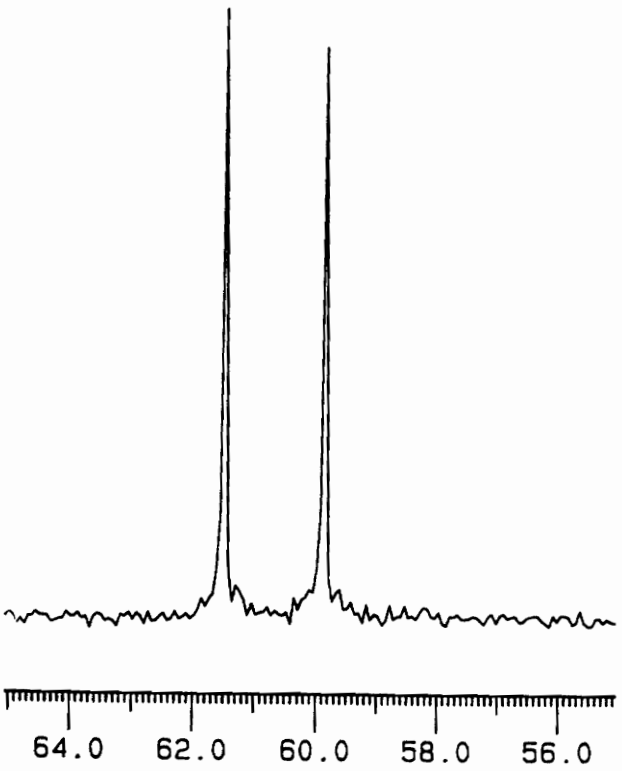

Figure 32. ^{31}P NMR spectrum of $Rh(DPPETS)_2Cl$.

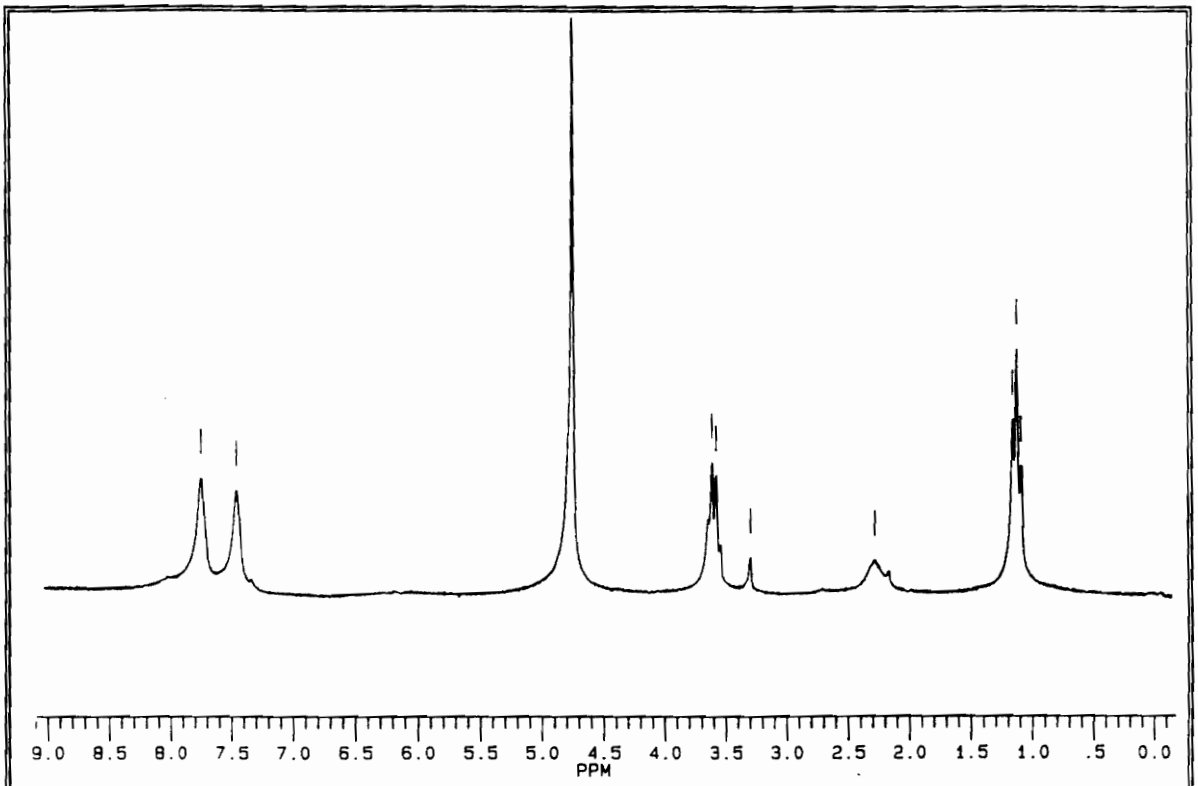

Figure 33. ^{1}H NMR spectrum of $Rh(DPPETS)_2Cl$.

5.1.2.D Rh(COD)(DPPETS)Cl

This compound is prepared from $Rh_2COD_2Cl_2$. A dilute solution of both the rhodium dimer and DPPETS is essential or the bis-DPPETS product $Rh(DPPETS)_2^+$ will form. The ^{1}H NMR spectrum (Figure 34) is remarkable in that the four aryl proton resonances are well-resolved and can be assigned. In the ^{31}P spectrum (Figure 35) the coupling constant J_{Rh-P} = 151.7 Hz is quite a bit larger than that of $[Rh(DPPETS)_2]Cl$ (J_{Rh-P} = 132.7 Hz.) and the resonances for the two componds are very close. $\delta(D_2O)$ for Rh(COD)(DPPETS)Cl = 59.24 ppm, while $\delta(D_2O)$ for $Rh(DPPETS)_2CL$ = 60.71. The ^{13}C spectrum is straightforward (Figure 36).

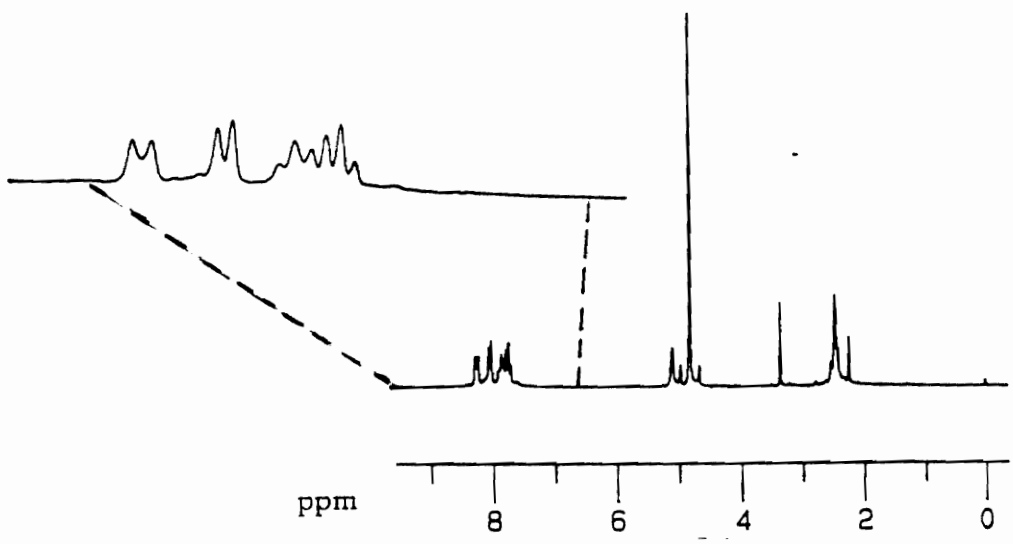

Figure 34. ^{1}H NMR spectrum of Rh(COD)(DPPETS)Cl.

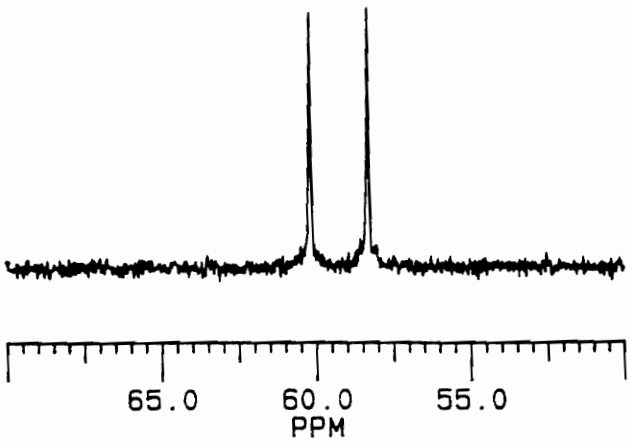

Figure 35. ^{31}P NMR spectrum of Rh(COD)(DPPETS)Cl.

The assignments of the peaks for the ^{13}C NMR spectrum for Rh(COD)(DPPETS)Cl are found on page 73. The inset in Figure 36 is the aryl region, with the resonance at 106 ppm being that of the sp^2 carbons on the COD moiety. The sp^3 carbons on COD are coincidentally equivalent at 32 ppm with the methylene carbons from DPPETS.

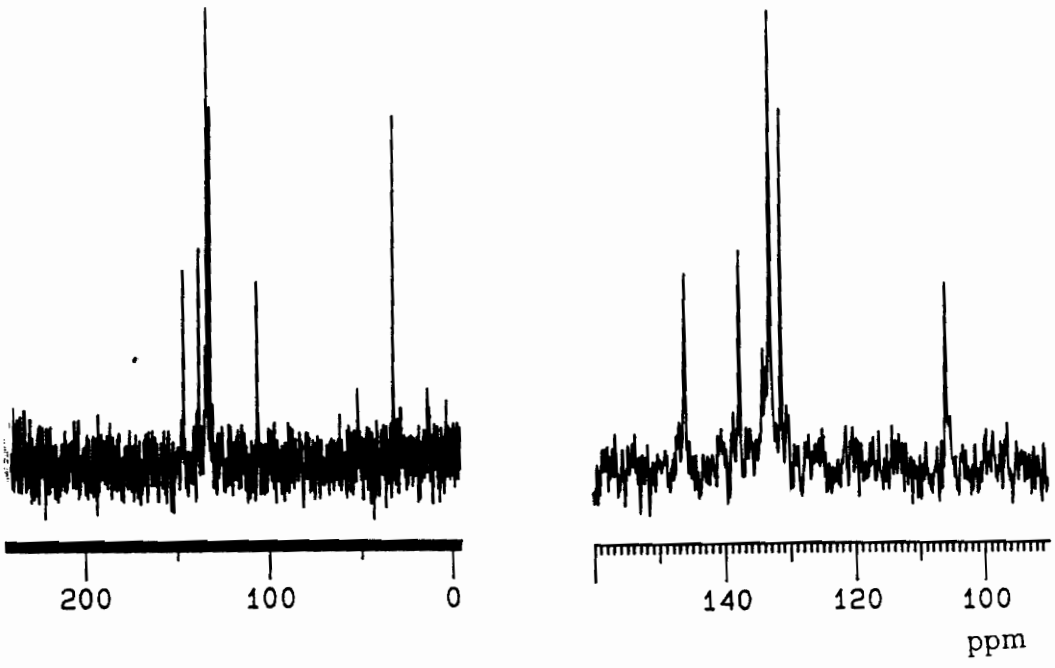

Figure 36. ^{13}C NMR spectrum of Rh(COD)(DPPETS)Cl.

5.1.2.E $Pt(DPPETS\text{-}H)Cl_2$

The ^{31}P NMR spectrum of $Pt(DPPETS\text{-}H)Cl_2$ (Figure 37) shows an apparent triplet at $\delta(D_2O) = 52.97$, with the intensity of the center peak approximately three times that of the outer peaks. The outer satellite peaks result from phosphorus with 100% spin 1/2 abundance coupling with ^{195}platinum, which has spin = 1/2 and 33.7% abundance. The center peak is from uncoupled phosphorus, since the remaining natural isotopes of platinum do not possess spin. A large isotropic J coupling constant (on the order of 3000 - 4000 Hz) is typical of platinum-phosphine compounds where there is *cis* geometry,[9, 138] and on the order of 1700 - 2500 Hz. for *trans* geometry. However, we found a coupling constant $J_{Pt\text{-}P} = 2310$ Hz, more consistent with *trans* geometry. This can be rationalized in view of the added steric distortions caused by the large sulfonate groups on the phenyl rings.[139] ^{35}Cl NMR spectra of this complex and $Pt(PhCN)_2Cl_2$ were compared for the presence of chlorine and were found to be remarkably similar. The complex was also found to be very stable at pH = 2 - 10. Another possibility is that the complex is actually octahedral with platinum (IV). This could result from the oxidative addition of HCl to Pt(II); the coupling constant data are more consistent with this oxidation state.

The ^1H NMR spectrum (Figure 38) displays four well-resolved peaks in the aryl region corresponding to the aryl protons . The triplet at $\delta = 2.62$ ppm is consistent with the methylene protons. The ^{13}C NMR spectrum (Figure 39) is unremarkable. The acid form of DPPETS (DPPETS-H) was used in making this and the palladium complex because both metals have a tendency to lose chloride and coordinate with solvent at pH > 7. The

analogous platinum complex, $Pt(DPPE)Cl_2$ has a chemical shift of 41.4 ppm in CH_2Cl_2 and $J_{Pt\text{-}P} = 3618$ Hz.[141]

This platinum complex has been sent to the National Cancer Institute via Starks CP Laboratories, Rockville, MD for testing as a possible anti-tumor agent. DPPE has shown anti-tumor activity.[140]

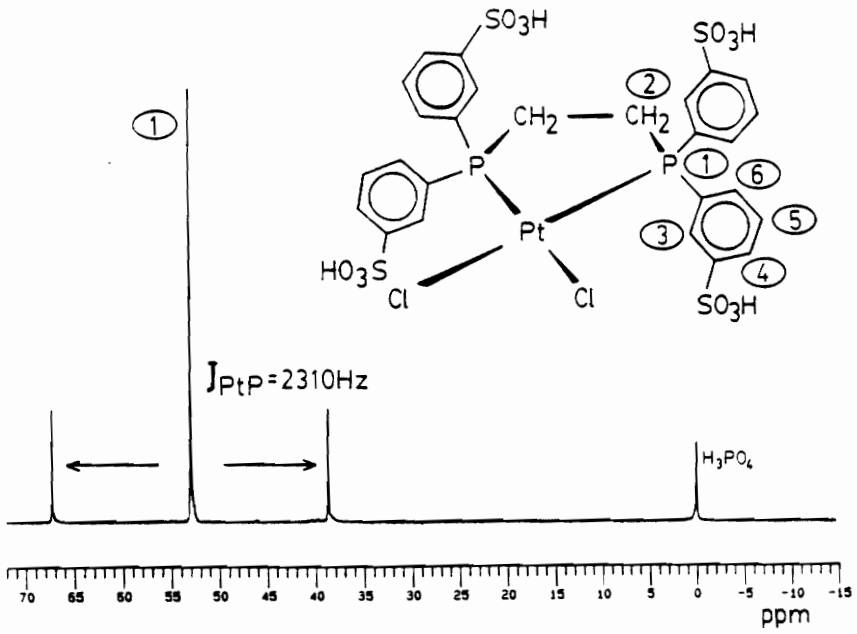

Figure 37. ^{31}P NMR spectrum of $Pt(DPPETS\text{-}H)Cl_2$

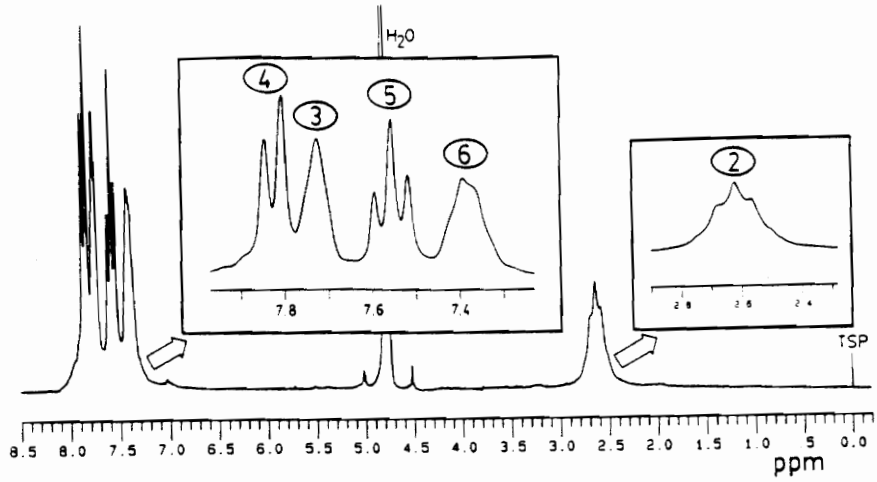

Figure 38. ^{1}H NMR spectrum of Pt(DPPETS-H)Cl_2

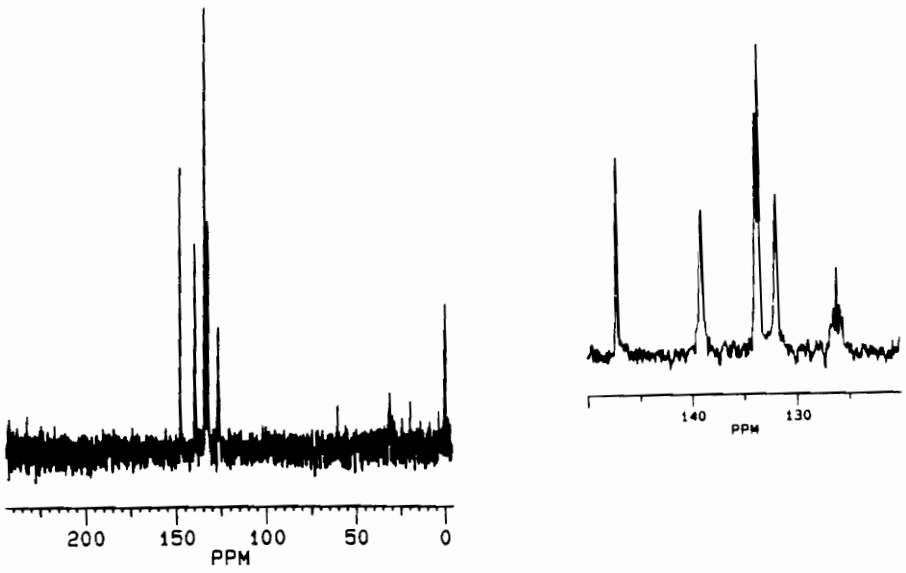

Figure 39. ^{13}C NMR sectrum of Pt(DPPETS-H)Cl_2

5.2 Results of T_1 Studies

5.2.1 T_1 and CSA Studies on DPPETS and Derived Complexes

^{31}P spin-lattice relaxation times in both solution- and solid-state were found for DPPETS and the complexes (except $Ni(CO)_2$(DPPETS)). The results are summarized in Table 1.

Table 1. ^{31}P T_1 values (solution- and solid-state) for DPPETS and derived complexes.

Compound	T_1, s (solution)‡	T_1, s (solid)‡‡
DPPETS	2.5	370
$Rh(DPPETS)_2Cl$	0.46	33
Rh(COD)(DPPETS)Cl	0.89	≈120*
$Pd(DPPETS\text{-}H)Cl_2$	0.59	---------
$Pt(DPPETS\text{-}H)Cl_2$	0.86	55

‡ at 9.4 Tesla
‡‡ at 7.05 Tesla
* this measurement is an estimate.

Interestingly, the T_1 of the free ligand is longer than any of the complexes, both in solid- and solution state. The T_1 plots of DPPETS, $Rh(DPPETS)_2Cl$ and $Pt(DPPETS\text{-}H)Cl_2$ are shown in figure 40. Included for the sake of comparison is the T_1 value of the unsulfonated analog of DPPETS, DPPE.

Table 2 compares the ^{31}P chemical shifts of the compounds in solid- and solution-state. It is informative to compare these values to see the effect of solvent interactions. All solution studies were done in degassed D_2O. There is a large difference in chemical shift upon comparing solution- to solid-state for Rh(COD)DPPETS)Cl. The only probable coupling in the solid-state spectra was observed for Pt(DPPETS-H)Cl_2. In the expanded solid-state spectrum two shoulders are barely visible at 60.886 ppm and 42.006 ppm, corresponding to the satellite coupling J_{Pt-P} = 2294 Hz. (Figure 41).

Table 2. ^{31}P NMR Chemical shifts of DPPETS and derived complexes in solid- and solution state.

Compound	δ, ppm (D_2O)	δ_{iso}, ppm (solid)
DPPETS	-12.45(s)	-13.4
Rh(DPPETS)$_2$Cl	60.71(d,J_{Rh-P}=132.7Hz)	63.5
Rh(COD)(DPPETS)Cl	59.24(d,J_{Rh-P}=151.7Hz)	77.3
Pd(DPPETS-H)Cl_2	61.21(s)	
Pt(DPPETS-H)Cl_2	52.97(t*,J_{Pt-P}=2310 Hz)	52.1

*not a true triplet; see text

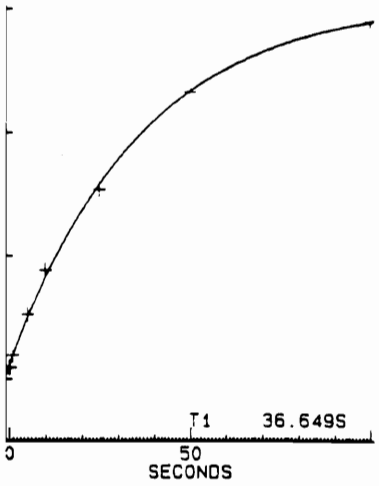

DPPETS

T_1 = 366 s

Program loop = 10

DPPE

T_1 = 171 s

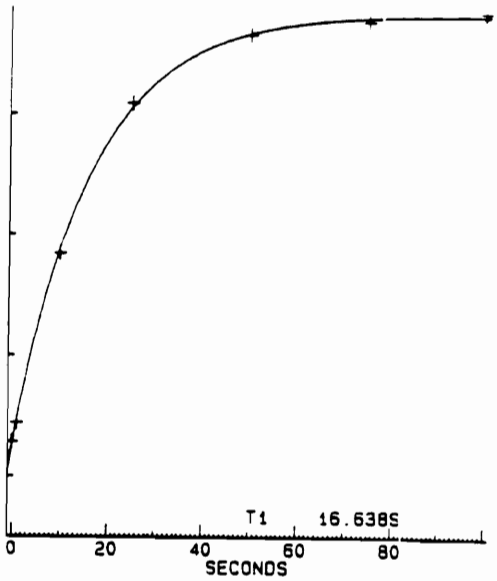

$Rh(DPPETS)_2Cl$

T_1 = 33 s

Program loop = 2

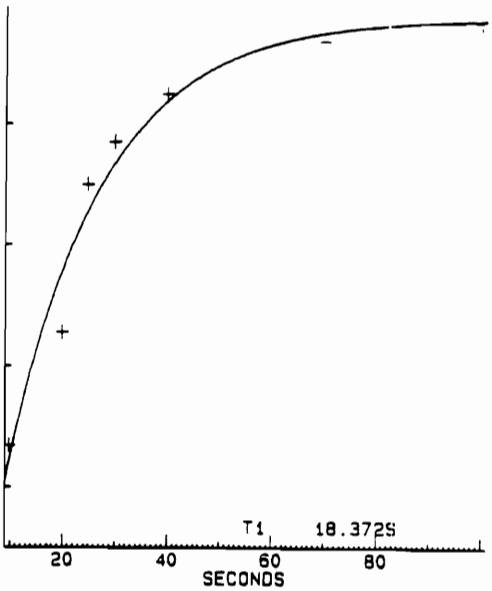

$Pt(DPPETS\text{-}H)Cl_2$

T_1 = 55s

Program loop = 3

Figure 40. ^{31}P T_1 plots of DPPETS and selected complexes in the solid-state.

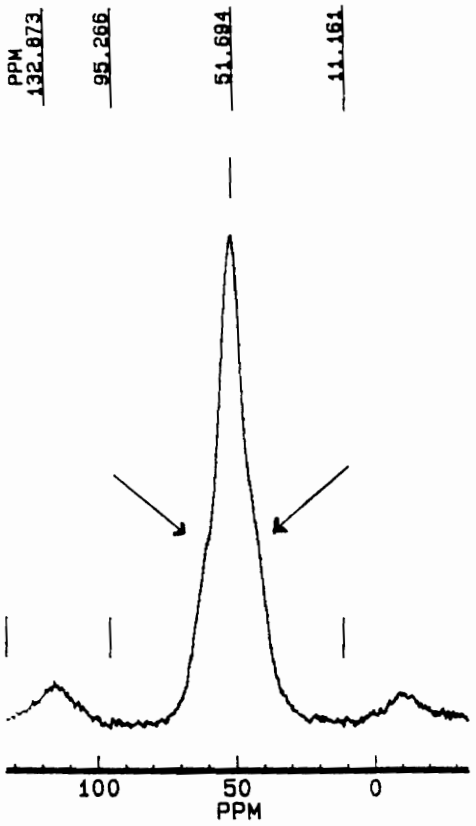

Figure 41. Expanded ^{31}P solid-state NMR spectrum of Pt(DPPETS-H)Cl_2; spin rate = 7500 Hz. Satellite peaks are barely visible as shoulders.

Fast- and slow-spinning experiments were undertaken to determine the isotropic chemical shift and the magnitude of the CSA for DPPE, DPPETS and Pt(DPPETS-H)Cl_2. Figures 42 and 43 depict the results for DPPETS and Pt(DPPETS-H)Cl_2. Table 3 lists the absolute magnitudes ($|\sigma_{33} - \sigma_{11}|$) of the chemical shift anisotropy at room temperature for all the complexes measured. The CSA of DPPETS can be almost eliminated by spinning at the magic angle at 8500 Hz. The powder pattern indicates the magnitude of the CSA at 83 ppm, which means that with dipolar interactions

eliminated by high power decoupling that spinning at 10,000 Hz. would eliminate the CSA.

The three complexes listed in Table 3 have very large CSA values, and normal spin rates can not completely eliminate the CSA (Figure 44). The small peak in the spectrum of $Rh(DPPETS)_2Cl$ at about -10 ppm is assigned to free DPPETS. The ^{31}P spectrum of RH(COD)(DPPETS)Cl appears to be that of two compounds; it is believed that the second compound is $Rh(DPPETS)_2Cl$. Rh(COD)(DPPETS)Cl is relatively unstable and gradually metamorphoses into the bis-compound. This has also been observed for mono-phosphines.[72,73]

Table 3. Magnitude of chemical shift anisotropy for DPPETS, DPPE, and some derived complexes.

Compound	CSA, ppm	CSA, Hz.
DPPE	65	7,897
DPPETS	83	10,084
$Rh(DPPETS)_2Cl$	200*	24,000
$Pt(DPPETS\text{-}H)Cl_2$	150	18,224
Rh(COD)(DPPETS)Cl	200*	24,000

*Estimated on the basis of two experiments

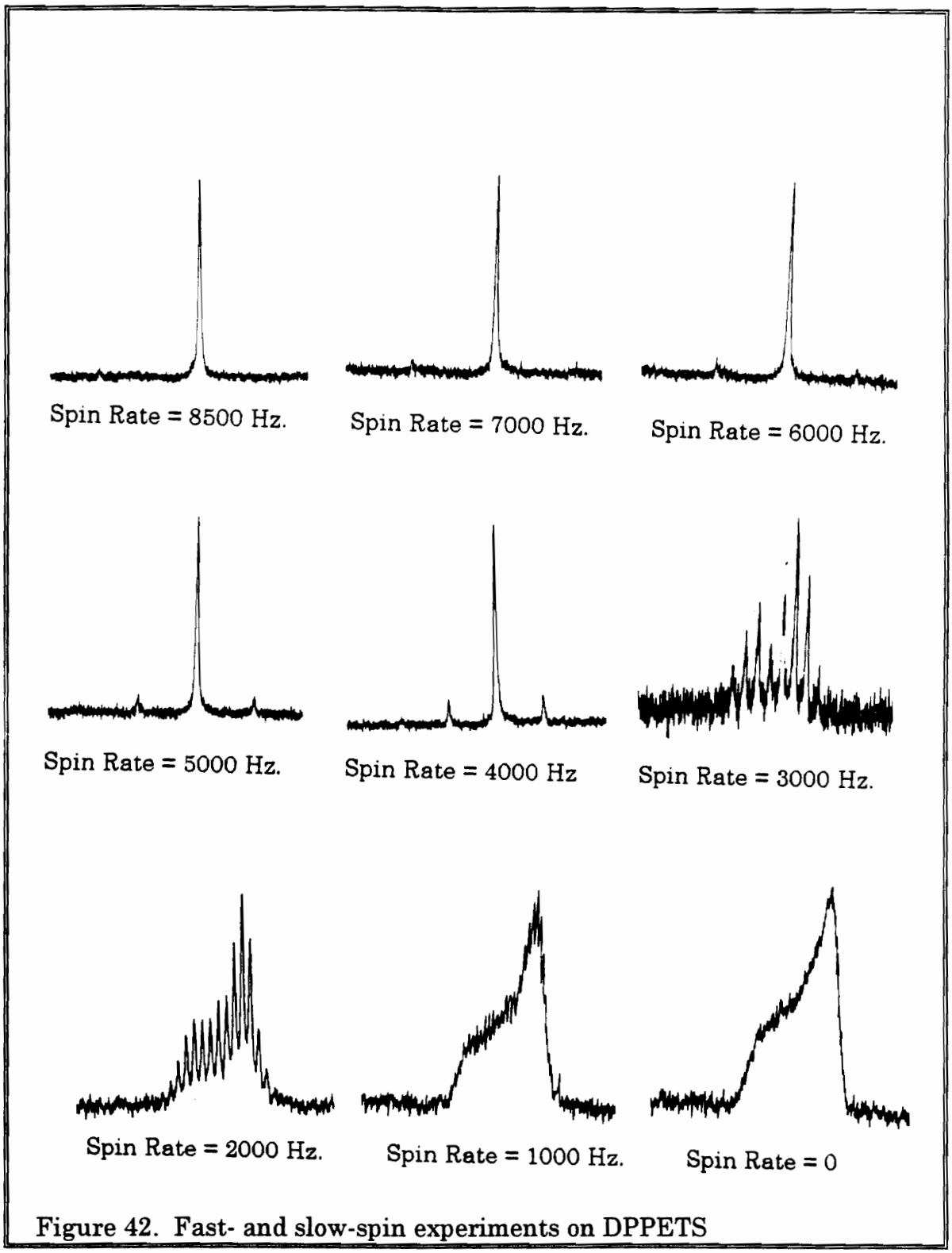

Figure 42. Fast- and slow-spin experiments on DPPETS

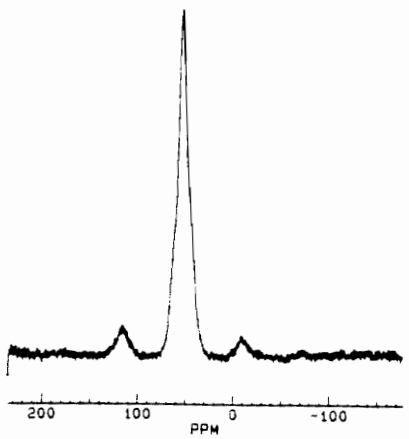

Spin rate = 7500 Hz.

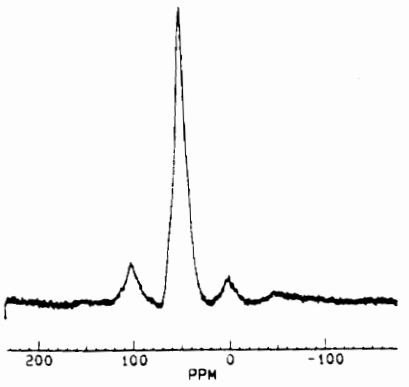

Spin rate = 6000 Hz.

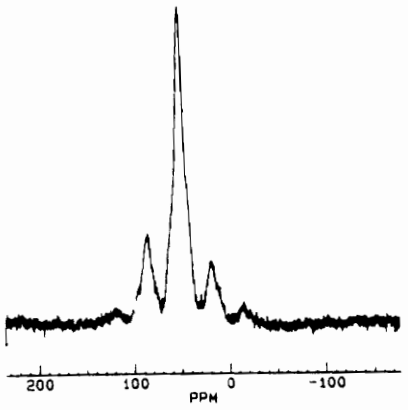

Spin rate = 4000 Hz.

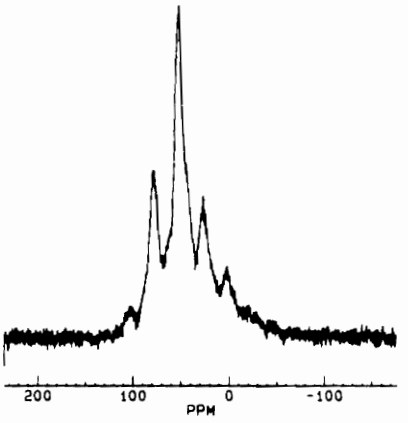

Spin rate = 3000 Hz.

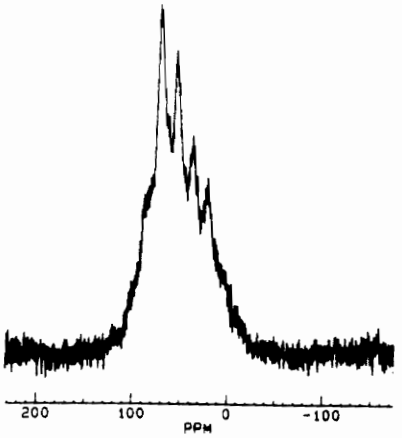

Spin rate = 2000 Hz.

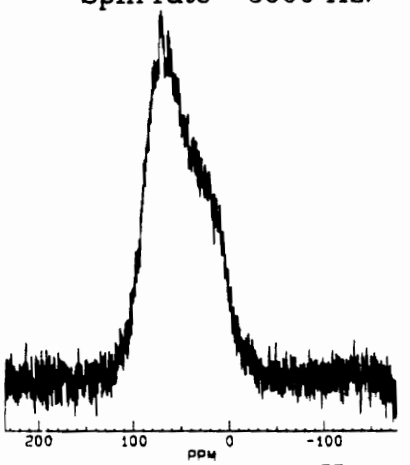

Spin rate = 1000 Hz.

Figure 43. Fast- and slow-spin experiments on Pt(DPPETS-H)Cl_2.

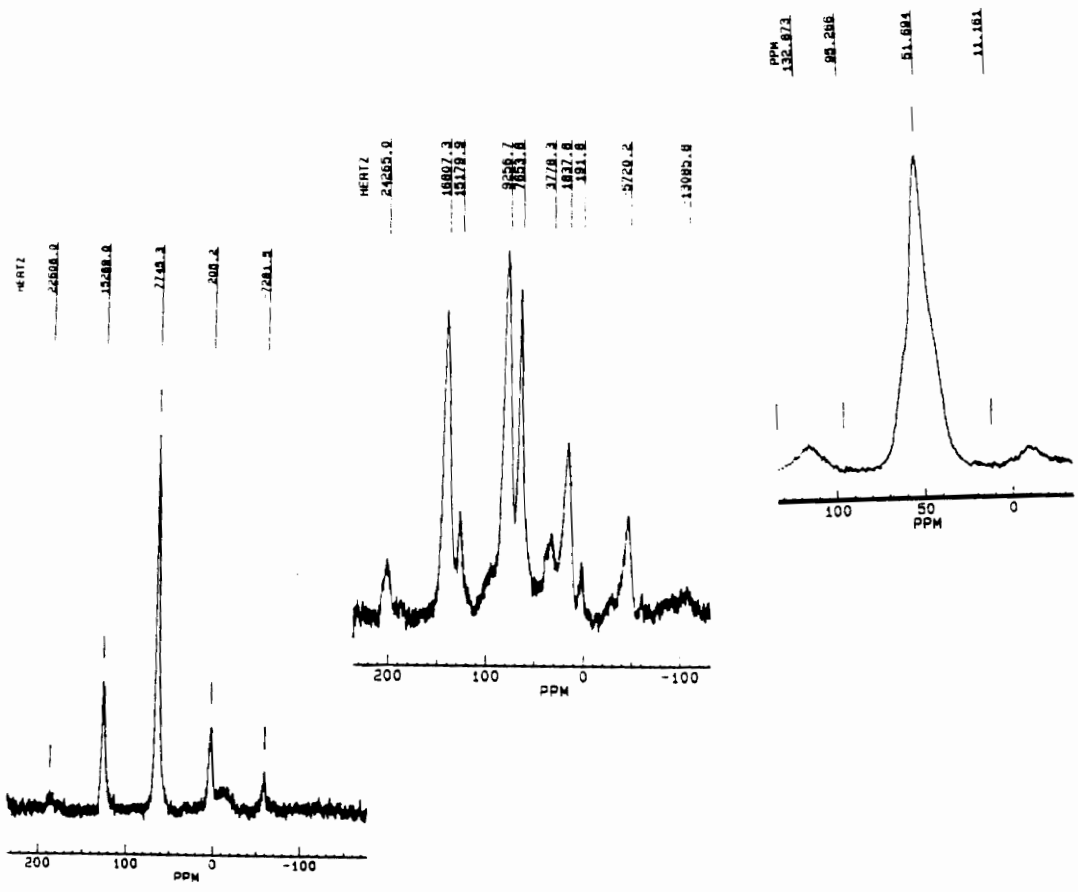

Figure 44. ^{31}P solid-state spectra of $Rh(DPPETS)_2Cl$, $Rh(COD)(DPPETS)Cl$ and $Pt(DPPETS\text{-}H)Cl_2$ at spinning rates greater than 7500 Hz.

Interestingly, based upon the shapes of the powder patterns, all the above compounds have axial symmetry, except DPPE. Powder patterns for DPPE and DPPETS are shown in Figure 45 for comparison. The approximate isotropic chemical shift is indicated with an arrow.

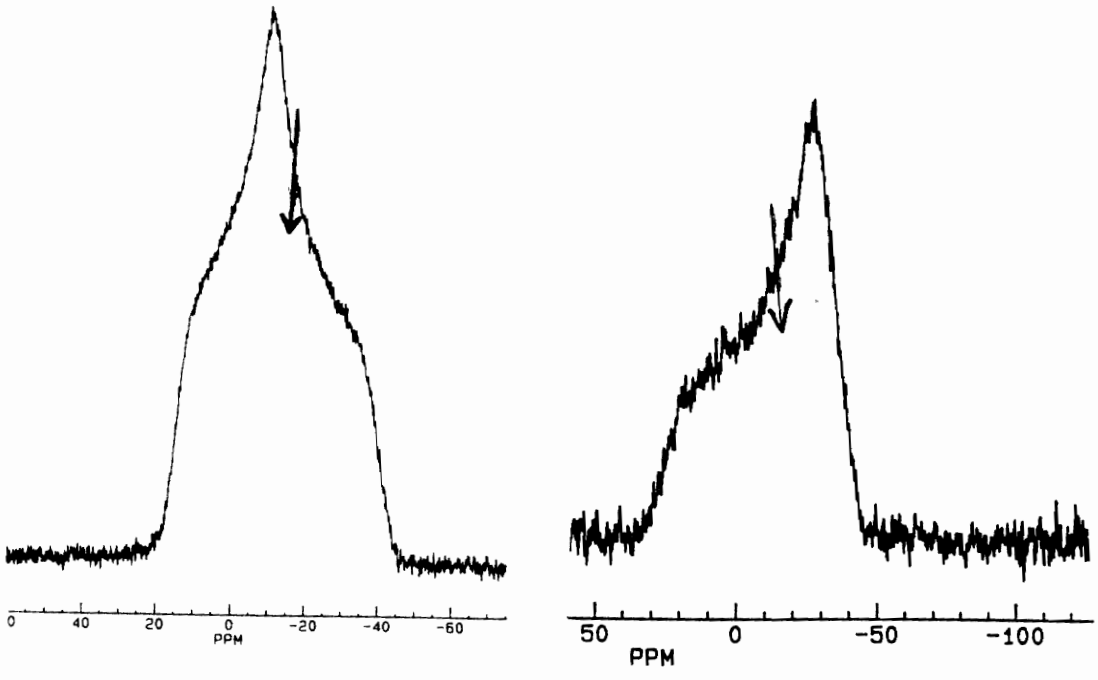

DPPE DPPETS

Figure 45. ^{31}P NMR powder patterns for DPPE and DPPETS. The approximate isotropic chemical shift is indicated with an arrow.

5.2.2 T_1 Studies on Supported Aqueous Phase Catalysts

Arhancet[17] found that by immobilizing a water-soluble catalyst on CPG-240 glass the rate of hydroformylation of terminal higher olefins approached that of homogeneous catalysis, without the problem of leaching and loss of the catalyst. He also found that the rate of hydroformylation of the organic substrate is proportional to the amount of water present in the support. Figure 46 is a plot of percent conversion as a function of time the supported phase was exposed to water vapor (hence the wt.% water, as is shown at the top of the graph).

It can be seen that at low wt.% water (2.9 wt.% by thermogravic methods) that there is a minimum of catalytic activity, while at 45 wt.% water the catalytic activity has virtually ceased. At 8.5 wt.% water the activity has reached a maximum. It was postulated that at small amounts of water the immobilized catalyst had limited mobility, and at large amounts of water, the pores of the support were filled and the organic substrate was unable to interact with the catalyst.

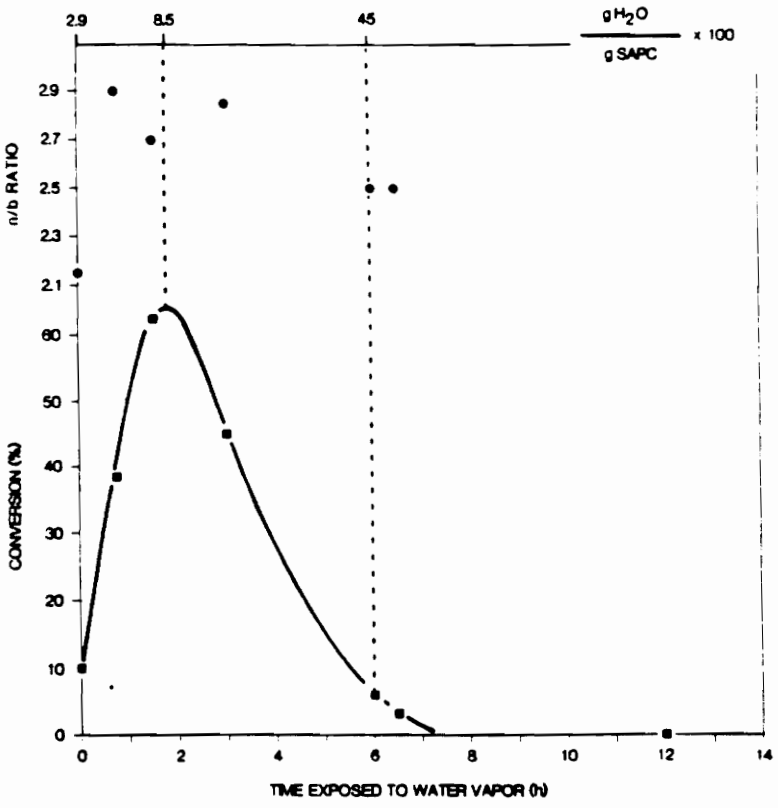

Figure 46. The influence of water in the SAP hydroformylation of 1-octene.[17]

It was also found that at 2.9 wt.% water, magic angle spinning techniques were required to obtain a resolved solid-state ^{31}P NMR spectrum of the supported phase, while at 45 wt.% water, what appeared to be a dry, free-flowing solid could be placed in an NMR tube and examined under solution conditions and produce a well-resolved spectrum.

There appeared to be a point at which a "liquid-like" character was taken on by the immobilized phase; that is, the immobilized phase seemed to behave as though it were free in solution; the question of the point at which this phenomenon occurs was addressed by measuring the spin-lattice relaxation (T_1) values of TPPTS and the complex $HRh(CO)(TPPTS)_3$ as pure materials and supported on the glass. T_1 relaxation is a complicated event that, as has been explained previously, depends upon several mechanisms. In the solid state however, two mechanisms dominate and both are related to the correlation time (τ_C) of the molecule (Figure 47).

$$\frac{1}{T_{1CSA}} = (\text{constants}) B_o^2 \left(\sigma_{\parallel} - \sigma_{\perp} \right)^2 \tau_C$$

$$\frac{1}{T_{1DD}} = (\text{constants}) \frac{\gamma_A^2 \gamma_X^2}{r^6} \tau_C$$

Figure 47. The relationship between the dominant T_1 spin-lattice relaxation mechanisms in the solid state and the correlation time, τ_C.

In the solid-state, when spin-lattice relaxation rates are slow the molecular correlation time τ_C is long indicating little motion. For a short T_1

in the solid state, there is more motion and as a result the correlation time is short. The T_1 times were measured by the inversion-recovery method outlined in the experimental section. The T_1 plots were generated by the program TIPLOTS . Each experiment yielded a data point, and required at least four transients to give a reasonable signal to noise ratio.

TPPTS, TPP, TPPTS=O, TPP=O, DPPE and DPPETS were investigated by solution- and solid-state NMR methods. The solid-state and solution-state (in degassed D_2O) data are presented in Table 4. The wt.% water in this table was determined by thermogravimetric analysis. The error on the T_1 measurements is ± 10%.

Table 4. ^{31}P Solid State and Solution State Parameters for Some Sulfonated Phosphines and Their Unsulfonated Analogs.

	Solid State			Solution State	
Compound	T_1,s	CSA,ppm	δiso,ppm	T_1,s	δ,ppm
TPP	1700	63	-10.3	30.8**	-9.1
TPPTS	1150*	56	-4.6	6.9	-5.14
TPP=O	93	288	29.2		29.6
TPPTS=O	27*	173	28.3	1.5	35.1
DPPE	171	65	-12.6		-13.2
DPPETS	366	83	-13.5	2.5	-12.6

* < 3 wt% water

** Pregosin, P.S.; Kunz, R.W.; *^{31}P and ^{13}C NMR of Transition Metal Phosphine Complexes,* Springer-Verlag, Berlin, 1979, p. 90.

Table 4 shows some interesting variations. For example, the unoxidized and oxidized monophosphines show reduced T_1 values when sulfonato groups are present, but the diphosphine shows the reverse. The magnitude of the chemical shift anisotropy at room temperature shows very little change upon sulfonation, yet what small change there is shows a decrease upon sulfonation for the monophosphines and an increase upon sulfonation for the diphosphine. The mono phosphine oxides have dramatically reduced T_1 values, which is a reflection of the increased chemical shift anisotropy (see Figure 47).

Since TPPTS is the ligand of interest for the supported aqueous phase studies, it is informative to focus on the difference in relaxation times going from solid- to solution-state. From a T_1 of 1200 seconds in the solid-state, there is a drop to 7 seconds in solution, a change of about three orders of magnitude.

Similar measurements were taken on $HRh(CO)(TPPTS)_3$ and other complexes; the data are shown in Tables 5 and 6. The unsulfonated analogues are reported when measured or when data was available in the literature.

Table 5. ^{31}P Solution state NMR parameters for some sulfonated transition metal complexes and their unsulfonated analogs. Unsulfonated complexes in CH_2Cl_2; sulfonated in D_2O.

Compound	T_1, s	δ, ppm	J_{M-P}, Hz.
$HRh(CO)(TPP)_3$		39.8*	155*
$HRh(CO)(TPPTS)_3$	0.99	43.9	155
$Rh(DPPE)Cl_2$		55.2	133
$Rh(DPPETS)^+$	0.46	60.7	133
Rh(COD)(DPPETS)Cl	0.44	59.2	151
$Pt(DPPE)Cl_2$		41.9**	3631**
$Pt(DPPETS\text{-}H)Cl_2$	0.86	53.1	2310
$Pd(DPPETS\text{-}H)Cl_2$	0.59	60.9	

*Horvath, I.T.; *et al* ; *Catal. Lett.*, **1989**, 2, 85.
Lindner, E.; *et al*; *Organometallics*, **1992, 11, 1033.

Table 6. ^{31}P Solid state NMR parameters for some sulfonated transition metal complexes and their unsulfonated analogs.

Compound	T_1,s	CSA,ppm	δ_{iso},ppm
$HRh(CO)(TPP)_3$			
$HRh(CO)(TPPTS)_3$	45	260	43.4
$Rh(DPPE)_2Cl$			
$Rh(DPPETS)_2^+$	33	200	63.7
Rh(COD)(DPPETS)Cl	≈120	≈200	63.7
$Rh(COD)(DPPE)ClO_4$***			56.8
$Pt(DPPE)Cl_2$*			44.1
$Pt(DPPETS)Cl_2$**	55	150	51.0

*$Pt(DPPE)Cl_2$ J_{Pt-P} = 3591 Hz
**$Pt(DPPETS\text{-}H)Cl_2$ J_{Pt-P} = 2425 Hz
***Rh(COD)(DPPE)ClO J_{Rh-P} = 126 Hz.

*Horvath, I.T.; *et al* ; *Catal. Lett.*, **1989**, 2, 85.
Lindner, E.; *et al*; *Organometallics*, **1992, 11, 1033.
***Davies, J.A.; *et al*; *Coord. Chem. Rev.*, **1992**, 114, 61.

Consider the T_1 values for the rhodium complex of interest, $HRh(CO)(TPPTS)_3$. In the solid-state, the relaxation time is 45 seconds, while in solution it is less than 1 second, a much smaller magnitude of change than that observed for the free ligand TPPTS. As can be seen from the tables, complexes generally have shorter relaxation times than do the free ligands.

Table 7 gives the values for TPPTS impregnated on CPG-240 support. The wt.% values were determined by TGA. The T_1 of TPPTS immobilized on CPG-240 is much smaller than that for the free ligand, even at a comparable amount of water. By the time there is 13.3% water associated with the immobilized phase, the T_1 is in the realm of the solution-state, even though at this point the substance appears completely dry and is a free-flowing powder.

Table 7. ^{31}P T_1 Times and wt% water in TPPTS impregnated on CPG-240 ; 16.92 % TPPTS on glass

Wt% H_2O	T_1,s
1.8	220
6.9	22.5
13.3	4.9

The rhodium complex of interest was also impregnated on CPG-240. Table 8 gives the results of T_1 measurements at various water levels.

Table 8. ^{31}P T_1 times and wt% water in $HRh(CO)(TPPTS)_3$ impregnated on CPG-240.

13.2% Rh(I) on Glass

Wt% H_2O	T_1,s
3.3	3.1
5.3	2.7
8.4	<1

Once again, it is informative to compare the T_1 of the free complex to that of the immobilized phase. At a comparatively small water content, the T_1 of the immobilized complex is already in the realm of solution-state relaxation measurements.

It was postulated that there was enough difference in the T_1 values of the free TPPTS that it could be used as a probe to investigate the role of water in the supported aqueous phase hydroformylation reaction. The relaxation rates could give a clue as to when the supported phase assumes a liquid-like character in terms of mobility.

Figure 48 is a plot of T_1 values of TPPTS and the % conversion of 1-octene as a function of the wt.% water of the supported phase. It can be seen that there is a relationship between maximum catalytic activity and the onset of a liquid-like character for the supported phase.

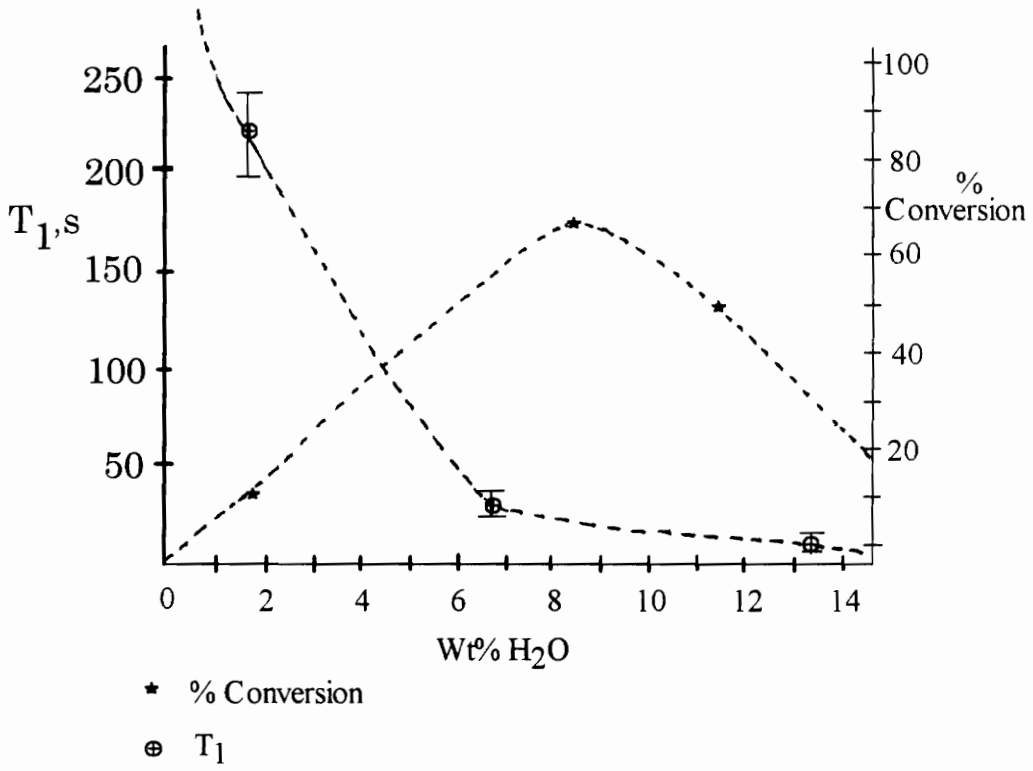

Figure 48. ^{31}P T_1 times and % conversion as a function of wt. % water. Influence of H_2O content on a Supported Aqueous Phase Catalyst on the hydroformylation of 1-Octene.

5.3 Results of Catalytic Work

A number of complexes were synthesized and characterized with DPPETS as the phosphine ligand in order to evaluate them as potential catalysts. These are shown in the reaction scheme below (Figure 49).

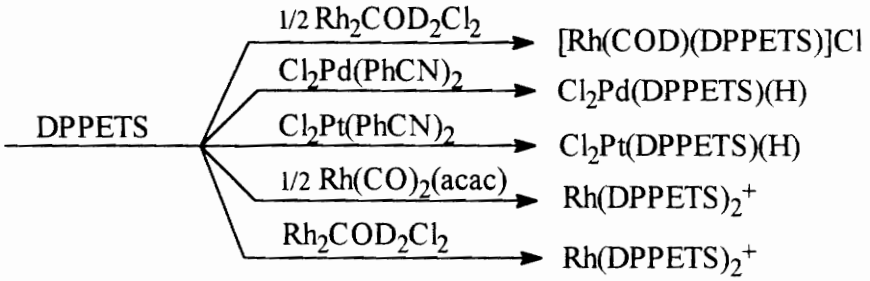

Figure 49. Reaction scheme outlining the synthesis of complexes with DPPETS.

$Ni(CO)_2$(DPPETS) was also synthesized and characterized, but its function was to investigate the electronic character of the phosphine and was not used in catalysis.

The biphasic hydroformylation of 1-octene with $Rh(DPPETS)_2^+$ (Figure 50) prepared *in situ* from DPPETS and $Rh(acac)(CO)_2$ sheds some light on the mechanism of hydroformylation in the aqueous phase, since it is reasonable to assume that the compound $Rh(DPPETS)_2^+$ forms under the influence of high P/Rh ratios. At high P/Rh ratios this compound was found to be inactive for hydroformylation since it is unlikely to provide an open coordination site at the metal by dissociating one chelating ligand. When the P/Rh ratio is low, the rate of hydroformylation is still slower than with TPPTS, although the selectivity is comparable to that of TPPTS.

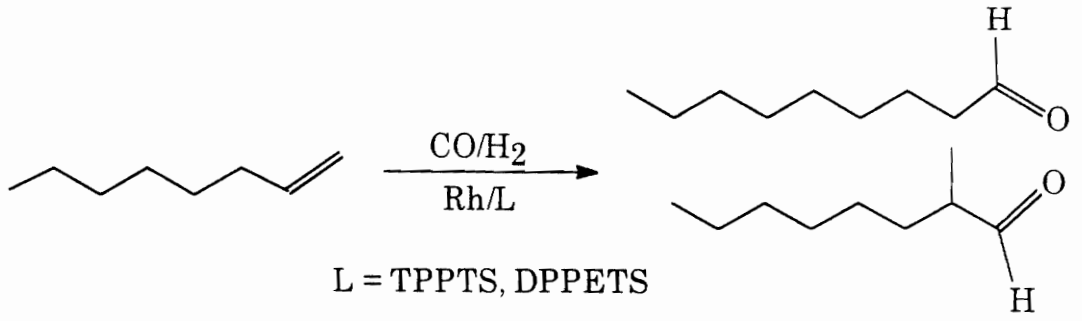

Figure 50. Hydroformylation of 1-octene.

The graph of the hydroformylation of 1-octene is shown in Figure 51 with a similar plot for TPPTS as the ligand for comparison in Figure 52.

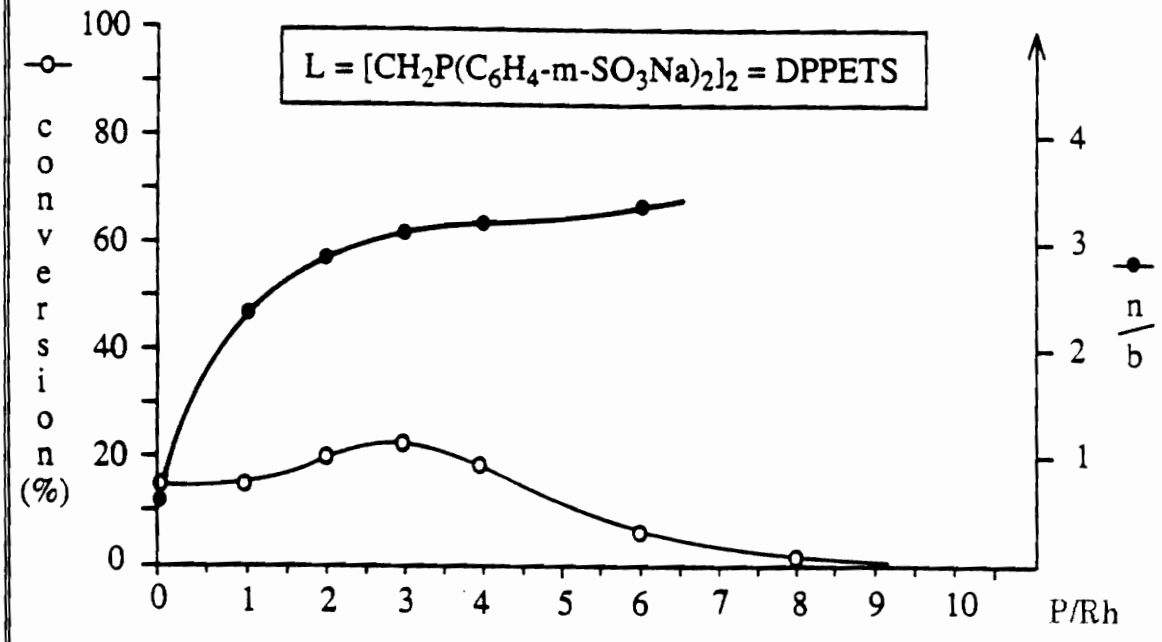

Figure 51. Plot of hydroformylation of 1-octene with Rh/DPPETS^{+}.
Pressure = 200 psig. Temperature = 120° Stirring rate = 360 rpm

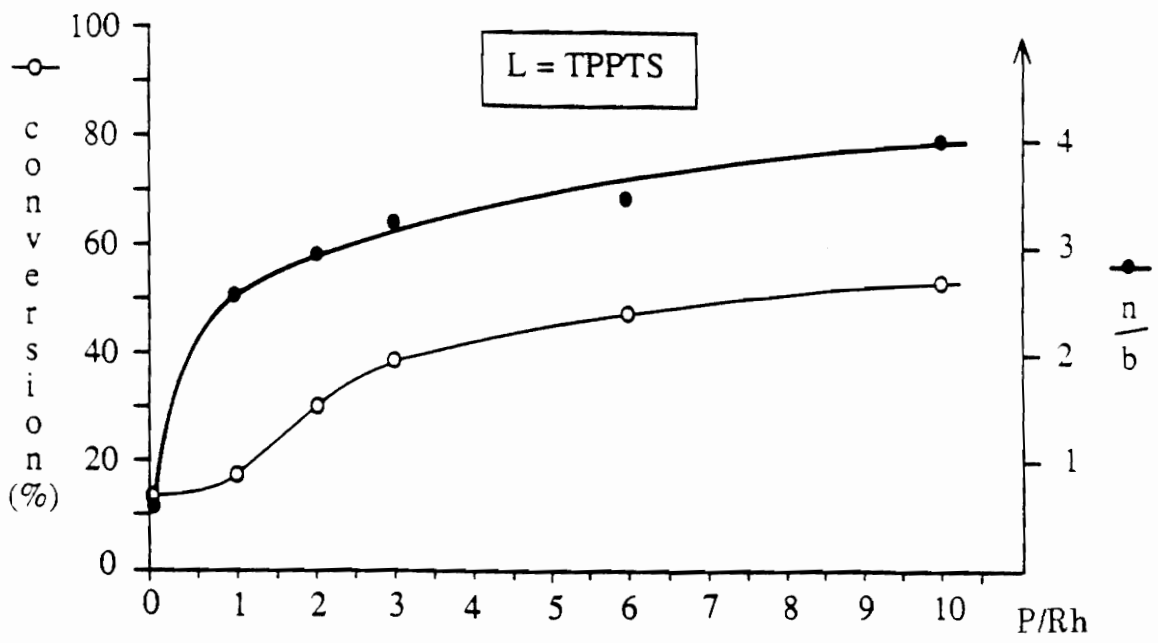

Figure 52. Plot of hydroformylation of 1-octene with Rh/TPPTS. Pressure = 200 psig. Temperature = 120° Stirring rate = 360 rpm

Another hydroformylation reaction was performed under similar conditions on styrene using the isolated complex $Rh(DPPETS)_2^+$ (Figure 53) and no additional ligand. Figure 54 shows the results using a 500/1 substrate/rhodium ratio. It can be seen that the normal to branched ratio is constant at about 1/1. This is also true for substrate/rhodium ratios of 1250/1.

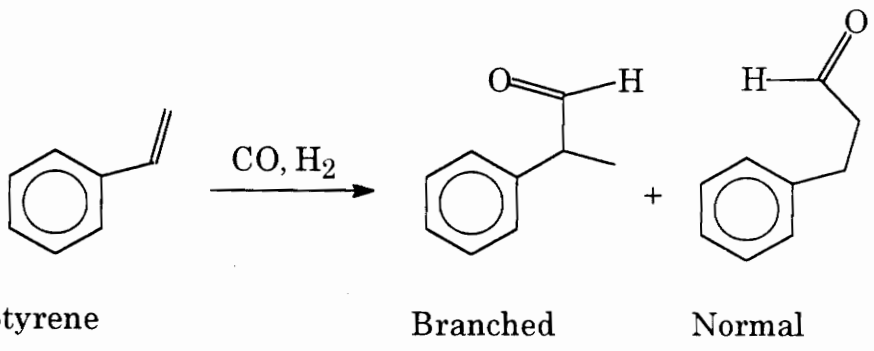

Figure 53. Hydroformylation of styrene

The outcome is about the same as was found for 1-octene, with less than 10% conversion after 6 hours; the percent conversion after 96 hours was only 56.3%. It has been postulated that the ability to form *trans* intermediates is crucial for the ability of rhodium hydroformylation complexes to be active and selective catalysts. It has been found that n/b ratios are usually low with chelating phosphines, which could be a result of olefin isomerization and also a lesser inclination for anti-Markownikoff addition to the terminal olefin with chelating phosphines.[141,142,143] Since similar n/b ratios were found with TPPTS and DPPETS, it is thought that the inherent selectivity which is determined by the sense of addition to the terminal olefin is the same for both species. It must be said though, that the chelating ligand BISBI gives good rates and good selectivity in the hydroformylation of olefins. Since BISBI can form a seven-membered ring with the metal center it may be able to approximate a *trans* arrangement.[11,14]

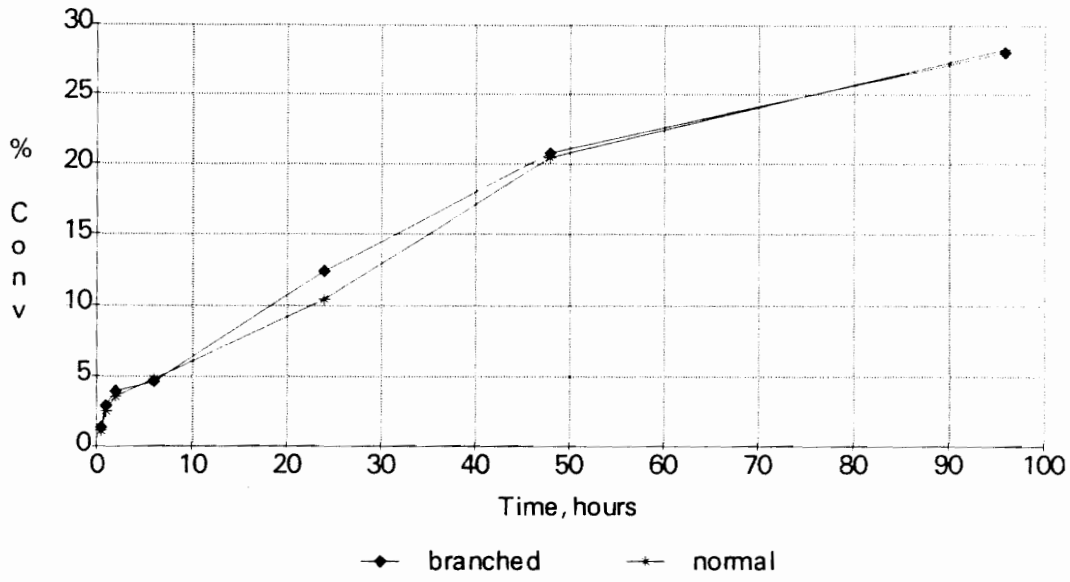

Figure 54. Plot of hydroformylation of styrene with $Rh(DPPETS)_2^+$.
Series A: Branched product • Series B: Normal product ✳
Substrate/Rh = 500/1
Pressure = 200 psig. Temperature = 120° Stirring rate = 360 rpm

The complex $Rh(DPPETS)_2Cl$ was also tested as a catalyst for the hydrogenation of trans-2-hexenal (Figure 55.). The substrate/rhodium concentration was varied and the temperature was varied. In both cases, there was almost 100% selectivity for the double bond, with little attack at the aldehyde functionality (Figure 56). An example of the amount of unsaturated alcohol formed is shown in Figure 57.

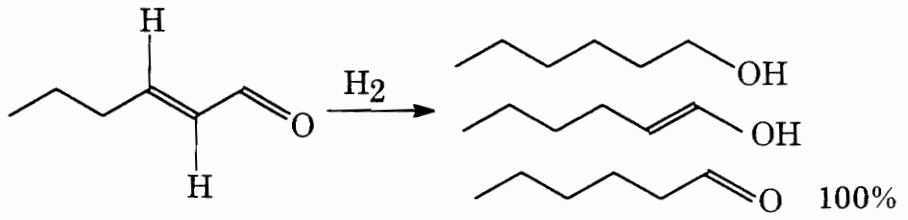

Figure 55. Hydrogenation of trans-2-hexenal.

It must be taken into acount that each point on all the graphs is from a separate catalytic run in a separate autoclave; therefore there is a certain amount of drift in the data. Indeed, this was found to be the case; however, when we consider the formation of the unsaturated alcohol, it appears that the bulk of the substrate is converted to unsaturated aldehyde before there is a significant attack on the carbonyl functionality to produce the unsaturated alcohol. This is typical for rhodium in that it is very selective for the double bond in these types of compounds.

If we consider the temperature at which the reaction took place, it appears that less alcohol is formed. The substrate concentration could have a role in amount of alcohol formed in the reaction. (Table 9)

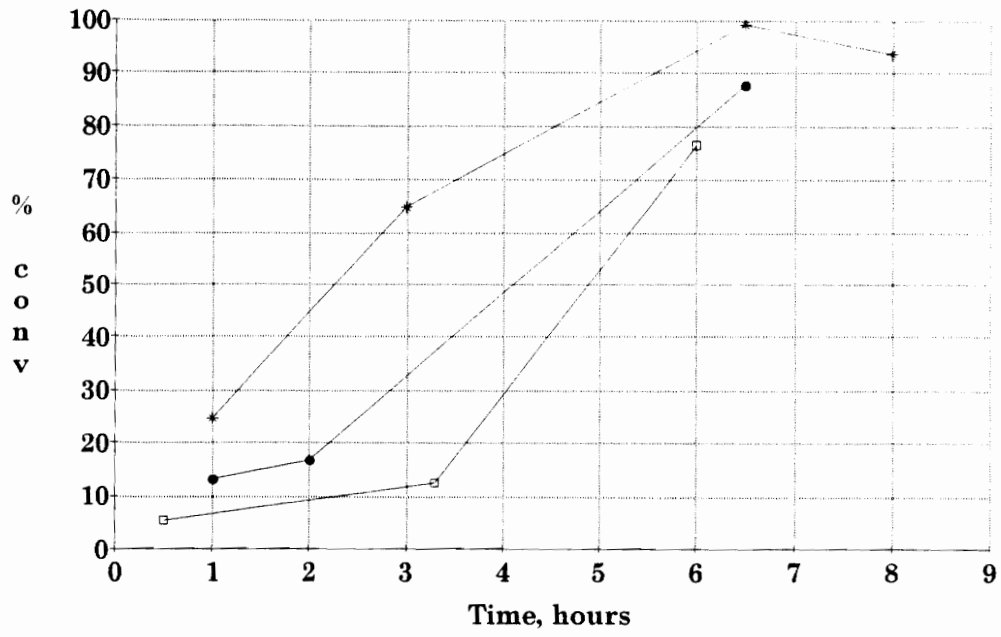

Figure 56. Plot of Hydrogenation of trans-2-hexenal with $Rh(DPPETS)_2^+$; temperature and concentration variation.

Series A: Substrate/Rh = 400/1, Temp = 60° ▫

Series B: Substrate/Rh = 400/1, Temp = 100° ✳

Series C: Substrate/Rh = 200/1, Temp = 60° •

Pressure = 200 psig H_2 Stirring Rate = 360 rpm

Table 9. Amount of unsaturated alcohol formed in funal run of hydrogenation reaction with $Rh(DPPETS)_2^+$

% Aldehyde	% Alcohol	Temperature	Substrate/Rh
76.37	0.27	60°	400/1
93.65	6.01	100°	400/1
69.18	---	60°	200/1

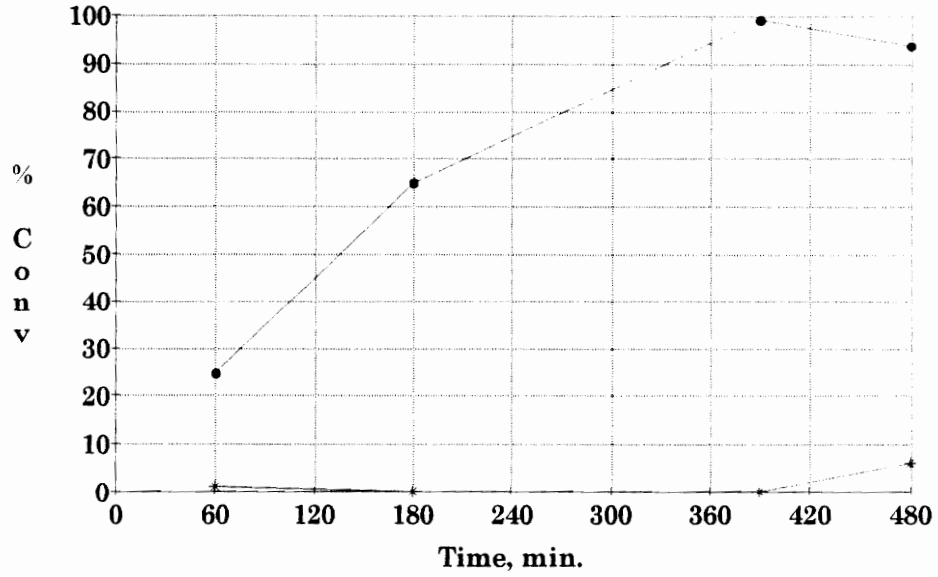

Figure 57. Plot of hydrogenation of trans-2-hexenal with $Rh(DPPETS)_2^+$ with formation of unsaturated alcohol.
Series A: aldehyde formation •
Series B: alcohol formation ✳
Substrate/Rh = 400/1 Temp. = 100°
Pressure = 200 psig H_2; Stir rate = 360 rpm

Another rhodium complex, Rh(COD)(DPPETS)Cl was prepared and isolated; it was also used in the hydrogenation of trans-2-hexenal, with similar results. As expected, rhodium catalysts are very selective for the double bond in hydrogenation reactions when other unsaturation is present.[145,62,64] Figure 58 gives the results of hydrogenation with Rh(COD)(DPPETS)Cl.

The palladium and platinum complexes were used in hydrogenation and carbonylation reactions and appeared to show little activity.

All data pertaining to the catalytic work can be found in Appendix B.

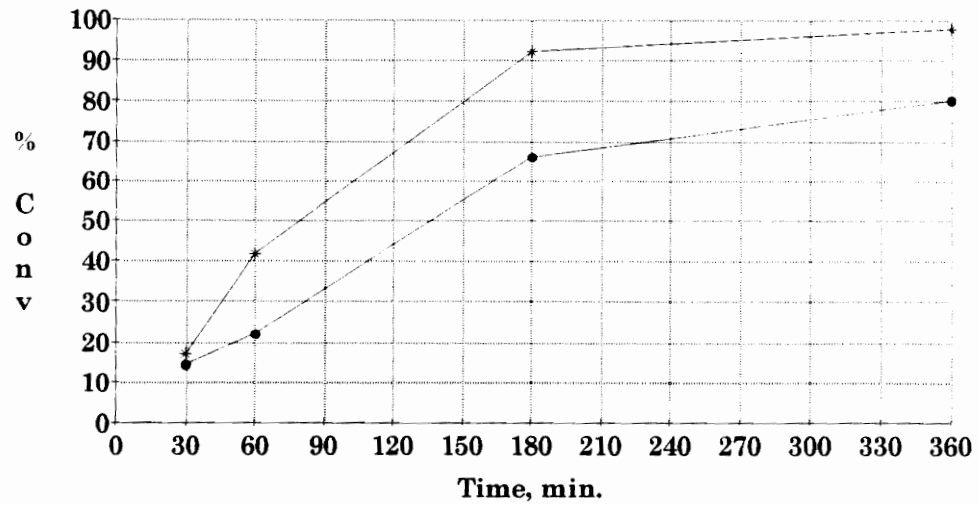

Figure 58. Plot of Hydrogenation of *trans*-2-hexenal as a function of time with Rh(COD)(DPPETS)Cl as catalyst; temperature variation.
Series A: 23° •
Series B: 60° ✳
Pressure = 200 psig H_2 ; Stirring rate = 360 rpm

Hydrogenation using DPPETS as a ligand looks very promising and more studies should be conducted; for example to monitor its behavior with ruthenium, since ruthenium complexes favor attacking the aldehyde functionality. Also, studies on simple olefins, terminal and internal and with multiple unconjugated bonds shoud be performed to see if there is a specific selectivity. Concentration of complex is another factor that can be easily observed. DPPETS is very favorable as a water-soluble phosphine ligand for all types of biphasic reactions.

5.4 Conclusions

This work included several diverse areas of chemistry, and indicated definitively how interdependent the various disciplines are upon each other.

^{31}P NMR spectroscopy has been shown to be a probe to determine the role of water in determining the rate of hydroformylation of terminal olefins in Supported Aqueous Phase Catalysis. It is possible to determine the onset of a "liquid-like" character for a supported phase by investigating the behavior of the ^{31}P spin-lattice relaxation times of that species. As the T_1 values of the immobilized phase diminish with the addition of water, it can be said that more mobility is afforded to the substance. It could be compared to kelp fronds that are made mobile by the action of the ocean waters in which they are immersed, even though the fronds are kept in one place by a "hold-fast".

This change in spin-lattice relaxation times coincided with the maximum catalytic activity which gives a method of determining the optimum amount of water in the system that permits maximum catalytic activity.

It was also found that a simple chelating water-soluble phosphine ligand can be prepared in gram-size quantities and purified to greater than 99%. This required careful reaction monitoring, rigorous attention to reaction conditions and patience in extraction and purification techniques. The synthesis of DPPETS allows the same type of study to be propagated for chelating phosphines that TPPTS engendered fifteen years ago. The great strides in biphasic catalytic work have been largely due to the availability of TPPTS at a relatively inexpensive cost and gram-size quantities. We have

provided a simple, relatively inexpensive route to pure DPPETS that will enable the same type of study to be possible for a chelating ligand that has up to now eluded researchers.

The initial studies on the rhodium complexes with DPPETS as a chelating ligand show promise for hydrogenation reactions, with high selectivity toward the double bond. The platinum and palladium initial results were disappointing, but deserve further study.

5.5. Recommendations for Future Work

All the complexes studied are potential catalysts for both biphasic and Supported Aqueous Phase Catalysis. More studies are cxertainly needed; the studies in this work were merely to evaluate the capability of the complexes for use, and to characterize them in relation to DPPETS. DPPETS should be investigated with ruthenium and rhodium as catalysts for α,β-unsaturated aldehydes and other doubly functionalized systems. The possibility exists that thew platinum complex has anti-tumor properties. This investgation should continue into other noble metal complexes with DPPETS as ligand.

Other means of sulfonation of DPPETS should be investigated. The idea of direct sulfonation of DPPE with SO_3 was that of Dr. Milos Hudlicky, Professor Emeritus at Virginia Tech. The idea is appealing for several reasons. It would settle the question of oxidation, because there would not be any protonation of the phosphorus atom during sufonation, since there would be no proton source. It would also allow the reaction to proceed at room temperature, and perhaps encourage it to proceed a little faster. It could also give more control over the actual process of sulfonation.

Of continuing interest is the possibility of complete oxidation of the phosphorus atom during sulfonation with subsequent reduction. While this has been accomplished by Larpent, *et al.*,[146] it is a tedious, multistep process. An easier way using redox methods with transition metals should be explored.

Efforts are being made to establish a patent on DPPETS.

References

1. Kuntz, E.; Chemtech, 1987, Sept., 587.
2. Arhancet, J.P.; Davis, M.E.; Merola, J.S.; Hanson, B.E.; *Nature*, **1989**, 339, 454.
3. Arhancet, J.P.; Davis, M.E.; Hanson, B.E.; *J. Catal.*, **1991**, 129, 94.
4. Arhancet, J.P.; Davis, M.E.; Hanson, B.E.; *J. Catal.*, **1991**, 129, 100.
5. Ahrland,S.; Chatt, J.; Davies, N.R.; Williams, A.A.; *J. Chem. Soc.*, **1958**, 276.
6. Dror, Y.; Manassen, J.; *J. Molecular Catal.*, **1977**, 2, 219.
7. Borowski, A.F.; Cole-Hamilton, D.J.; Wilkinson, G.; *Nouv. J. Chem.*, **1978**, 2, 137.
8. Harris, R.K.; *Nuclear Magnetic Resonance Spectroscopy,* Pitman, London, 1983, p.230.
9. ^{31}P and ^{13}C NMR of Transition Metal Phosphine Complexes; *NMR: Basic Principles and Progress,* Diehl, P.; Fluck, P.; Kosfeld, R.; eds., Springer-Verlag, Berlin, 1979, p. 2.
10. Ebsworth, E.A.B.; Rankin, D. W.H.; Cradock, S.; *Structural Methods in Inorganic Chemistry,* Blackwell, Oxford, 1987, p. 39.
11. Hermann, W.A.; Kohlpaintner, C.W.; Bahrmann, H.; Konkol,W.; *J. Molecular Catal.*, **1992**, 73, 191.
12. Amrani, Y.; Lecomte, L.; Sinou,D.; Bakos, J.; Toth, I.; Heil, B.; *Organometallics*, **1989**, 8, 542.
13. (a) Nuzzo, R.G.; Feitler, D.; Whitesides, G.M.; *J. Am. Chem. Soc.*, **1979**, 101, 3683.
    (b) Nuzzo, R.G.; Haynie, S.L.; Wilson, M.E.; Whitesides, G.M.; *J. Org. Chem.*, **1981**, 46, 2861.
14. Avey, A,; Schut, D.M.; Weakley, T.J.R.;Tyler, D.R.;*Inorg. Chem.*,**1993**,32, 233.
15. Lecomte, L.; Triolet, J.; Sinou, D.; Bakos, J.; Toth, I, Heil, B.; *J. Chromatogr.*, **1987**, 408, 416.
16. Herrmann, W.A.; Kulpe. J.A.; Konkol, W.; Bahrmann, H.; *J. Organometallic Chem.*, **1990**, 389, 101.
17. Arhancet, J.P.; Ph.D. Dissertation, Virginia Tech, 1989.
18. (a) Chan, A.S.C.; *Chemtech*, **1993**, March, 46.
    (b) Noyori, R.; *Chemtech*, **1992**, June, 360.
19. (a) Douglas, B.; McDaniel, D.H.; Alexander, J.J.; Concepts and Models of Inorganic Chemistry, 2nd ed., Wiley, New York, 1983, pp. 473, 720.
    (b) Cotton, F.A.; Wilkinson, G.; Advanced Inorganic Chemistry, 5th ed., Wiley, New York, 1988, p. 1224.
20. Alper, H.; *Adv. in Organometallic Chem.*, **1981**, 19, 183.

21. Ellis, J.W.; Harrison, K.N.; Hoye, P.A.T.; Orpen, A.G.; Pringle, P.G.; Smith, M.B.; *Inorg. Chem.*, **1992**, 31, 3026.
22. Kalck, P.; Monteil, F.; *Adv. in Organometallic Chem.*, **1993**, 34, 219.
23. Amrani, Y.; Sinou, D.; *J. Molecular Catal.*, **1984**, 24, 231.
24. Sinou,D.; Amrani, Y.; *J. Molecular Catal.*, **1986**, 36, 319.
25. Smith, R.T.; Baird, M.C.; *Trans. Met. Chem.*, **1981**, 6, 197.
26. Smith, R.T.; Ungar, R.K.; Baird, M.C.; *Trans. Met. Chem.*, **1982**, 7, 288.
27. Smith,R.T.; Ungar, R.K.; Sanderson, L.J.; Baird, M.C.; *Organometallics,* **1983**, 2, 1138.
28. Renaud, E.; Baird, M.C.; *J. Chem. Soc. Dalton,* **1992**, 2905.
29. Nuzzo, R.G.; Haynie, S.L.; Wilson, M.E.; Whitesides, G.M.; *J. Org. Chem.*, **1981**, 46, 2861.
30. Benhamza, R.; Amrani, Y.; Sinou,D.; *J. Organometallic Chem.*, **1985**, 288, C-37.
31. Nagel, U.; Kinzel, E.; *Chem. Ber.*, **1986,** 119, 1731.
32. Tóth, I.; Hanson, B.E.; *Tetrahedron Asymmetry*, **1990**, 1, 895.
33. Tóth, I.; Hanson, B.E.; Davis, M.E.; *Tetrahedron Asymmetry*, **1990**, 1, 913.
34. Tóth, I.; Hanson, B.E.; Davis, M.E.; *J. Organometallic Chem.*, **1990**, 396, 363.
35. Darensbourg, D.J.; Joó, F.; Kannisto, M.; Katho, A.; Reibenspeiss, J.H.; *Organometallics,* **1992**, 11, 1990.
36. Ahrland, S.; Chatt, J.; Davies, N.R.; Williams, A.A.; *J.Chem. Soc.*, **1958**, 276.
37. (a) Kuntz, E.; *Chemtech,* **1987**, Sept., 570.
(b) Kuntz, E.; US Patent 4,260,750, **1981**.
(c) Murray, R.E.; US Patent 4,822,915, **1989**.
38. Barton, M.; Atwood, J.D.; *J. Coord. Chem.*, **1991**, 24, 43.
39. Herrmann, W.A.; Kulpe, J.A.; Konkol, W.; Bahrmann,H.B.; *J. Organometallic Chem.*, **1990**, 389, 85.
40. Herrmann, W.A.; Kellner, J.; Riepl, H.; *J. Organometallic Chem.*, **1990,** 389, 103.
41. Herrmann, W.A.; Kulpe, J.A.; Kellner. J.; Riepl, H.; Bahrmann, H.; Konkol, W.; *Angew. Chem. Int. Ed. Eng.*, **1990**, 29, 391.
42. Aquino, M.A.S.; Macartney, D.H.; *Inorg. Chem.*, **1988**, 27, 2868.
43. Darensbourg, D.J.; Bischoff, C.J.; *Inorg. Chem.*, **1993**, 32, 47.
44. Fontal, B.; Orlewski, J.; Santini, C.C.; Basset, J.M.; *Inorg. Chem.*, **1986**, 25, 4322.
45. Renaud, E.; Russell, R.B.; Fortier, S.; Brown, S.J.; Baird, M.C.; *J. Organometallic Chem.*, **1991**, 419, 403.

46. Ganguly, S.; Mague, J.T.; Roundhill,D.M.; *Inorg. Chem.*, **1992**, 31, 3500.
47. Bartik, T.; Bartik, B.; Hanson, B.E.; Glass, T.; Bebout, W.; *Inorg. Chem.*, **1992**, 31, 2667.
48. Bartik, T.; Bartik, B.; Hanson, B.E.; Guo, I.; Tóth, I.; *Organometallics*, **1993**, 12, 164.
49. Darensbourg, D.J,; Bischoff, C.J.; Reibenspeis, J.H.; *Inorg. Chem.*, **1991**, 30, 1144..
50. Joò, F. and Tòth, Z.; Beck, M.T.; *Inorg. Chim. Acta.*, **1977**, 25, L61.
51. Joò, F. and Tòth, Z.; *J. Molecular Catal.*, **1980**, 8, 369.
52. Amrani, Y.; Lecomte, L.; Sinou, D.; *Organometallics*, **1989**, 8, 542.
53. Quinn, P.J.; Taylor, C.E.; *J. Molecular Catal.*, **1981**, 13, 389.
54. Mignani, G.; Morel, D.; Colleuille, *Tet. Lett.*, **1985**, 26, 6337.
55. Jensen, C.M.; Trogler, W.C.; Science, **1986**, 233, 1069.
56. Ramprasad, D.; Yue, H.J.; Marsella, J.A.; *Inorg. Chem.*, **1988**, 27, 3151.
57. Casalnuovo, A.L.; Calabrese, J.C.; *J. Am. Chem. Soc.*, **1990**, 112, 4324
58. Okano, T.; Uchida,I.; Nakagaki, T.; Konishi, H.; Kiji, J.; *J. Molecular Catal.*, **1989**, 54, 65.
59. Bahrmann, H.; Bach, H.; *Phosphorus and Sulfur,* **1987**, 30, 611.
60. Escaffre, P.; Thorez, A.; Kajck, P.; *J. Chem. Soc. Chem. Commun.*, **1987**, 146.
61. Grosselin, J.M.; Mercier, C.; Allmang, G.; Grass, F.; *Organometallics*, **1991**, 10, 2126.
62. Benyei, A.; Joó, F.; *J. Molecular Catal.*, 1990, 58, 151.
63 Sinou,D.; Safi, M.; Claver, C.; Masdeu, A.; *J. Molecular Catal.*, **1991**, 68, L9.
64. Alario, F.; Amrani, Y.; Colleuille, Y.; Dang, T.P.; Jenck, J.; Morel, D.; Sinou, D.; *J. Chem. Soc. Chem. Commun.*, **1986**, 202.
65. Joó, F.; Benyei, A.; *J. Organometallic Chem.*, **1989**, 363, C19.
66. Joó, F.; Somsak, T.; Beck, M.T.; *J. Molecular Catal.*, **1984**, 24, 71.
67. Tóth, Z.; Joó, F.; Beck, M.T.; *Inorg. Chim. Acta.*, **1980**, 42, 153.
68. Fache, E.; Senocq, F.; Santini, C.; Basset, J-M.; *J. Chem. Soc. Chem. Commun.*, **1990**, 1776.
69. Fache, E.; Santini, C.; Senocq, F.; Basset, J.M.; *J. Molecular Catal.*, **1992**, 72, 337.
70. Bartik, T.; Bartik, B.; Hanson, B.E.; *J. Molecular Catal.*, in press.
71. Vigh, L.; Joó, F.; van Hassalt, P.R.; Kuiper, P.J.C.; *J Molecular Catal.*, **1983**, 22, 15.
72. Larpent, C.; Dabard, R.; Patin, H.; *Inorg. Chem.*, **1987**, 26, 2922.
73. Larpent, C.; Dabard, R.; Patin, H.; *New J. Chem.*, **1988**, 12, 907.

74. Willner, I.; Maidan, R.; *J. Chem. Soc. Chem. Commun.*, **1988**, 876.
75. Horváth, I.T.; Kastrup, R.V.; Oswald, A.A.; Mozeleski, E.J.; *Catal. Lett.*, **1989**, 2, 85.
76. Cotton, F.A.; Wilkenson, G.; Advanced Inorganic Chemistry, 5th ed., 1988, Wiley, New york, p.1271.
77. Hartley, F.R.; Supported Metal Complexes, Reidal, Dordrecht, 1985.
78. Joò, F.; Beck, M.T.; *J. Molecular Catal.*, **1984**, 24, 135.
79. Arhancet, J.P.; Davis, M.E.; Merola, J.S.; Hanson, B.E.; *J. Catal.*, **1990**, 121, 327.
80. Davis, M.E.; *Chemtech*, **1992**, August, 498.
81. Horváth, I.T.; *Catal. Lett.*, **1990**, 6, 43.
82. Renaud, E.; Baird, M.C.; *J. Molecular Catal.*, **1993**, 80, 43.
83. Davies, J.A.; Dutremez, S.; *Coord. Chem. Rev.*, **1992**, 114, 201.
84. Yamasaki, A.; *Coord. Chem. Rev.*, **1991**, 109, 107.
85. Davies, J.A.; Dutremez, S.; *Coord. Chem. Rev.*, **1992**, 114, 61.
86. Suwelack, D.; Rothwell, W.P.; Waugh, J.S.; *J. Chem. Phys.*, **1980**, 73, 2559.
87. Rothwell, W.P.; Waugh, J.S.; *J. Chem. Phys.*, **1981**, 74, 2721.
88. Duncan, T.M.; *J. Phys. Chem. Ref. Data*, **1987**,16, 125.
89. Tolman, C.A.; *Chem. Rev.*, **1977**, 77, 313.
90. Bartik, T.; Himmler, T.; *J. Organomet. Chem.*, **1985**, 293, 343.
91. Bartik, T.; Himmler, T.; Schulte, H.-G.; Seevogel, K.;. *J. Organomet. Chem.*, **1984**, 272, 29.
92. Herzfeld, J.; Berger, A.E.; *J. Chem. Phys.*, **1980**, 73, 6021.
93. Shindo, H.; Wooten, J.B.; Pheiffer, B.H.; Zimmerman, S.B.; *Biochemistry*, **1980**,19, 518.
94. (a) Soderquist, A.; Hughes, C.D.; Horton, W.J.; Facelli, J.C.; Grant, D.M.; *J. Am. Chem. Soc.*, **1992**, 114, 2826.
(b) Orendt, A.M.; Sethi, N.K.; Facelli, J.C.; Horton, J.W.; Pugmire, R.J.; Grant,D.M.; *J. Am. Chem. Soc.*, **1992**, 114, 2832.
95. Diesveld, J.W.; Menger, E.M.; Edzes, H.T.; Veeman, W.S.; *J. Am. Chem. Soc.*, **1980**, 106, 7935.
96. Naito, A.; Sastry, D.L.; McDowell, C.A.; *Chem. Phys. Lett.*, **1985**, 115, 19.
97. Torchia, D.A.; Szabo, A.; *J. Mag. Res.*, **1982**, 49, 107.
98. Wang, J.; Ellis, P.D.; *J. Am. Chem. Soc.*, **1993**, 115, 212.
99. Power, W.P.; Wasylishen, R.E.; *Inorg. Chem.*, **1992**, 31, 2176.
100. Grim, S.O.; Keiter, R.L.; McFarlane, W.; *Inorg. Chem.*, **1967**, 6, 1133.
101. Rahn, J.A.; Baltusis, L.; Nelson, J.H.; *Inorg. Chem.*, **1990**, 29, 750.
102. Lindner, E.; Fawzi, R.; Mayer, H.A.; Eichele, K.; Pohmer, K.; *Inorg. Chem.*, **1991**, 30, 1102.

103. Bowmaker, G.A.; Cotten, J.D.; Healy, P.C.; Kildea, J.D.; Silong, S.B.; Skelton, B.W.; White, A.H.; *Inorg. Chem.,* **1989**, 28, 1462.
104. Healy, P.C.; Hanna, J.V.; Kildea, J.D.; Skelton, B.W.; White A.H.; *Aust. J. Chem.,* **1991**, 44, 427.
105. Attar, S.; Bearden, W.H.; Alcock, N.W.; Alyea, E.C.; Nelson. J.H.; *Inorg. Chem.,* **1990**, 29, 425, and references therein.
106. Davies, J.A.; Dutremez, S.G.; *Magn. Reson. Chem.,* **1993**, 31, 439.
107. Yamamoto, A.; *Organotransition Metal Chemistry,* John Wiley and Sons, New York, 1986, p. 335.
108. Kessler, J.M.; Nelson, J.H.; Frye, J.S.; DeCian, A.; Fischer, J.; *Inorg. Chem.,* **1993**, 32, 1048.
109. Wu, G.; Wasylishen, R.E.; *Inorg. Chem.,* **1992**, 31, 145.
110. Eckert, H.; Liang, C.S.; Stucky, G.D.; *J. Phys. Chem.,* **1989**, 93, 452.
111 Lindner, E.; Bader,A.; Mayer, H.A.; *Inorg. Chem.,* **1991**, 30, 3783.
112. Penner, G.H.; Wasylishen, R.E.; *Can. J. Chem.,* **1989**,67, 1909.
113. Davies, J.A.; Dutremez, S.; Pinkerton,A.A.; *Inorg. Chem.,* **1991**, 30, 2387.
114. Frye, J.S.; *Concepts in Magnetic Resonance,* **1989**, 1, 27.
115. Wu, G.; Wasylishen, R.E.; *Organometallics*, **1992**, 11, 3242.
116. Robert, J.B.; Wiesenfeld, L.; *Molecular Physics*, **1981**, 44, 319.
117. Dutasta, J.P.; Robert, J.B., Wiesenfeld, L.; ACS Symp. Ser., 171 (Phosphorus Chemistry), **1981**, 581.
118. Dutasta, J.P.; Robert, J.B.; Weisenfeld, L.; *Chem. Phys. Lett.*, **1981**, 77, 336.
119. Gobetto, R.; *Materials Chemistry and Physics*, **1991**, 29, 221.
120. Chu, P.J.; Potrzebowski, M.J.; *Magn. Reson. Chem.*, **1990**, 28, 477.
121. Bemi, L.; Clark, H.C.; Davies, J.A.; Fyfe, C.A.; Wasylishen, R.E.; *J. Am. Chem. Soc.*, **1982**, 104, 438.
122. Rahn, J.A.; O'Donnell,D.J.; Palmer, A.R.; Nelson,J.H.; *Inorg. Chem.*, **1989**, 28, 2031.
123. Andersen, K.V.; Bildsøe, H.; Jakobsen, H.J.; *Magn. Resn. Chem.*, **1990**, 28, (special issue), S-47.
124. Harris, R.K.; *Chemistry in Britain*, **1993**, July, 601.
125 Jelinski, L.W.; *Chemtech*, **1986**, March, 186.
126. Dybowski, C.; *Chemtech*, **1985**, March, 186.
127. Maciel, G.E.; *Science*, **1984**, 19 Oct., 282.
128. Becker, E.D.; Anal. Chem., 1993, 65, 295A.
129. Levy, G.C., ed. "Topics in Carbon-13 Spectroscopy", Vol. 4, John Wiley and Sons, NY, 1984, pp.239-275.
130. (a) Harris, R.K.; "Nuclear Magnetic Resonance", Pitman, London, 1983, pp 66-68.

(b) Sanders, J.K.M.; Hunter, B.K.; "Modern NMR Spectroscopy", Oxford University Press, Oxford, 1990, pp. 20-21.
(c) Farrar, T.C.; Becker, E.D.; "Pulse and Fourier Transform NMR", Academic Press, Orlando, 1971. pp. 46-65.
131. Granger, P.; Harris, R.K.; "Multinuclear Magnetic Resonance in Liquids and Solids - Chemical Applications", Kluwer Academic Publishers, Dordrecht, 1988, pp.33-50.
132 Spiess, H.W.; "NMR Basic Principles and Progress", Vol. 15, Springer-Verlag, Berlin, 1978.
133. Fyffe, C.A.; "Solid State NMR for Chemists", C.F.C. Press, Guelph, Ont., 1983,p.46.
134. Bartik, T.; Bartik, B.; Hanson, B.E.; *J. Mol. Catal.* submitted.
135. Bruker MSL 300 Operating Manual
136. Chatt, J.; Hart, F.A.; *J. Chem. Soc.*, **1960**, 1378.
137. Sanger, A.R.; *J.Chem. Soc. Dalton Commun.*, **1977**, 120.
138. Power, W.P.; Wasylishen, R.E.; *Inorg. Chem.*, **1992**, 31, 2176.
139. Mather, G.G.; Pidcock, A.; Rapsey, G.N.; *J. Chem. Soc. Dalton Trans.*, **1973**, 2095.
140. Khokhar, A.R.; Xu, Q.; Siddick, Z.H.; *J. Inorg. Biochemistry*, **1990**, 39, 117.
141. Appleton, T.G.; Bennett, M.A.; *Inorg. Chem.*, **1978**, 17, 738.
142. Kiss, T.; Horvath, I.T.; *Organometallics*, **1991**, 10, 3798.
143. Sanger, A.R.; *J. Molecular Catal.*, **1977/78**, 3, 221.
144. Pittman, C.U. Jr.; Hirao, J.; *J. Org. Chem.*, **1977**, 43, 1978.
145. Grosselin, J.M.; Mercier, C.; Allmang,G.;Grass,F.; *Organometallics*, **1991**, 10, 2126.
146. Larpent, C.; Patin, H.; Thilmont, N.; Valdor, J.F.; *Syn. Commun.*, **1991**, 21, 495.

Bibliography for Sections 3.1, 3.2 and 3.3

The texts listed below are representative of an extensive offering of NMR basics.

a. Fyfe, C.A.; Solid State NMR for Chemists, CFC Press, Guelph, Ontario, 1983, pp.6-25.; 139-180.
b. Saunders, J.K.M.; Hunter, B.K.; Modern NMR Spectroscopy, Oxford Press, Oxford, 1990, pp. 9-13.
c. Freibolin, H.; Basic One- and Two- Dimensional NMR Spectroscopy VCH Publishers, New York, 1991, pp. 2-10.
d. NMR Spectroscopy Techniques, Dybowski, C.; Lichter, R.L.; eds., Marcel Dekker, New York, 1987, pp.1-4; 253-326.
e. Modern NMR Techniques for Chemistry Research, Derome, A.E.; Pergamon Press, Oxford, 1988, pp.9-29.
f. Nuclear Magnetic Resonance Spectroscopy, Harris, R. K.; Pitman, London, 1983, pp.2-33.
g. Multinuclear Magnetic Resonance in Liquids and Solids - Chemical Applications, Granger, P.; Harris, R.K.; Kluwer Academic Publishers, Dordrecht, The Netherlands, 1988, pp. 241-338.
3. Granger, p.317.

Appendix A

NMR Parameters for Solid-state Experiments

Bruker Parameter Naming Conventions

SR	Hz	Spectrum reference; difference between basic frequency of spectrometer and frequency of observed nucleus
O1	Hz	Offset frequency; combined with SY to generate exact synthesizer frequency for observed nucleus. (Carrier frequency)
SY	Hz	Synthesizer setting
TD	K	number if digital words that defines spectral width
SI	K	Spectrum Size; number of points in transformed spectrum 1K = 1024 points
SW	Hz	Spectral width; frequency range of spectrum
Hz/Pt	Hz	Digital resolution
RG		Receiver gain
NE		Number of experiments
NS		Number of transients (scans)
TE	K	Absolute temperature
DW		Dwell time; interval (time) between collection of each data point
FW	Hz	Bandwidth filter that prevents aliasing of noise
O2	Hz	Adjusts decoupler channel frequency. (Decoupler frequency)
DP		Controls the amplitude of the decoupler channel output
D0	s	Recycle delay
D1	μs	90° pulse for observed nucleus
D2	μs	180° pulse for observed nucleus
D3	μs	Deadtime delay (ringdown delay)
LB		Line broadening (exponential)
CX		x axis length
CY		y axis length
SR		Spectrum reference; (O1 frequency equal to 0 ppm)
AI		Absolute intensity for scaling spectra to same CY value
ZG		Zero go; starts simple pulse programs
GS		Go setup; pulses nucleus but no data collection
AU		Starts complicated pulse programs
AQ		Aquisition time

Default Parameters Common to All Experiments

SF	121.496 MHz (^{31}P)	O1	10,500 Hz
SI	16384	TD	8192
SW	50,000 Hz	Hz/Pt	6.104
TE	297 K	DW	10.0
FW	60,000	O2	19,741.0 Hz
DP	63L D0	D11	5.0μs
^{1}H gain	20	D7	30 ms

TPPP31 (QUADCYCL.PC)

```
START<C*,       D1      [F1 @PLS  RGATE]
                D3      <I*[STA  RGATE]
                D0      <I*[++PLS]
GOTO<C*  START
BEGIN<C* LISTS
PLS<C*,     +X -X +Y -Y
RLS<C*,     +X -X +Y -Y
END<C*     LISTS
```

HPDEC.PC

```
START<C*,    10U
             D1       <I*[F1 @PLS1]      ; 90 DEG. PULSE
             D3       <I*[F2 +X STA]     ; DECOUPLING AND TRIGGER
             D7       <I*[F2 +X]         ; ACQUISITION
             D0
             <I*++PLS1
             ++PLS1<C*
GOTO<C*  START
BEGIN<C* LISTS
PLS1C<*,     +X +X -X -X +Y +Y -Y -Y
RLS<C*       +X +X -X -X +Y +Y -Y -Y
END<C*     LISTS
```

MMIRTONE.PC

```
START <C*,          LOOP 2 TIMES
              D0
              END<I*  LOOP
              END<C*  LOOP
              D2     <I*[F1 @PLS1]        ;180 DEGREE PULSE
              LOOP<C*  2 TIMES
              END<C*  LOOP
              D1     <I*[F1 @PLS2  F2 +X  RGATE]   ;90 DEGREE PULSE
              DE<C*     [F2 +X STA  RGATE]
              D7     <I*[F2 +X]
              ++PLS1<C*
              ++PLS2<C*
GOTO<C*  START
BEGIN<C*  LISTS
PLS1<C*,   +X -X
PLS2<C*,   +X +X -X -X
RLS<C*,    +X +X -X -X
END<C*  LISTS
```

NMR Parameters for Solid-state Experiments

T/G/H = TPPTS/Glass Support/ H_2O
complex = $HRh(CO)(TPPTS)_3$
Rh/G/H = $Hrh(CO)(TPPTS)_3$/Glass Support/H_2O

Sample	T/G/H	T/G/H	T/G/H	TPPTS
Comp.	16.92%T	16.92%	16.92	pure
H_2O	no	added	added	no
Wt.% H_2O	1.53	1.83	6.90	3.19
T_1	150	220	22.5	805
CSA	x	x	x	x
File:BBB	50	51	53	55
RG	23	22	15	15
NE	8	6	8	7
NS	8	8	64	4
D0	100s	100	25	40
Loop	50	40	10	100
D1	4.0	5.0	4.0	4.1
^{31}P gain	10	10	10	10
D2	8.0	10.0	8.0	8.2
D3	17.0	10.0	17.0	17.0
LB	50	50	50	50
SR	6905.03	6911.13	6911.13	6905.03
LOOP	50	40	10	100
Std.dev.	0.020130	0.017061	0.078607	0.010021
iterations	8 in 4	7 in 3	7 in 2	6 in 3
δ	-4.85			-4.65
RO	6500	6400	6870	6888
Loop	50	40	10	100
VD list ; 1	100	x	25	40
2	0.02	0.02	0.025	1
3	10	10	1	0.1
4	60	60	0.1	20
5	2	2	15	10
6	20	20	0.0025	5
7	80	80	10	30
8	40	x	5	

Sample	complex	complex	complex	DPPE	DPPETS	TPPTS
Comp.	pure	pure	pure	pure	pure	pure
H_2O	no	no	no	x	x	no
Wt.% H_2O		1.52	5.70	x	x	2.82
T_1		1.51	7.9	171	344	1145
CSA	x	x	x	6390	9100	6100
File:BBB	56	58	60	100	103	105
RG	15	15	20	20	20	20
NE	8	6	8	8	8	9
NS	32	32	32	8	8	16
D0	25	50	45	100	100	80
Loop	10	5	5	10	10	50
D1	3.6	3.9	4.75	3.9	3.8	3.9
^{31}P gain	10	10	10	10	10	10
D2	7.2	7.8	9.5	7.8	7.6	7.8
D3	10.0	10.0	17.0	10.0	10.0	10.0
LB	25	25	25	10	10	5
SR	6935.55	6947.75	6953.86	6978.27	6972.17	6978.27
LOOP	10	5	5	10	10	50
Std.dev.		0.003412	0.016680	0.001834	0.007851	0.003084
iterations		4 in 31	7 in 3	8 in 12	8 in 4	7 in 3
δ		42.5		-12.0567	-13.4333	-4.6971
RO	6000	7029	6533	8000	8000	8400
Loop	10	5	5	10	10	50
VD list ; 1	25	50	45	100	100	80
2	0.01	0.02	0.01	0.5	0.1	0.1
3	20	20	30	50	50	40
4	2	0.2	0.1	1	1	2
5	5	10	20	10	25	1
6	1	2	1	5	5	20
7	10		10	25	10	10
8	0.1		5	75	0.2	

Sample	T/G/H	T/G/H	T/G/H	TPPTS=O	complex	complex
Comp.	16.92	16.92	16.92	16.92	pure	pure
H_2O	yes	yes	yes	yes	yes	yes
Wt.% H_2O	2.09	2.03	13.28	13.2	8.73	
T_1	201	210	4.92	2.56	3.55	1.5
CSA						
File:BBB	107a	108	109	109	110	111
RG	1	1	5	5	15	20
NE	8	8	8	8	10	8
NS	16	16	16	16	8	64
D0	80	75	20	20	40	40
Loop	10	20	1	1	5	1
D1	3.9	3.5	3.4	3.4	3.4	3.4
^{31}P gain	10	10	10	10	10	10
D2	7.8	7.0	6.8	6.8	6.8	6.8
^{1}H gain	20	20	20	20	20	20
LB	50	50	50	50	50	50
SR	6984.38	6978.27	6984.38	6984.38	6984.38	6984.38
LOOP	10	20	1	1	5	1
Std.dev.	0.027534	0.023340	0.019030	0.024471	0.037849	
iterations	8 in 4	8 in 3	8 in 3	8 in 3	8 in 2	
δ	-8.71	-7.90	-6.03	32.98	43.25	
RO	7250	7100	7060	7060	7050	7050
Loop	10	20	1	1	5	1
VD list ; 1	80	75	20	20	40	20
2	0.1	0.1	0.001	0.001	0.001	0.005
3	60	60	15	15	30	15
4	1	1	0.01	0.01	0.01	5
5	45	45	10	10	20	10
6	10	10	0.1	0.1	0.1	0.5
7	30	30	5	5	10	5
8	20	20	1	1	1	1

Sample	complex	complex	Rh/G/H	complex	complex
Comp.	pure	pure	13.2	pure	pure
H_2O	yes		no	no	solution
Wt.% H_2O					WP-200
T_1	0.74	2.72	1.43	1.65	1.464
CSA	26,880	x	x	x	x
File:BBB	112	114	115	116	
RG	20	24	1	1	
NE	10	8	8	8	
NS	64	64	256	64	
D0	5	50	20	15	
Loop	1	1	1	1	
D1	3.4	3.4	3.4	3.7	
^{31}P gain	10	10	10	10	
D2	6.8	6.8	6.8	7.4	
^{1}H gain	20	20	20	20	
LB	25	25	25	25	
SR	6984.38	6984.38	6984.38	6984.38	
LOOP	1	1	1	1	
Std.dev.	0.03...	0.014169	0.041530	0.044124	0.046155
iterations	10 in 3	4 in 3	8 in 3	8 in 3	
δ	43.0	42.5	43.4	42.45	
RO	7080	7080	7080	6800	
Loop	1	1	1	1	
VD list ; 1	5	50	20	15	
2	0.005	0.001	0.001	0.01	
3	4	5	1	1	
4	0.01	40	5	5	
5	3	0.01	0.1	0.1	
6	0.05	10	10	10	
7	2	30	2	2	
8	0.1	0.1	0.01	8	
9	1	20			
10	0.5				

Sample	TPP	TPP=O	TPPTS=O	TPPTS	complex
T_1	1707				
CSA	8284		26475		
SR	6727.37				
Std.dev.	0.016223				
iterations					
δ	-9.6403				
RO					

T_1 (solution)		1.54 Varian	9.0 Varian	1.46 WP200

Sample	T/G/H	T/G/H	T/G/H	T/G/H	TPPTS
Comp.	17.29	16.15	16.15	16.15	pure
time hydrated	29h	13h	2h	none	none
Wt.% H_2O		1.80	1.52	1.10	869
T_1	160	130	109	120	1.08
File:BBB	45	44	43	42	41
std dev	0.006743	0.038823	0.036652	0.044669	
Sample	Rh/G/H	T/G/H	TPPTS		TPPTS
Comp.	9.73	17.3	pure		pure
time hydrated	no	12h	no		16h
Wt.% H_2O	1.73	7.41	1.26		1.47
T_1	0.112				1098
File:BBB	34	32	31		23
std dev	0.039937				0.011883

1. (a) Bruker Operating Manual 890701
(b) Bruker DISMSL Pulse Program Library VSN 890701

Summary

Compound	T1	Wt.% water	T1 (sol'n)
TPPTS	805	3.19	6.9 (V)
	1145	2.82	
	1098	1.47*	
		1.26*	
T/G/H 16.92%	150	1.53	
	220	1.83	
	22.5	6.90	
	201	2.09	
	210	2.03	
	4.92	13.28	
T/G/H 16.15%	130	1.80	
	109	1.52	
	120	1.10	
	869	1.08	
Complex, pure	1.51	1.52	1.46 (WP)
	7.9	5.70	
	3.55	8.73	
	1.50		
	0.74		
	2.72		
	1.65		
Rh/G/H 9.73%	0.112	1.73*	
Rh/G/H 13.2%	1.43		
	1.65		
	1.50		

Potentiometric Data for DPPETS

mL NaOH	pH	mL NaOH	pH
0.00	2.16	1.00	2.35
1.50	2.42	2.00	2.49
2.50	2.55	3.00	2.63
3.50	2.71	4.00	2.79
4.50	2.89	5.00	3.01
5.50	3.19	5.80	3.31
6.00	3.47	6.20	3.67
6.40	4.05	6.50	4.70
6.55	5.60	6.60	5.93
6.65	6.19	6.70	6.40
6.75	6.75	6.80	6.93
6.85	7.28	6.90	7.47
6.95	7.64	7.00	7.94
7.05	8.10	7.10	8.24
7.15	8.46	7.20	8.56
7.26	8.74	7.32	8.82
7.37	8.95	7.40	9.01
7.46	9.07	7.52	9.18
7.60	9.27	7.70	9.40
7.84	9.51	8.00	9.67
8.20	9.80	8.40	9.92
8.60	10.01	8.80	10.10
9.00	10.16	9.20	10.22
9.40	10.27	9.60	10.31
9.80	10.35	10.00	10.39
10.20	10.43	10.40	10.46
10.60	10.48	10.80	10.50
11.00	10.52		

Appendix B: Catalytic Data

Hydrogenation of trans-2-hexenal with Rh(COD)DPPETS)Cl

GC Setting: initial temp. = 40°
Hold = 2 min.
Final temp. = 200 °
Ramp = 10°/min.
Hold = 2 min.

Compound	B.P.	R.T.
pentane	36°	0.85
hexanal	131°	3.81
t-2-hexenal	146-7°	4.57
t-2-hexenol	158-60°	4.58
1-hexanol	157°	5.48
Decane	175°	7.77

Pressure (initial) = 200 psig H_2
Stirring rate = 360 rpm
In each autoclave:
0.5 mL substrate (4.33 mmol)
400/1 Substrate/Rh= 0.0108mmol/exp; 11.4 mg/exp.
1.0 mL catalyst solution (11.4 mg/mL)
1.0 mL pentane
0.25 mL decane
1.0 mL water

Temp: runs 5,6,7,8 = 23 °
Run # 5 30 min.

peak	%	RT	compound
1	53.671	0.88	pentane
2	3.166	3.53	hexanal
3	18.784	5.00	hexenal
4	24.379	7.92	decane

14.42% conversion to hexanal

Run # 6 60 min.

1	53.547	0.87	pentane
2	4.651	3.67	hexanal
3	16.285	5.1	hexenal
4	0.156	6.97	hexanol
5	25.361	7.98	decane

22.05% hexanal; 0.74% hexanol

Run#7 180 min.

1	56.778	0.87	pentane
2	13.052	3.95	hexanal
3	6.227	4.87	hexenal
4	0.518	6.96	hexanol
5	23.426	7.96	decane

65.93% hexanal; 2.62% hexanol

run#8 360 min.

1	62.764	0.86	pentane
2	13.221	3.76	hexanal
3	3.258	4.56	hexenal
4	20.757	7.79	decane

80.23% hexanal

Temp: runs 9.10.11.12 = 40°

run#9 30 min.

1	32.921	0.85	pentane
2	2.096	3.39	hexanal
3	0.416	3.68	hexanal
4	21.524	5.17	hexenal
5	0.103	6.8	hexanol
6	22.941	7.76	decane

10.41% hexanal; 0.43% hexanol

run#10 60 min.

1	54.937	0.85	pentane
2	11.276	3.7	hexanal
3	0.847	3.7	hexanal
4	0.196	3.77	hexanal
5	10.365	4.74	hexenal
6	0.094	6.74	hexanol
7	22.285	7.68	decane

54.08% hexanal; 0.41% hexanol

run#11 120 min.

1	54.971	0.85	pentane
2	10.038	3.7	hexanal
3	12.231	4.88	hexenal
4	0.105	6.76	hexanol
5	22.655	7.76	decane

44.86% hexanal; 0.47% hexanol

run#12 360 min

1	55.495	0.85	pentane
2	17.856	3.87	hexanal
3	4.148	4.62	hexenal
4	22.5	7.8	decane

81.15% hexanal

Temp: runs 13,14,15,16 = 60°

run#13 30 min.

1	51.28	0.85	pentane
2	4.196	3.4	hexanal
3	20.342	4.98	hexenal
4	0.111	6.74	hexanol
5	24.071	7.74	decane

17.02% hexanal; 0.45% hexanol

run#14 60 min.

1	56.808	0.85	pentane
2	8.583	3.64	hexanal
3	11.92	4.82	hexenal
4	0.098	6.77	hexanol
5	22.591	7.72	decane

41.66% hexanal; 0.48% hexanol

run#15 120 min.

1	55.008	0.84	pentane
2	21.068	3.86	hexanal
3	1.796	4.46	hexenal
4	22.128	7.74	decane

92.14% hexanal

run#16 312 min.

1	53.87	0.86	pentane
2	22.059	3.87	hexanal
3	0.501	4.35	hexenal
4	23.571	7.76	decane

97.78% hexanal

Hydrogenation of trans-2-hexenal with $Rh(DPPETS)_2Cl$

GC Setting: initial temp. = 40°
Hold = 2 min.
Final temp. = 200 °
Ramp = 10°/min.

Compound	B.P.	R.T.
pentane	36°	0.85
hexanal	131°	3.81
t-2-hexenal	146-7°	4.57
t-2-hexenol	158-60°	4.58
1-hexanol	157°	5.48
Decane	175°	7.77

Pressure = 200 psig H_2
Stirring rate = 360 rpm
In each autoclave:
0.5 mL substrate (4.51mmol)
1.0 mL catalyst solution
1.0 mL water
0.25 mL decane
1.0 mL pentane

Temp for runs 17,18,19,20 = 60°
Catalyst: 400/1 0.113 mmol/exp (19.79 mg/exp)

Run#17 30 min.

1	53.154	0.84	pentane
2	1.353	3.27	hexanal
3	24.002	5.12	hexenal
4	0.073	6.78	hexanol
5	21.417	7.68	decane

5.32% hexanal; 0.29% hexanol

run#18 192 min

1	51.99	0.86	pentane
2	3.194	3.39	hexanal
3	22.475	5.11	hexenal
4	0.102	6.78	hexanol
5	21.224	7.77	decane
6	0.148	13.38	
7	0.265	14.41	
8	0.115	14.42	
9	0.218	14.5	
10	0.27	18.67	

(next thing was to clean column)
12.39% hexanal; 0.40% hexanol

run#19 360 min.

1	52.159	0.85	pentnane
2	18.736	3.93	hexanal
3	5.731	4.74	hexenal
4	0.066	5.86	hexanol
5	21.041	7.84	decane
6	1.276	7.85	decane
7	0.162	13.39	
8	0.589	14.41	
9	0.079	14.51	
10	0.161	14.52	

76.37% hexanal; 0.27% hexanol

run#20 600 min

1	51.2	0.86	pentane
2	12.132	3.79	hexanal
3	13.549	4.96	hexenal
4	0.096	5.97	hexanol
5	23.023	7.86	decane

47.07% hexanal; 0.37% hexanol

Temp for runs 21,22,23,24 = 100°
Catalyst: 400/1 0.113 mmol/exp (19.79 mg/exp)
run#21 60 min.

1	56.409	0.85	pentane
2	5.831	3.46	hexanal
3	17.559	4.87	hexenal
4	0.253	6.74	hexanol
5	19.948	7.7	decane

24.66% hexanal; 1.07% hexanol

run#22 180 min

1	41.239	0.86	pentane
2	19.499	3.82	hexanal
3	0.255	3.89	hexanal
4	10.724	4.77	hexenal
5	28.282	7.79	decane

64.81% hexanal; 0.0% hexanol

run#23 390 min.

1	48.618	0.86	pentane
2	0.154	2.82	
3	28.133	3.88	hexanal
4	0.253	4.29	hexenal
5	22.844	7.74	decane

99.11% hexanal

run#24 480 min.

1	51.079	0.86	pentane
2	0.078	2.05	
3	24.178	3.89	hexanal
4	0.087	4.28	hexenal
5	1.552	5.26	hexanol
6	22.194	7.71	decane
7	0.078	12.4	
8	0.212	13.36	
9	0.067	13.56	
10	0.474	14.34	

93.65% hexanal; 6.01% hexanol

Temp for runs 25,26,27,28 = 60°
Catalyst: 200/1 0.113mmol/exp (19.79 mg/exp);substrate =0.25 mL;

run# 25 60 min.

1	69.135	0.86	pentane
2	1.571	3.36	hexanal
3	10.43	4.78	hexenal
4	18.865	7.79	decane

13.09% hexanal

run#26 120 min.

1	72.132	0.86	pentane
2	1.996	3.37	hexanal
3	9.915	4.66	hexenal
4	15.957	7.68	decane

16.76% hexanal

run#27 390 min.

1	66.939	0.86	pentane
2	10.918	3.77	hexanal
3	1.537	4.43	hexenal
4	20.605	7.8	decane

87.66% hexanal

run#28 1200 min.

1	68.488	0.86	pentane
2	8.357	3.71	hexanal
3	3.723	4.58	hexenal
4	19.432	7.82	decane

69.18% hexanal

Hydroformylation of 1-hexene with $PtCl_2$(DPPETS-H)

GC:
init. temp = 40°
Hold = 4 min
ramp = 15°/min
final temp = 200°
hold 1 min

1-hexene	63°	1.19
heptane	98°	2.33
hexanal	128-31°	4.16
2-hexanol	140°	5.16
1-hexanol	158°	7.74
decane	175°	11.62

400/1 substrate/ Pt
0.60 mL 1-hexene = 4.77 mmol
153 mg Pt/exp = 0.01200mmol/ exp
1.0 mL heptane
0.25 mL decane
2.0 mL Pt solution

Pressure = 200 psig CO/H_2 (1/1)
Stir rate = 360 rpm

Temp = 120° run# 29,30,31,32
run # 29, 30 min

1	33.822	1.22	1-hexene
2	50.268	2.67	heptane
3	15.91	12.12	decane

run#30 120 min

1	34.566	1.17	1-hexene
2	50.637	2.27	heptane
3	14.797	11.48	decane

run#31 435 min. not analyzed

run #32 1260 min.

1	0.149	0.86	
2	30.015	1.19	1-hexene
3	52.045	2.46	heptane
4	0.504	2.9	
5	16.372	7.52	
6	0.41	18.17	
7	0.506	18.64	

run #33 120 min (With detergent)

1	0.189	0.87	
2	30.871	1.22	1-hexene
3	51.048	2.79	heptane
4	17.891	12.32	decane

Hydrogenation of trans-2-hexenal with $PtCl_2$(DPPETS-H)

400/1 = 0.00894 mmol Pt complex/exp
Temp. = 60°
1.0 mL pentane
0.25 mL decane
0.41 mL substrate (3.58 mmol)
1.5 mL Pt solution
GC: as for hydrogenation

run#34 30 min

1	50.812	0.87	pentane
2	25.366	5.18	hexenal
3	23.822	7.89	decane

run#35 120 min

1	50.865	0.87	pentane
2	25.331	5.01	hexenal
3	23.804	7.83	decane

run#36 240 min.

1	49.584	0.87	pentane
2	4.706	3.45	hexanal
3	21.866	5.0	hexenal
4	23.844	7.8	decane

17.71% hexanal

run#37 480 min

1	49.087	0.87	pentane
2	25.718	5.12	hexenal
3	25.042	7.87	decane
4	0.153	13.41	

Carbonylation of Benzyl Chloride with $PtCl_2$(DPPETS-H)

Pressure =200 psig CO
Temp = 60°
Stir rate = 360 rpm

1.0 mL hexane	98°	1.11
Toluene	111°	2.64
Octane	125°	3.43
BzCl	177-81°	6.87
Benzyl alcohol	205°	
Phenylacetic acid	266°	10.00
dibenzyl	285°	
1,3-diphenylacetone	331°	

0.25 mL octane
Runs 38, 39, 40, 41 ruined (no NaOH)
2.5 mol/L used 1.0 mL NaOH Solution

acidify aqueous layer to pH=2
Extract with diethylether three times; combine with organic layer
Reduce volume to about 0.5 mL

GC: initial Temp = 50°
hold = 3 min.
Final temp = 250°
hold 2 min.
ramp 15°/min

Pt solution = 0.0266 mmol/ exp (1.0 mL of solution)
200/1 substrate/catalyst = 5.32 mmol BzCl = 0.60 ml
Rh(acac)$(CO)_2$, 0.015 M in MeOH, and DPPETS, 0.100 M in H_2O

run#42 60 min

1	7.624	0.83	
2	7.961	1.08	hexane
3	19.529	3.56	octane
4	64.159	7.3	BzCl
5	0.601	7.68	impurity in BzCl
6	0.127	8.02	

run#43	120 min.	
1	10.891	0.83
2	11.364	1.08
3	17.29	3.49
4	59.628	7.17
5	0.66	7.59
6	0.119	7.96
7	0.048	11.69
run#44	360 min	
1	22.754	0.81
2	20.93	1.08
3	11.247	3.5
4	35.756	7.21
5	0.599	7.36
6	0.379	7.64
7	0.074	8.0
8	0.148	11.71
9	0.297	14.32
10	3.857	22.81
11	3.959	23.45
run#45	480 min	
1	25.739	0.81
2	15.386	1.07
3	14.467	3.5
4	42.038	7.1
5	1.195	7.28
6	0.505	7.58
7	0.086	7.94
8	0.431	11.73
9	0.153	14.31

Hydroformylation of 1-octene using $Rh(acac)(CO)_2$ and DPPETS to form $Rh(DPPETS)_2^+$ *in situ*

$Rh(acac)(CO)_2$, 0.015 M in MeOH, and DPPETS, 0.100 M in H_2O
Nonane = 0.34 mL
Temp. = 120°
Pressure = 200 psig
Stirring rate = 360 rpm

Hydroformylation of styrene using $Rh(DPPETS)_2^+$

GC: Initial Column Temp = 50°
Inj. Temp = 200°
Detector Temp = 200°
Initial hold = 2 min.
Final hold = 2 min.
Ramp = 10°/min

Temp = 120°
Pressure = 220 psig CO/H (1/1) (Initial)
Stir rate = 360 rpm

toluene 111°
styrene 146°
ethylbenzene 136°
normal
branched

For runs 001-004
Stock solution = 0.0039 mol/L
(used 0.8 mL with 1.2 mL h_2O)
Styrene = 0.46 mL (4 mmol)
Nonane = 0.3 mL
Toluene = 1.25 mL
detergent (about 0.01g)

Substrate/Rh = 1250/1

Run# 001 30 min

%	RT	Substance
65.84	2.78	toluene
22.737	4.66	styrene
11.228	5.03	nonane
0.122	7.6	branched
0.073	8.52	normal

0.53% branched; 0.32% normal

Run#002 1 hr

64.273	2.22	toluene
25.389	4.2	styrene
9.692	4.51	nonane
0.012	4.69	
0.317	6.95	normal
0.317	7.85	branched

1.22% branched; 1.22% normal

Run#003 2 hr

69.301	3.03	toluene
20.542	4.92	styrene
9.191	5.25	nonane
0.012	5.44	
0.403	7.77	branched
0.09	7.78	branched
0.462	8.68	normal

2.29% branched; 2.15% normal

Run#004 6 hr

67.133	3.01	toluene
21.929	4.95	styrene
8.78	5.26	nonane
0.015	5.44	
1.103	7.86	branched
1.04	8.79	normal

4.58% branched; 4.32% normal

For runs 005-011

Stock solution: 0.0109 mol/L
(used 0.80 mL with 1.2 mL H_2O
0.50 mL styrene (4.36 mmol)
0.30 mL nonane
1.2 mL toluene
detergent (about 0.01g)

substrate/Rh = 500/1

Run#005 30 min

51.323	2.62	toluene
31.978	4.62	styrene
15.872	4.98	nonane
0.451	7.58	branched
0.376	8.49	normal

1.37% branched; 1.15% normal

Run#006 1 hr

46.822	2.61	toluene
21.912	4.54	styrene
10.771	4.66	
16.248	5.02	
0.673	7.64	branched
0.584	8.55	normal
0.177	13.62	
0.086	16.96	
0.229	17.2	
0.793	18.19	
1.704	18.72	

2.90% branched; 2.52% normakl

Run#007 2 hr

49.16	2.63	toluene
30.636	4.67	styrene
17.737	5.05	nonane
1.294	7.68	branched
1.172	8.59	normal

3.91% branched; 3.54% normal

Run#008 6 hr

55.162	2.79	toluene
26.549	4.82	styrene
15.536	5.2	nonane
0.018	5.37	
1.345	7.76	branched
1.391	8.69	normal

4.59% branched; 4.75% normal

Run#009 24 hr

76.019	1.8	toluene
0.332	2.83	
8.556	3.45	styrene
12.591	3.97	nonane
1.368	6.75	branched
1.147	7.66	normal

12.36% branched; 10.36% normal

Run#010 48 hr

73.515	2.49	toluene
0.55	3.61	
7.459	4.16	styrene
13.246	4.67	nonane
2.634	7.54	branched
2.596	8.45	normal

20.76% branched; 20.46% normal

Run#11 96 hrs

71.228	2.45	toluene
0.841	3.38	
5.003	4.02	styrene
16.155	4.66	nonane
3.203	7.44	branched
3.23	8.42	normal
0.341	12.99	

28.01% branched; 28.24% normal

Appendix C

Publications Generated by this Research

"Synthesis, Reaction and Catalytic Chemistry of the Water-Soluble Chelating Phosphine 1,2-[Bis(d-m-sodium sulfonatophenyl)phosphino]ethane (DPPETS) with Nickel, PAlladium, Platinum and Rhodium"
Tamas Bartik, Barbara B. Bunn, Berit Bartik, and Brian E. Hanson
Iorganic Chemistry, in press

"^{31}P Solid-State NMR as a Tool for the Characterization of Supported Aqueous Phase Catalysis"
Barbara B. Bunn, Brian E. Hanson, Tamas Bartik, Berit Bartik, William R. Bebout, Thomas E. Glass
Journal of Catalysis, submitted

VITA

Barbara B. Bunn was born on September 22, 1940 in Orange, New Jersey, to Wilbur B. and Eleanor K. Batt. She was reared in Clearwater, Florida and graduated from Clearwater High School in 1958. She married The Rev. George S. Bunn, III on March 31, 1959 and is the mother of three children, David Strother, an attorney in Bristol, Tennessee, Jonathan Rudman, an attorney in Bristol, Viginia, and Gabrielle Elizabeth, enrolled in the College of Veterinary Medicine at the University of Tennessee, Knoxville, TN.

The author matriculated at East Tennessee State University, Johnson City, TN the summer of 1982. She graduated with the Bachelor of Science degree in chemistry in 1986, and recieved the Master's degree in physical chemistry in 1988 under the direction of Dr. Thomas T.-S. Huang. She remained at ETSU as adjunct faculty, assistant professor until 1990, when she began her studies for the Ph.D. degree in inorganic chemistry under the guidance of Dr. Brian E. Hanson. While at Virginia Tech she was a lecturer in General Chemistry. She received the doctorate in December, 1993.

B.B. Bunn lives at "The Little Farm", 518 Beech Forest Rd., Bristol, TN 37620 with her husband, George, three horses, Ginger, Ruach and June Bug; Wolfie the goat, Bismarck the dog, and assorted cats. Her interests include horses, gardening and church work as well as chemistry.